INFORMATION TO USERS

This manuscript has been reproduced from the microfilm master. UMI films the text directly from the original or copy submitted. Thus, some thesis and dissertation copies are in typewriter face, while others may be from any type of computer printer.

The quality of this reproduction is dependent upon the quality of the copy submitted. Broken or indistinct print, colored or poor quality illustrations and photographs, print bleedthrough, substandard margins, and improper alignment can adversely affect reproduction.

In the unlikely event that the author did not send UMI a complete manuscript and there are missing pages, these will be noted. Also, if unauthorized copyright material had to be removed, a note will indicate the deletion.

Oversize materials (e.g., maps, drawings, charts) are reproduced by sectioning the original, beginning at the upper left-hand corner and continuing from left to right in equal sections with small overlaps.

Photographs included in the original manuscript have been reproduced xerographically in this copy. Higher quality 6" x 9" black and white photographic prints are available for any photographs or illustrations appearing in this copy for an additional charge. Contact UMI directly to order.

ProQuest Information and Learning
300 North Zeeb Road, Ann Arbor, MI 48106-1346 USA
800-521-0600

DISSERTATION

CYCLIN A-CDK2 INHIBITION BY p21, p27, and p57

Submitted by
Joshua N. Adkins
Department of Biochemistry and Molecular Biology

In partial fulfillment of the requirements for the
Degree of Doctorate of Philosophy
Colorado State University
Fort Collins, Colorado
Spring 2001

UMI Number: 3013819

UMI Microform 3013819

Bell & Howell Information and Learning Company
300 North Zeeb Road
P.O. Box 1346
Ann Arbor, MI 48106-1346

COLORADO STATE UNIVERSITY

March 15, 2001

WE HEREBY RECOMMEND THAT THE DISSERTATION PREPARED UNDER OUR SUPERVISION BY JOSHUA N. ADKINS ENTITLED

CYCLIN A-CDK2 INHIBITION BY p21, p27, and p57

BE ACCEPTED AS FULFILLING IN PART REQUIREMENTS FOR THE DEGREE OF DOCTORATE OF PHILOSOPHY.

Committee on Graduate Work

Robert W. Woody

James R Bamburg

Adviser

Department Head

ABSTRACT

CYCLIN A-CDK2 INHIBITION BY p21, p27, and p57

Progression through the eukaryotic cell cycle is regulated by phosphorylation, which is catalyzed by cyclin-dependent kinases. Cyclin-dependent kinases are regulated through several mechanisms, including negative regulation by the p21 (variously called CAP20, Cip1, Sdi1, and WAF1) family of inhibitors. It has been proposed that multiple p21 molecules are required to inhibit cyclin-dependent kinases, such that p21 acts as a sensitive buffer of cyclin-dependent kinase activity or as an assembly factor for the complexes formed by the cyclins and cyclin-dependent kinases. Using purified, full-length proteins of known concentration (determined by absorbance) and cyclin A-Cdk2 of known activity (calibrated with staurosporine), we find that a 1:1 molar ratio of p21 to cyclin A-Cdk2 is able to inhibit Cdk2 activity both in the binary cyclin A-Cdk2 complex and in the presence of proliferating cell nuclear antigen (PCNA). Our results indicate that the mechanism of p21 inhibition of cyclin A-Cdk2 does not involve multiple molecules of bound p21.

p27 contributes to cell-cycle regulation by inhibiting the enzymatic activity of cyclin-dependent kinases. In contrast to the ordered conformation observed in the crystal structure of the p27-cyclin A-Cdk2 complex, we find that the human p27 Cdk-inhibitor is intrinsically disordered in isolation under conditions where the domain inhibits cyclin A-Cdk2. Using proline- and alanine-mapping mutatgenesis, we show the p27 domain contains marginally stable helical structure that is localized to the region that folds as an α-helix, but not the 3_{10} helix, upon binding cyclin A-Cdk2. Reducing or increasing the helical propensity in the isolated p27 domain with proline and alanine mutagenesis did not affect formation of the p27-inhibited cyclin A-Cdk2

complex in either energetic or functional terms. We conclude that non-local (quaternary) contacts between p27 and cyclin A-Cdk2 are more important determinants of p27-cyclin A-Cdk2 assembly than pre-existing local (helical) interactions in the intrinsically disordered p27.

Biophysical characterization and functional analysis of human p57 and the isolated inhibition domain of p57 completes a general characterization of this family of proteins. The inhibition domain of p57 is based on the homologous residues of p27 that were used in the crystal structure of p27-cyclin A-Cdk2. Circular dichroism spectra of both full-length p57 and the excised inhibition domain exhibit similar features expected of an unfolded protein. Sedimentation equilibrium and gel filtration indicate this protein is monomeric and in an extended conformation. Cdk-inhibition by both full-length p57 and the inhibition domain indicates that these proteins are active in a 1:1 stoichiometry with slightly greater K_d as compared to p27ID. We conclude p57 is unordered in isolation and behaves in a similar manner to that of p21 and p27.

Joshua N. Adkins
Department of Biochemistry and
Molecular Biology
Colorado State University
Fort Collins, Colorado 80523-1870
Spring 2001

Acknowledgements

I would like express my great respect and deep appreciation for my adviser, Dr. Kevin Lumb, for his guidance, availability for questions, and high expectations. He has been and will remain a force pushing me to higher goals and expectations. Even, if occasionally, that higher goal is another pint.

I would like to thank my committee members, Dr. James Bamburg, Dr. Paul Laybourn, Dr. Christopher Rithner, and Dr. Robert Woody for their time, helpful suggestions, and the often-used equipment and materials. Dr. Rithner also provided critical help in collecting the data shown in figure 2.7.

I am indebted to the people who shared their technical knowledge and assistance. These people include, but are not limited to Lynn Taylor, Dr. Alan Kennan, and Dr. Phillip Ryan with the rest of the MRF staff.

I would like to thank Mary Robinson, Ryan Ogg, and Dr. Laurie Stargell for the honor of our collaboration on TFIIA.

I cannot thank enough the members of the Lumb laboratory past and present. Kathleen Campbell, thank you for being a great lab partner and good listener for five years (probably very long years for you). Dr. Ewa Bienkiewicz, dziękuję (thank you) for the years of friendship, quality of advice, and productive collaborations. Andrew Vendel, I could never have wished for a better partner in crime. Yu Wei, Shannon Flaugh, Santano Mestas, and Teresa Groesch have all been good friends and great lab partners.

To my parents (including in-laws), I would like to thank you for your unique contributions to my motivations, concerns, and aspirations.

Lastly, I am deeply indebted to my wife and children. Patty, your support and understanding has always been appreciated and welcomed. Sarah, your bright eyes and inquisitive nature make me appreciate the world and really see "the moon." Ethan, your easy smile and joyous ways make me realize my only wish for you and your sister is happiness.

Dedicated to the memory
of my grandmother V. M. Chartier

Table of Contents

Figures and Tables

Abbreviations

4HB	four-helix bundle of yeast TFIIA
t-Boc	*tert*-butyloxycarbonyl
CD	circular dichroism
Cdk	cyclin-dependent kinase
DIEA	N,N-diisopropylethylamine
DMF	N,N-dimethyl formamide
DNP	2,4-dinitrophenyl
DTT	dithiothreitol
HBTU	2-(H-benzotriazole-1-yl)-1,1,3,3-tetramethyluronium hexafluorophosphate
HF	hydrogen fluoride
HPLC	high performance liquid chromatography
IPTG	isopropyl-β-D-thiogalactose
krpm	thousands of revolutions per minute
MALDI	matrix-assisted laser desorption ionization
MPF	maturation promoting factor
MBHA	4-methylbenzhydrylamine
NMR	nuclear magnetic resonance
PAGE	polyacrylamide gel electrophoresis
PCNA	proliferating cell nuclear antigen
SDS	sodium dodecyl-sulfate
TFA	trifluoroacetic acid

Chapter 1
Cell-Cycle Regulation

1.0 THE CELL CYCLE

In 1665, Robert Hooke published *Micrographia*, which among other items described small structures he had observed under an early compound microscope as "little boxes or cells." This is usually considered the origin of the word "cell" as it is known today (Hooke, 1665). The cell theory is composed of the ideas of Theodore Schleiden, Jacob Schwann, and Rudolf Virchow and was proposed in two parts: every "living" organism is made up of one or more cells, and new cells only arise from pre-existing cells (Pauly, 1987).

Early optical microscopy studies of the cell-division cycle, or the cell cycle, identified two major phases. The first phase, mitosis, is when chromosomes condense and sister chromatids separate, and the cell divides (cytokinesis) into daughter cells. The second phase was referred to simply as interphase and comprised the majority of the life cycle of most cells because no obvious subdivisions could be observed with microscopy. However, two obvious processes must occur during a standard interphase: doubling the size of the cell and replication of DNA. Through studies of DNA content, subdivisions of interphase were made. Interphase was subdivided into G1 or Gap1 phase, S or (DNA) Synthesis phase, and G2 or Gap2 phase (Figure 1.1).

Early in the 1970's, studies of *Xenopus laevis* oocytes further developed knowledge of the cell cycle. A component of the cytoplasm in unfertilized

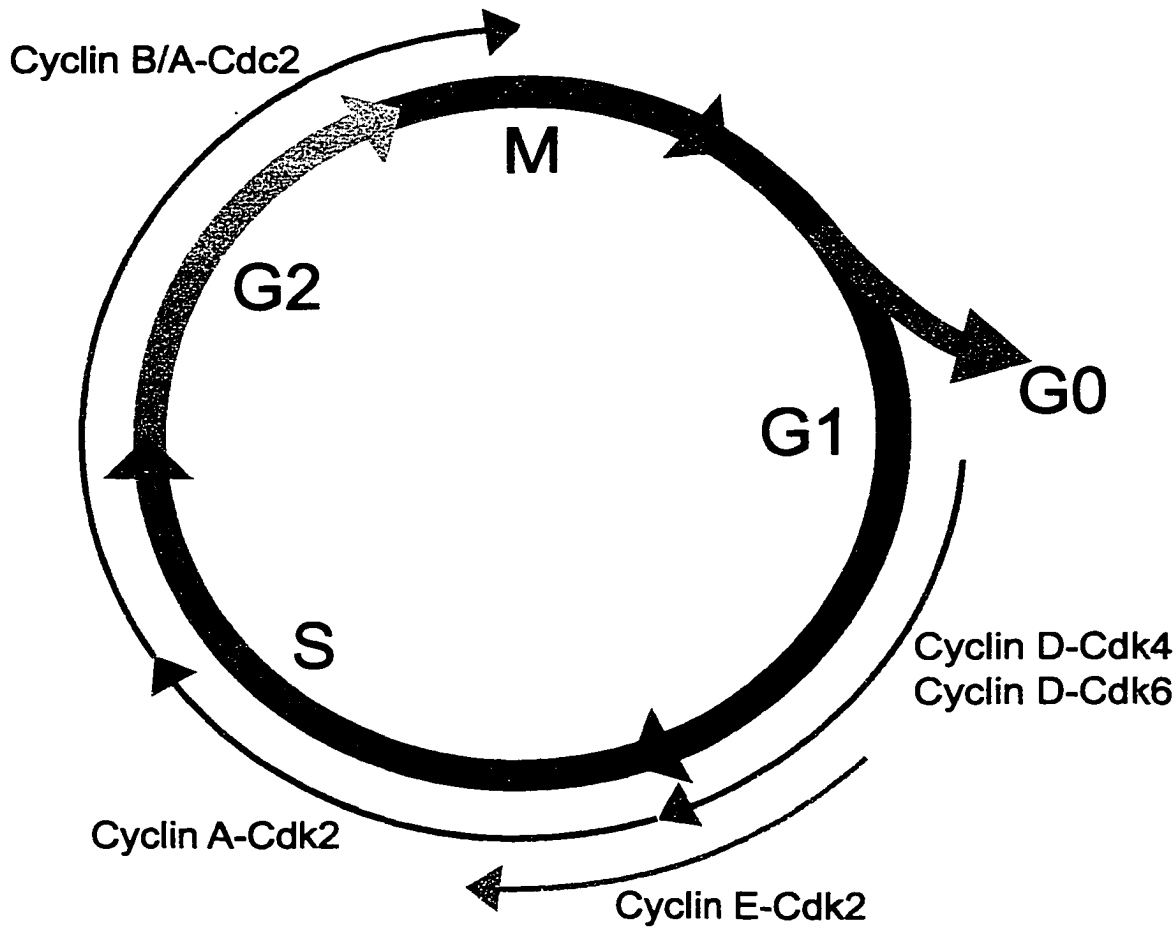

Figure 1.1. The Cell Cycle

The cell cycle contains four phases called G1, S, G2 and M phases. The length of the phases corresponds with approximate length of most actively proliferating cells. Cyclin-Cdk pairs are shown during the period of the cell cycle when they are activated (Sherr, 1993).

oocytes induces meiosis II metaphase arrest with progesterone, i.e. maturation, and is capable of being transferred to other unfertilized oocytes to induce maturation (Murray and Hunt, 1993). This maturation continued with serial cytoplasmic transfers from matured oocytes to immature oocytes and therefore was not an effect of residual progesterone. The component that induces this maturation was therefore called maturation-promoting factor (MPF) (Masui and Markert, 1971). MPF activity cycled in mitotic cells, but a protein that cycled with this activity was elusive in *Xenopus laevis*. The first protein that increased and decreased within the same cycle as MPF was found in sea urchin eggs (Murray and Hunt, 1993). This oscillating protein is now called cyclin and was found to disappear following mitosis, but would gradually reappear and gradually increase until the end of the next round of mitosis (Figure 1.2).

The cyclin by itself is not MPF (Murray and Hunt, 1993; Alberts et al., 1994). The discovery of a partner to cyclin was found in both budding yeast *Saccharomyces cerevisiae* and fission yeast *Schizosaccharomyces pombe* as temperature-sensitive mutants of the cell-division cycle. At the restrictive temperature, cell-division cycle (cdc) mutants were unable to progress past specific points in the cell cycle (Alberts et al., 1994; Morgan, 1997). Among the cdc mutants were the kinases *Saccharomyces cerevisiae* Cdc28 and *Schizosaccharomyces pombe* Cdc2. These catalytic proteins required a cyclin in order to function; therefore Cdc28 and Cdc2 were the first characterized cyclin-dependent kinases (Cdks).

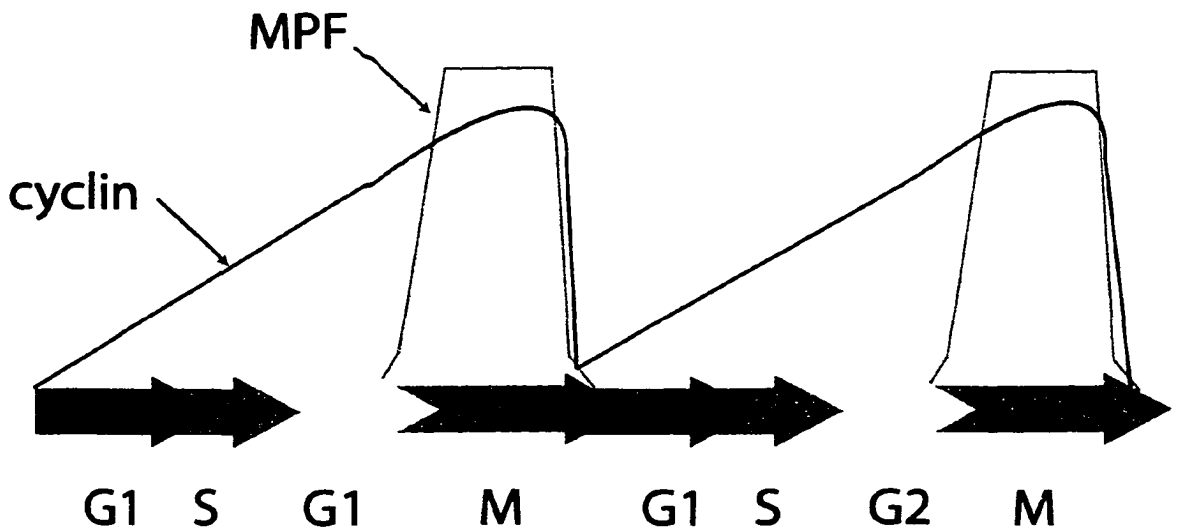

Figure 1.2. Cyclin Level Associated with MPF Activity
Cyclin was first characterized in sea urchin fertilized eggs because it can make up to 5 % of the protein synthesized in early cell cycles. Cyclin (later referred to as mitotic cyclin in fission yeast and cyclins A and B in vertebrates) gradually appears until mitosis, quickly disappears by the end of mitosis, and repeats this cycle during subsequent cell cycles. Adapted from Murray and Hunt (1993) and Alberts et al. (1994).

1.1 CYCLINS AND CYCLIN-DEPENDENT KINASES

Vertebrates have more than ten Cdc2-related proteins and at least eight major cyclin types. The majority of Cdks are not critical to the cell cycle (Morgan, 1997). Cdks are unable to phosphorylate other proteins without a cyclin partner and therefore will generally be discussed here as cyclin-Cdk complexes. The primary vertebrate cyclin-Cdk pairs functioning in G1 phase are cyclin D-Cdk4, cyclin D-Cdk6 (reviewed in Sherr and Roberts, 1999), and cyclin E-Cdk2 (Koff et al., 1991; Koff et al., 1992) (Figure 1.1). The cyclin E-Cdk2 complex is also active during early S phase, while cyclin A-Cdk2 activity starts just prior to entry to S phase and abates by mid-G2 phase. G2 phase is predominately controlled by cyclins A and B with Cdc2 (Cdk1) and their activity continues into early mitosis (Figure 1.1).

Cyclin-Cdk pairs coordinate cell cycle progression and are the targets for cell-cycle regulatory signals. Growth signals from Ras and MAP kinase pathways lead to induction of cyclin D and the activation of Cdk4 and Cdk6 (Hunter and Pines, 1994). The G1 Cdks are also activated by integrins that promote anchorage-dependent growth (Zhu et al., 1996). Very little is known about many of the signals and how they regulate cyclin-Cdk pairs, but more is known about the mechanisms of cyclin-Cdk regulation.

1.2 REGULATION OF CYCLIN-DEPENDENT KINASES

1.2.a Positive Regulation by Cyclins

The transitions to and from active Cdks are driven by the increases and decreases in cyclin concentrations. Cells stay dormant or quiescent in the

cell-cycle phase called G0 until induced by mitogenic stimuli. Cyclin D then induces the cell to progress through the restriction point by binding Cdk4 and Cdk6. The restriction point is the position in the cell cycle when the cell is committed to cell division (Hunter and Pines, 1994). Cyclin E expression is then induced, which is important in the G1-S phase transition and initiation of DNA replication (Heichman and Roberts, 1994). Both cyclin D and E are rapidly degraded by ubiquitin-mediated proteolysis at the beginning of S phase (Koepp et al., 1999). Cyclins A and B expression is induced during S phase, but cyclin A is localized to the nucleus and cyclin B is sequestered in the cytoplasm until the end of G2 (Yang and Kornbluth, 1999). Cyclin A is then required for progression through S phase. In the presence of cyclins A and B bound to cdc2, the cell progresses through the G2/M transition (Hunter and Pines, 1994). At the beginning of M phase cyclins A and B are then degraded by ubiquitin-mediated proteolysis (Hunter and Pines, 1994).

Cdks share a large degree of sequence similarity (40-75 % from Cdk1 through Cdk7). Hence, structural studies of Cdk2 are likely to give insight to the entire range of Cdks. The cyclin family is more diverse, but they share a sequence similarity in the region known as the cyclin box that contains between 30-50 % similarity (Hadwiger et al., 1989). This further suggests that general lessons from cyclin A will translate to other cyclins. Cyclin A and Cdk2 are relatively promiscuous compared to other cyclins and Cdks, with one or the other active through most of the cell cycle.

Cdk2 is structurally very similar to other eukaryotic protein kinases with a conserved catalytic core (Taylor and Radzio-Andzelm, 1994; Jeffrey et al., 1995). This catalytic core consists of an N-terminal lobe rich in β-sheet and a larger C-terminal lobe rich in α-helix (Figure 1.3A) (De Bondt et al., 1993). A deep catalytic cleft is located between the N- and C-terminal lobes (Jeffrey et al., 1995). Cdk2 does have some conserved features specific to other Cdks; these are the PSTAIRE (one letter amino acid code) helix region and the regulatory T-loop.

The truncated cyclin A fragment (175-432) is a globular protein consisting of twelve α-helices. In the cyclin A-Cdk2 crystal structure, these proteins share a large buried surface area in the complex (Figure 1.3B) (Jeffrey et al., 1995). This buried surface area is substantially larger than most other heterologous protein-protein interactions (Jeffrey et al., 1995). Cyclin A makes significant contacts with both the PSTAIRE helix and T-loop segments of Cdk2. The cyclin box motif of cyclin A clamps onto the PSTAIRE helix and moves portions of the T-loop by as much as 20 Å. The movement of the PSTAIRE helix orients Glu51 of Cdk2 in the catalytic cleft to help coordinate ATP for catalysis. The T-loop blocks the catalytic cleft of Cdk2 when unbound, but binding of cyclin A relieves much of this blockage by the T-loop (Jeffrey et al., 1995). Therefore, cyclin A binding to Cdk2 not only positions Glu51 of the triad of catalytic residues, it also increases access to the catalytic site by substrates.

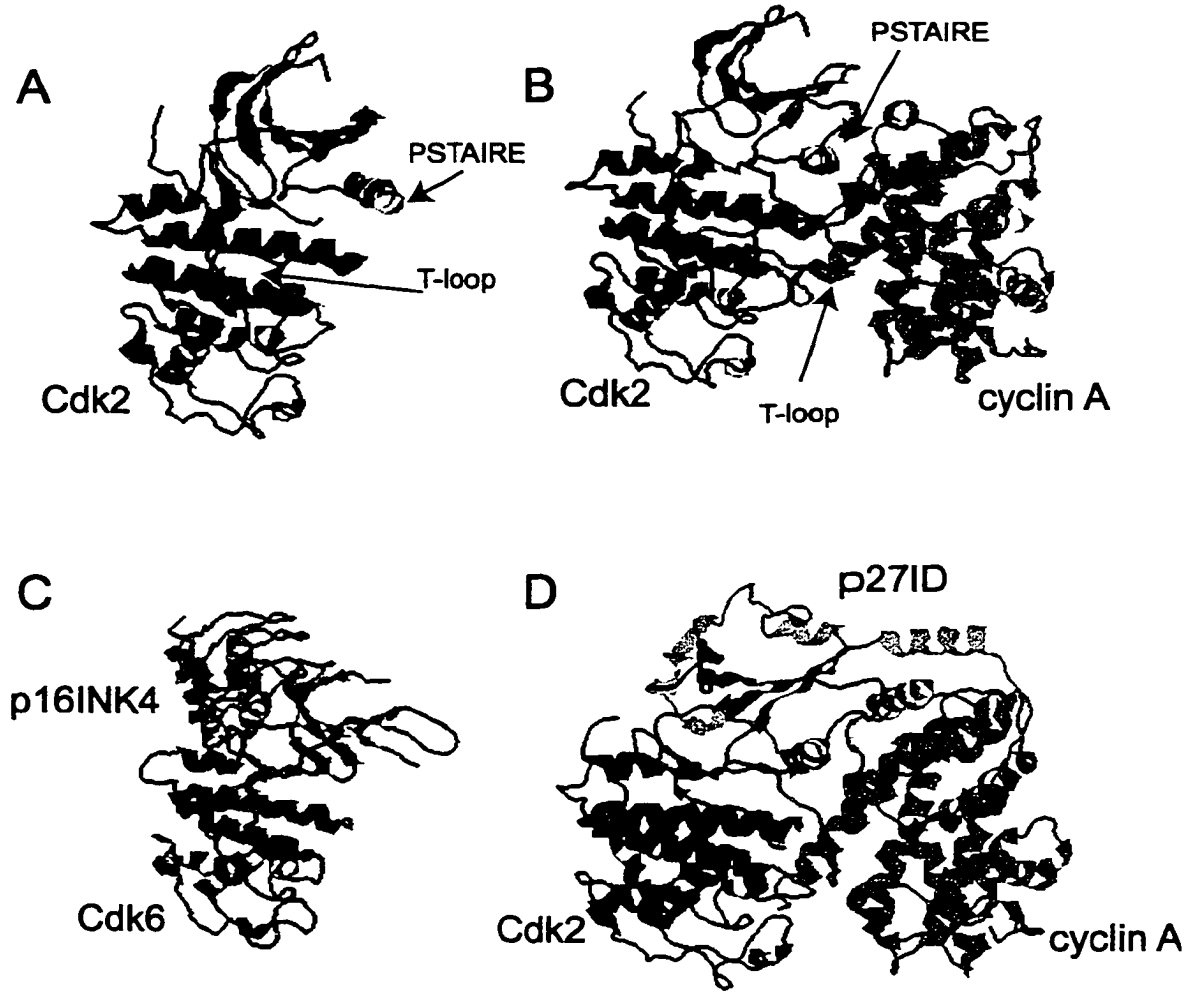

Figure 1.3. Crystal Structure of Cdks Alone and with Various Partners
A. Cdk2 (De Bondt et al., 1993).
B. Cyclin A-Cdk2 (Jeffrey et al., 1995).
C. $p16^{Ink4a}$-inhibited Cdk6 (Russo et al., 1998).
D. p27-inhibited cyclin A-Cdk2 (Russo et al., 1996a).

1.2.b Positive Regulation by Phosphorylation

Cyclin A-Cdk2 has become the structural archetype for understanding other cyclins and Cdks. One major difference between cyclin A-Cdk2 kinase activity and other cyclin-Cdk complexes is that cyclin A-Cdk2 has some activity in the absence of stimulatory phosphorylation on a conserved Thr (Thr160 for Cdk2). The activity of cyclin A-Cdk2 when Thr160 is phosphorylated is 300-fold greater than that of the unphosphorylated form (Songyang et al., 1994; Russo et al., 1996b).

There is some uncertainty as to the kinase that performs the stimulatory phosphorylation on most Cdks *in vivo* (Kaldis and Solomon, 2000). That kinase is usually considered to be cyclin H and Cdk7 (MO15) (Solomon et al., 1993; Fisher and Morgan, 1994; Kaldis and Solomon, 2000). Another protein, Cak1p, from budding yeast is a monomeric protein kinase that can also catalyze stimulatory phosphorylation on Cdks (Kaldis et al., 1996).

Cdk2 is stimulated when phosphorylated at Thr160, which is located on the T-loop. When Thr160 is phosphorylated, three Arg residues coordinate the negative charges of the phosphate group (Russo et al., 1996b). This phosphorylation moves part of the T-loop by as much as 7 Å, making the substrate binding site of Cdk2 more accessible than by cyclin A binding alone, and also increases buried surface area between the already significant contacts between the interface of cyclin A and Cdk2 (Russo et al., 1996b).

KAP (Cd*k*-*a*ssociated *p*hosphatase) and PP2A (*p*rotein *p*hosphatase *2A*) are two inhibitory phosphatases that catalyze the dephosphorylation of Thr160 on Cdk2 (Lew and Kornbluth, 1996; Karaiskou et al., 1999).

1.2.c Negative Regulation by Phosphorylation

In addition to positive regulation by phosphorylation, Cdks can also be inhibited by phosphorylation. The sites for inhibitory phosphorylation on Cdk2 are Thr14 and Tyr15. Wee1, performs the phosphorylation of Tyr15 (Russell and Nurse, 1987; Lew and Kornbluth, 1996). Phosphorylation of Tyr15 is the most common inhibitory phosphorylation of Cdks *in vivo*. Myt1 catalyzes Thr14 phosphorylation and may phosphorylate a specific cytoplasmic sub-population of Cdks (Lew and Kornbluth, 1996).

There are no crystal structures of inhibitory phosphorylation states of Cdk2. The p27-inhibited cyclin A-Cdk2 and staurosporine-inhibited crystal structures suggest a method of inhibition (Russo et al., 1996a; Lawrie et al., 1997). Thr14 and Tyr15 are both on the edge of the catalytic cleft of Cdk2, facing the solvent away from this cleft. The locations of the residues are closest to the ATP-binding site where the ATP phosphates hydrogen bond with Lys33. When Thr14/Tyr15 residues are phosphorylated, they may hydrogen bond with Lys33, preventing ATP from binding in this site (Pines, 1995).

Myt1 and Wee1 phosphorylate Thr14 and Tyr15 respectively and inhibit Cdk activity (Russell and Nurse, 1986; Lew and Kornbluth, 1996). Cdc25 is the opposing phosphatase that catalyzes the dephosphorylation of both Thr14 and Tyr15 residues, thereby reactivating Cdk activity.

1.2.d Negative Regulation by the Ink4-Famliy of Inhibitors

The binding of a protein inhibitor from the Ink4 family (*in*hibitor of Cd*k4*) can inhibit cyclin D-Cdk4 and cyclin D-Cdk6 complexes. The Ink4 family of inhibitors, including $p16^{Ink4a}$, $p15^{Ink4b}$, $p18^{Ink4c}$, and $p19^{Ink4d}$, are biochemically indistinguishable, but appear to control cell cycle progression in response to differing proliferative stimuli (Carnero and Hannon, 1998; Chellappan et al., 1998).

Crystal structures of $p16^{Ink4a}$ (Russo et al., 1998) and its close relative $p19^{Ink4d}$ (Brotherton et al., 1998) bound to Cdk6 illustrate how these proteins inhibit their Cdk targets (Figure 1.3C). These inhibitors bind to Cdk6 by making contacts with both the β-sheet-rich N-terminal lobe and the α-helix-rich C-terminal lobe. This binding partially blocks the ATP binding site, but does not occupy or contact the cyclin-binding region of Cdk6. Compared to the cyclin A-Cdk2 structure (Figure 1.3B), the Ink4 inhibitors twist the N-terminal lobe 15° relative to the C-terminal lobe and appear to prevent cyclin D binding (Pavletich, 1999). This twist also reorients the PSTAIRE helix

such that equivalent cyclin A binding with Cdk2 would require a major deformation of at least one of the proteins to be accommodated (Pavletich, 1999). Comparisons between the cyclin A-Cdk2 structures and the Ink4-Cdk6 structures do suggest this mechanism of inhibition, but it should be noted that Cdk6 with or without cyclin D has not been crystallized. Hence, the uninhibited Cdk6 could vary in ways that actually are more or less accommodating than the equivalent effects in the Cdk2 structures.

1.2.e Negative Regulation by the p21$^{Cip1/Waf1}$ Family of Inhibitors

A more promiscuous family of Cdk inhibitors is the p21 family. This family comprises p21 (Cip1, Harper et al., 1993; Waf1, El-Deiry et al., 1993; Cap20, Gu et al., 1993; Sdi1, Noda et al., 1994), p27^{Kip1} (*k*inase-*i*nhibitory *p*rotein*1*; Polyak et al., 1994), and p57^{Kip2} (*k*inase-*i*nhibitory *p*rotein*2*; Lee et al., 1995; Matsuoka et al., 1995). These proteins bind to most cyclin-Cdk pairs and have differing affinities for those complexes (Harper et al., 1995; Chen et al., 1996; Lee et al., 1996; Hengst and Reed, 1998). They share a highly homologous N-terminal domain (approximately 43 % identity) that inhibits Cdk activity (Figure 1.4).

Inhibition occurs only when the inhibition domain binds to both the cyclin and Cdk (Morgan, 1997). The p27^{Kip1} inhibited cyclin A-Cdk2 crystal structure gives insight to the mechanism of Cdk inhibition (Figure 1.3.d).

A

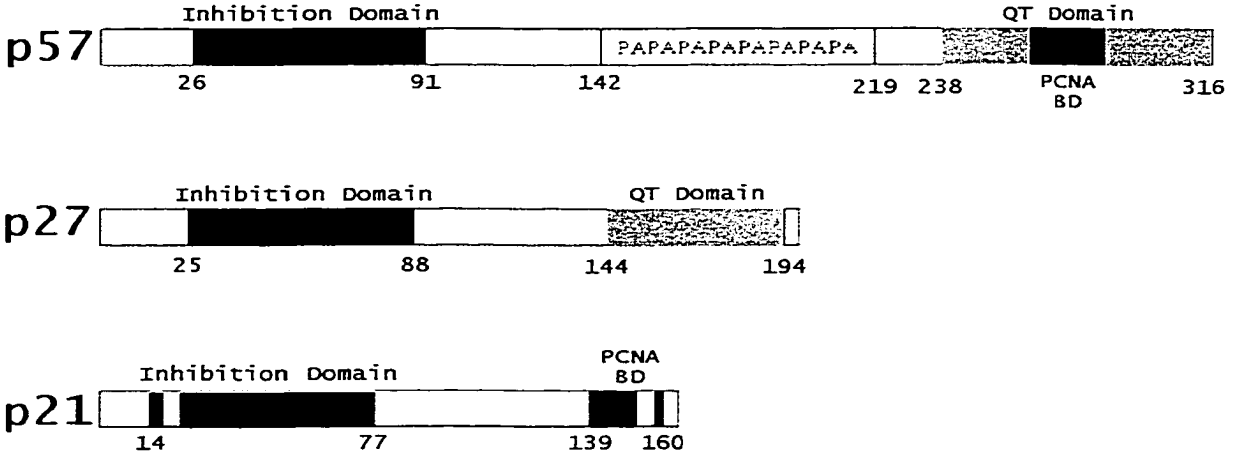

B

p21 (16-77) SKACRRLFGPVDSEQLSRDCDALMAGCIQEARERWNFDFVTETPLEG DFAWERVRGLGLPKLY
p27 (26-88) PSACRNLFGPVDHEELTRDLEKHCRDMEEASQRKWNFDFQNHKPLEG KYEWQEVEKGSLPEFY
p57 (27-91) TSACRSLFGPVDHEELSRELQARLAELNAEDQNRWDYDFQQDMPLRGPGRLQWTEVDSDSVPAFY

Figure 1.4. Domain Structure of the Cip Family of Cdk Inhibitors

A. Full-length p21, p27, and p57 with domains labeled. Light bars on p21 are cyclin binding regions.
B. Sequence comparison of the Cdk-inhibition domains of p21, p27 and p57.

An obvious feature of the crystal structure is a C-terminal 3_{10}-helix of p27 inserted in the catalytic cleft of Cdk2. Tyr88 of the 3_{10}-helix of p27 binds Lys33 of Cdk2, which is important in stabilization of the ATP phosphates (see also Section 1.2.c). Surprisingly, if the 3_{10}-helix is removed p27 can still inhibit cyclin-Cdk complexes (Polyak et al., 1994). This secondary inhibition occurs by changing the shape of the catalytic cleft through the β-sheet rich N-terminal lobe (Pavletich, 1999). Connecting this C-terminal region to the N-terminal cyclin binding domain is an α-helix that is extended over both cyclin A and Cdk2. Removal of the N-terminal cyclin binding region disrupts inhibition (Fotedar et al., 1996; Ball et al., 1997; Schulman et al., 1998). The cyclin-binding region appears to be important for the high affinity of binding and may have a role in cyclin-Cdk specificity (Chen et al., 1996; Lee et al., 1996; Morgan, 1997;.

1.3 THE BIOLOGICAL ROLE OF THE p21 FAMILY OF INHIBITORS

1.3.a p21

p21 has been found to arrest cells in G1 when overexpressed or transcriptionally activated by the tumor suppressor p53 (Elledge et al. 1996; Hengst and Reed 1998). p53 activates p21 transcription in response to DNA damage. When p53-negative cells are subjected to DNA damage the cells do not accumulate p21, leading to the conclusion that p21 is the agent responsible for p53-mediated G1 arrest (El-Deiry et al., 1993; Harper et al., 1993). This conclusion was complicated by comparisons of p53-nullizygous mice with p21-nullizygous mice (Kiyokawa and Koff, 1998). The p53-

nullizygous mice developed spontaneous tumors at a high rate and had a complete loss of the ability for G1 arrest (Donehower et al., 1992). In contrast, the p21-nullizygous mice have no spontaneous tumorigenesis and, albeit impaired, the cells still have the ability to arrest in G1 (Brugarolas et al., 1995; Deng et al., 1995). The only phenotype of p21-deficient mice is a defective DNA-damage checkpoint control. The mutation rate of p21 in human cancers is very low and those are usually loss-of-function mutations, resulting from N-terminus truncations (Gao et al., 1995). p21 does have a role in G1 arrest, but this role is not absolutely critical to mouse development or the oncogenesis.

p21 functions through two known mechanisms; Cdk inhibition through the inhibition domain (discussed previously) and blocking replication by binding proliferating cell nuclear antigen (PCNA) (Chen et al., 1996). PCNA is a homotrimeric ring that interacts with DNA and functions as the processivity factor for DNA polymerase δ (Warbrick et al., 1995; Gulbis et al., 1996). One molecule of p21 can bind one molecule of PCNA, therefore three p21 molecules can occupy the three molecule of PCNA in the trimer. This binding appears to disrupt replication functions of PCNA, but not DNA repair functions (Chen et al., 1996; Gulbis et al., 1996).

1.3.b p27

p27, like p21, is capable of inducing G1 arrest when overexpressed (Polyak et al., 1994). The analysis of p27 function *in vivo* that has given the greatest

insight to p27 function has also been through nullizygous mice (Fero et al., 1996; Kiyokawa et al., 1996). p27-nullizygous mice were 20-40% larger than wild-type littermates. The thymus was hyperplasic as a result of hyperproliferation and not a decrease in apoptosis for the individual cells. Pituitary gland hyperplasia was also seen, including an increase in size through time, suggesting p27 plays an important role in quiescence in this cell lineage. Female p27-null mice are infertile. The underlying cause of infertility was unclear due to the complexity of the processes involved in oogenesis, ovulation, and embryo implantation (Kiyokawa and Koff, 1998; Weinberg, 1995). Finally, these mice also exhibited severe disruption of the retina (Nakayama et al., 1996). The retina is an area of interest due to the association of retinoblastomas in humans with the Cdk4 and Cdk6 substrate pRb (retinoblastoma protein) (Kiyokawa and Koff, 1998). The phenotypic changes of p27-nullizygous mice are more obvious than those of the p21-nullizygous mice, but the results suggest that the Cip/Kip family of inhibitors may not be important molecules in carcinogenesis. Analyses of mutations in cancers have found very little correlation with mutations of p27 (reviewed in Hengst and Reed, 1998).

1.3.c p57

There appear to be two p57 variants that arise in human cells due to alternate splicing (Matsuoka et al., 1995). One variant is primarily made up of the N-terminal inhibition domain (residues 1-96) and the longer variant has a more diverse domain structure (residues 1-316) than either p21 or p27.

Overexpression of p57 causes cell cycle arrest in G1 phase, like the other members of the p21 protein family (Lee et al., 1995; Matsuoka et al., 1995). The longer of the two-p57 variants is expressed in a tissue specific manner, unlike the near universal expression of p21 and p27. Highest expression of p57 is in the skeletal muscle, brain, heart, lungs, eyes, and tongue (Lee et al., 1995; Matsuoka et al., 1995). The shorter variant appears to be expressed largely in the placenta (Lee et al., 1995; Matsuoka et al., 1995).

The p57 gene is paternally imprinted in both mice and humans. Localized to chromosome 11p15.5, p57 is in a region predicted to have a tumor suppressor gene or genes involved in human cancers, such as Wilms' Tumor, and Beckwith-Weidemann syndrome (Hatada et al., 1996; Kondo et al., 1996; Matsuoka et al., 1996). Mice null for p57 have major developmental defects affecting palate, abdomen muscle, intestine, and endochondral bone ossification (Yan et al., 1997; Zhang et al., 1997). p57-null mice also have abnormalities in chrondrocytes, renal medulla, and adrenal cortex with lens cell hypertrophy and apoptosis (Yan et al., 1997; Zhang et al., 1997). While the majority of these mice did not survive postnatal day one, many of these embryonic phenotypes are seen in humans suffering from Beckwith-Weidemann syndrome (Yan et al., 1997). The heterozygous mice with the wild-type p57 allele paternally inherited and the p57 null allele maternally inherited had essentially the same phenotype as the p57 null mice. In mice paternal imprinting is complete, while in humans

imprinting is incomplete (Zhang et al., 1997). The incomplete imprinting is believed to explain why humans with a defective maternal p57 allele develop Beckwith-Wiedemann syndrome rather than die one day postnatally (Zhang et al., 1997).

Diseases such as Wilm's tumor (Reid et al., 1996), Beckwith-Wiedemann syndrome (Hatada et al., 1996), lung cancer (Kondo et al., 1996), and even bladder cancer (Oya and Schulz, 2000) have a high rate of mutation or loss of the p57 maternal allele. Other studies have confirmed earlier results linking p57 function to development and maintenance of muscle, bone, brain, and lens (Dyer and Cepko, 2000; Reynaud et al., 2000; Takahashi et al., 2000; Tsugu et al., 2000; Urano et al., 2000).

Chapter 2
Stoichiometry of Cyclin A-Cdk 2 Inhibition by $p21^{Cip1/Waf1}$

This chapter describes work published in *Biochemistry* (Adkins and Lumb, 2000). Experimental detail and analysis have been expanded beyond those reported in the paper, including sedimentation equilibrium data, and is summarized in Appendix A.

2.0 INTRODUCTION

Cyclin-dependent kinases catalyze regulatory phosphorylation events during cell-cycle progression (Morgan, 1997). Cdk activity is positively regulated by association with cyclins and by phosphorylation at a conserved Thr (Thr 160 in human Cdk2) and negatively regulated by phosphorylation at a Thr or Tyr residue (Thr 14 and Tyr 15 in human Cdk2) (Morgan, 1997). Proteins that inhibit Cdk catalysis are another way Cdk activity can be negatively regulated (Harper and Elledge, 1996; Hengst and Reed, 1998; Sherr and Roberts, 1999). One such Cdk inhibitor is p21 (variously called CAP20, Cip1, Sdi1, and WAF1) (El-Deiry et al., 1993; Gu et al., 1993; Harper et al., 1993; Xiong et al., 1993). p21 has been implicated in a variety of cellular processes associated with cell growth and differentiation, including the p53-mediated G1 checkpoint and certain cancers (Harper and Elledge, 1996; Chellappan et al., 1998; El-Deiry, 1998; Hengst and Reed, 1998; Kiyokawa and Koff, 1998). p21 contains an N-terminal domain that binds cyclin-Cdk complexes and inhibits kinase activity and a C-terminal domain that binds the DNA replication factor PCNA (El-Deiry et al., 1993; Gu et al., 1993; Harper et al., 1993; Xiong et al., 1993; Chen et al., 1995; Warbrick et al., 1995; Chen et al., 1996; Gulbis et al., 1996).

p21 has been found in non-transformed cells and is reported to be a component of active cyclin D-Cdk4 (LaBaer et al., 1997) and cyclin A-Cdk2 complexes (Zhang et al., 1994a; Zhang et al., 1994b; Harper et al., 1995). These observations led to a proposal that p21 binds to cyclin-Cdk complexes

in normal cells without affecting Cdk activity and that p21 inhibition of Cdk activity is effective only when p21 levels are elevated such that multiple p21 molecules are bound to cyclin-Cdk complexes (Zhang et al., 1994a; Zhang et al., 1994b; Harper et al., 1995). It has been suggested that p21 buffering might exert large effects upon Cdk activity by only small changes in p21 levels (Harper et al., 1995) and that p21 may act as an assembly factor for cyclin-Cdk complexes at low stoichiometric amounts and as an inhibitor only when multiple p21 molecules are bound to the cyclin-Cdk complex (Zhang et al., 1994a; LaBaer et al., 1997; Cheng et al., 1999).

A central feature of a "buffer" mechanism of p21 function is that active cyclin-Cdk complexes are usually associated with p21 and that multiple molecules of p21 need to be bound for the Cdk activity to be abolished (Zhang et al., 1994a; Zhang et al., 1994b; Harper et al., 1995). A direct test of a buffering mechanism for p21 inhibition is to monitor Cdk activity as the molar ratio of p21 is changed, which determines directly if a 1:1 or higher ratio of p21 to cyclin-Cdk is required for complete inhibition.

Investigations of stoichiometry in protein complexes or enzyme mechanisms depend critically upon accurate concentration determinations. However, prior studies of Cdk2 inhibition by p21 were executed under conditions under which accurate concentration determinations are difficult (Zhang et al., 1994a; Zhang et al., 1994b; Harper et al., 1995; Cai and Dynlacht, 1998; Hengst et al., 1998). Previous experiments were performed in the undefined

context of cell lysates, immunoprecipitates, or affinity columns, or used problematic dye-binding (Coomassie Blue) assays for the estimation of concentration (Zhang et al., 1994a; Zhang et al., 1994b; Harper et al., 1995; Cai and Dynlacht, 1998; Hengst et al., 1998). In addition, the population of active enzyme was not known. Such conditions preclude firm conclusions regarding the stoichiometry of Cdk2 inhibition by p21, and hence the importance of a buffer mechanism for p21. Indeed, different studies have led to different conclusions regarding the stoichiometry of p21-inhibited cyclin-Cdk complexes (Zhang et al., 1994a; Zhang et al., 1994b; Harper et al., 1995; Cai and Dynlacht, 1998; Hengst et al., 1998). Reports using polyclonal antibodies for p21, cyclin A, Cdk2 for immunoprecipitations and glutathione affinity chromatography with GST-tagged proteins reported that an excess of p21 was required for inhibition (Zhang et al., 1994a; Harper et al., 1995). Among these co-immunoprecipitations and GST pull-downs, other proteins were present including PCNA. In contrast, reports using monoclonal antibodies for p21 and Coomassie blue staining for estimates of concentration found that a 1:1 stoichiometry was sufficient for complete inhibition (Cai and Dynlacht, 1998; Hengst et al., 1998).

The best method to determine protein concentration, and the one used here, is to measure the absorbance of a purified protein stock solution in 6 M GuHCl in the aromatic region of the UV spectrum (Edelhoch, 1967; Gill and von Hippel, 1989; Pace et al., 1995). This method yields protein concentrations with a typical accuracy of 2-5 % (Edelhoch, 1967; Gill and von

Hippel, 1989; Pace et al., 1995). Stoichiometry determinations also require calibration of cyclin A-Cdk2 activity, which we measured using the chemical kinase inhibitor staurosporine. Using proteins of known concentration and calibrated cyclin A-Cdk2, we find that a single bound molecule of p21 effectively inhibits cyclin A-Cdk2.

2.1 METHODS

2.1.a Cyclin A Expression and Purification

Human cyclin A was expressed using the plasmid pET3a-Cyclin A (gift of J. W. Harper; Connell-Crowley et al. 1993). 1 ml of an overnight culture of pET3a-Cyclin A-transformed *Escherichia coli* strain BL21 (DE3) was used per 1 L LB medium culture containing 50 mg/ml ampicillin for inoculation. Six 1 L cultures were incubated at 37 °C with shaking until the optical density at 600 nm was 0.7-0.9. Cooling the exterior of the culture flasks with tap water and light swirling was found to prevent cyclin A from being sequestered to inclusion bodies, as judged by SDS-PAGE using 12 % gels (resolving gel was made with 40 ml 40% Acrylamide/Bis Solution 37.5:1 (BioRad 161-0148), 25 ml 1.5 M Tris-HCl pH 8.8, 1 ml 10 % SDS, 33.5 ml H_2O, 50 µl TEMED, 500 µl 10 % ammonium persulfate and the stacking gel was made with 3.3 ml 40% Acrylamide/Bis Solution 37.5:1 (BioRad 161-01 48), 6.3 ml 0.5 M Tris-HCl pH 6.8, 250 µl 10 % SDS, 15 ml water, 25 µl TEMED, 125 µl 10 % ammonium persulfate) of the soluble and insoluble cell lysate fractions. The cells were then induced with 0.5 mM IPTG at 25 °C for 3 hours.

After induction, the cultures were transferred to 1 L centrifuge bottles and centrifuged at 4.2 krpm in a Beckman JS-4.2 rotor for 30 minutes at 4 °C. The cell pellets were resuspended in 10 ml 20 mM Tris-base, 1 mM EDTA, 20 mM NaCl, 1 mM dithiothreitol (DTT), 5 % glycerol, 1 mM PMSF, pH 7.5 per 1 L cell culture. The resuspended cell pellet was lysed by freezing in liquid nitrogen, thawed, and sonicated on ice 5 times for 15 seconds. The lysate was centrifuged using a Beckman JA-20 rotor at 15 krpm for 25 minutes at 4 °C. The supernatant was dialyzed (SpectraPor MWCO 25 kDa) overnight at 4 °C against 4 L 20 mM Tris-base, 1 mM EDTA, 20 mM NaCl, 1 mM DTT, 5 % glycerol, 1 mM PMSF, pH 7.5.

The dialysate was filtered (0.8 μm) and loaded onto a 40 ml DEAE Fast Flow column (Pharmacia) (3 cm diameter) in 20 mM Tris-base, 1 mM EDTA, 20 mM NaCl, 5 % glycerol, pH 7.5. The column was washed with buffer until the flow-through contaminants were eluted as detected by absorbance at 280 nm. Cyclin A was eluted using a 0-300 mM linear NaCl gradient over 300 ml. Ten ml fractions were collected. Fractions were analyzed by SDS-PAGE using 12 % gels and peak fractions were pooled. Cyclin A eluted from the DEAE column at approximately 180-250 mM NaCl. The pooled fractions were dialyzed (SpectraPor MWCO 25 kDa) overnight at 4 °C against 4 L 20 mM Tris-base, 1 mM EDTA, 20 mM NaCl, 1 mM DTT, 5 % glycerol, 1 mM PMSF, pH 7.5.

The dialysate was loaded onto a 5 ml SP HiTrap column (Pharmacia) in 20 mM Tris-base, 1 mM EDTA, 20 mM NaCl, 5 % glycerol, pH 7.5. The column was washed with buffer until the void volume was eluted, as detected by absorbance at 280 nm. Cyclin A was eluted using a 0-600 mM linear NaCl gradient over 300 ml. Ten ml fractions were collected. Cyclin A eluted from the SP column at approximately 240-300 mM NaCl. Fractions were analyzed by SDS-PAGE using 12 % gels, and peak fractions were pooled. The pooled fractions were divided into 1-ml aliquots in microcentrifuge tubes, frozen with liquid nitrogen, and stored at –70 °C. Yields ranged from 0.7-2 mg/L.

An aliquot of cyclin A was dialyzed (Bio-Tech International, Seattle, WA, dialysis device 920403; 2000 MWCO) against water and lyophilized for analysis by MALDI mass spectrometry. The expected and observed masses agreed to within 1 Da (expected mass 48536.3 Da; observed 48536 Da).

2.1.b Preparation of Mini-cyclin A

Full-length cyclin A was also converted to mini-cyclin A (residues 173-432) with subtilisin (Lees and Harlow, 1993; Jeffrey et al., 1995). Mini-cyclin A is a more soluble form of cyclin A that can be made from a subtilisin digestion of full-length cyclin A. A stock solution of subtilisin (Boehringer Mannheim 165905) was prepared at 1 mg/ml. Full-length cyclin A was digested from 1 ml aliquots with 5-10 μg/ml subtilisin for 15-45 minutes. The digestion was monitored by SDS-PAGE using 16 % gels. No significant difference was

found for the range of digestion conditions studied and all visible (by SDS-PAGE) cyclin A was converted to mini-cyclin A.

The resulting mini-cyclin A was dialysed (SpectraPor MWCO 10 kDa) against 20 mM Tris-base, 1 mM EDTA, 20 mM NaCl, 5 % glycerol, pH 7.5. The dialysate containing mini-cyclin A was loaded onto a 5 ml SP HiTrap (Pharmacia) column in 20 mM Tris-base, 1 mM EDTA, 20 mM NaCl, 5 % glycerol, pH 7.5. The column was washed with buffer until the UV detector read zero. Mini-cyclin A was eluted using a 0-600 mM linear NaCl gradient over 300 ml. Fractions were analyzed by SDS-PAGE using 12 % gels and peak fractions were pooled. The mini-cyclin A was made, dialyzed, and used immediately in sedimentation equilibrium experiments, and therefore no long-term storage scheme was performed or tested. Mini-cyclin A behaved well for analytical ultracentrifugation studies. Mini-cyclin A was not ideal for this study because interactions with p21 may be different when full-length cyclin A is used.

2.1.c PCNA Expression and Purification

Human PCNA was expressed using the plasmid pT7-PCNA (kind gift of B. Stillman; Fien and Stillman, 1992). One ml of an overnight culture of pT7-PCNA transformed *Escherichia coli* strain BL21(DE3) was used for inoculation per 1 L LB medium containing 50 mg/L ampicillin. Four 1-L cultures were incubated at 37 °C until the optical density at 600 nm was approximately 0.7 and then induced with 1 mM IPTG at 37 °C for 3 hours.

The cells were harvested by centrifugation at 4.2 krpm in a Beckman JS-4.2 rotor at 4 °C for 30 minutes. The cell pellets were each resuspended in 10 ml 20 mM Tris-base, 1 mM EDTA, 1 mM DTT, 1 mM PMSF, pH 7.5. The cells were lysed by sonication and centrifuged at 15 krpm using a Beckman JA20 rotor at 4 °C for 25 minutes. The resulting soluble fraction was dialyzed (SpectraPor MWCO 25 kDa) overnight against 10 mM Tris-base, 10 mM NaCl, 1 mM EDTA, 1 mM DTT, 5 % glycerol, pH 7.5 at 4 °C.

The dialysate was loaded onto tandem 5-ml HiTrap SP and Q columns (Pharmacia) pre-equilibrated with 10 mM Tris-base, 10 mM NaCl, 1 mM EDTA, 1 mM DTT, 5 % glycerol, pH 7.5 at 4 °C. The SP and Q columns were washed with buffer until the flow-through contaminants were eluted, as detected by absorbance at 280 nm. The HiTrap SP column was taken out of line; human PCNA does not bind to the SP resin column. The HiTrap Q column was washed with equilibration buffer containing 250 mM NaCl. After washing, PCNA was eluted with a linear gradient of 250–450 mM NaCl over 200 ml. Ten ml fractions were collected. PCNA fractions were identified using SDS-PAGE with 16 % gels (resolving gels were made with 52.8 ml 40% Acrylamide/Bis Solution 37.5:1 (BioRad 161-0148), 25 ml 1.5 M Tris-HCl pH 8.8, 1 ml 10 % SDS, 20.7 ml H_2O, 50 µl TEMED, 500 µl 10 % ammonium persulfate and stacking gels were made as described earlier), pooled, and dialyzed (SpectraPor MWCO 25 kDa) at 4 °C against 20 mM sodium phosphate, 10 % glycerol, 1 mM DTT, pH adjusted to 7.0. Fractions containing PCNA were loaded onto a 4-ml hydroxyapatite Bio-Gel HTP (Bio-

Rad 130-0420) column (15 mm diameter x 30 mm bed height) equilibrated in 20 mM sodium phosphate, 10 % glycerol, 1 mM DTT, pH adjusted to 7.0, and eluted with a linear sodium phosphate, pH 7.0 gradient (20-500 mM) over 200 ml. PCNA started to elute around 150 mM sodium phosphate. Fractions were analyzed using SDS-PAGE with 16 % gels, and peak fractions were pooled. PCNA was dialysed against 10 mM Tris-base, 10 mM NaCl, 1 mM EDTA, 1 mM DTT, 5 % glycerol, pH 7.5 at 4 °C. The pooled fractions were divided into 1-ml aliquots in microcentrifuge tubes, frozen with liquid nitrogen, and stored at –70 °C. Yield was about 1 mg/L. MALDI and electrospray mass spectrometries were unable to measure the mass of PCNA. The PCNA used here was functional for trimerization and p21 binding (see pages 41 and 42).

2.1.d Escherichia coli-expressed Human Cdk2

N-Terminally hemagglutinin A (HA) tagged Cdk2 (pXHA-Cdk2; gift of Dr. J. Wade Harper, Connell-Crowley et al., 1993) and wild-type Cdk2 (using pET-11a-Cdk2 that I made as a PCR product from pXHA-Cdk2) were expressed in *Escherichia coli* strain BL21(DE3). Cultures were grown in a shaking incubator at 37 °C to an optical density at 600 nm of 1.0. The cultures were transferred to 20 °C incubator and induced with 0.5 mM IPTG for about 16 hours. *Escherichia coli*-derived human Cdk2 with and without an HA tag did not consistently bind ATP-agarose and was not functional for histone phosphorylation. Therefore, Cdk2 was prepared using the baculovirus

expression system instead of *Escherichia coli* derived human Cdk2 as described above.

2.1.e Cdk2 Baculovirus Expression and Purification

Human Cdk2 with a C-terminal hemagglutinin A antibody tag (SMAYPYDVPDYASLGPGL) was expressed in baculovirus-infected High Five cells (the virus was a kind gift of D. O. Morgan; Rosenblatt et al., 1993). Infection of High Five cells took place in 70 % confluent adherent 8-ml cultures (Corning Tissue Culture Dish 25020) grown in High Five Serum-Free Medium (Invitrogen B100-01) for 5 days. Expression of Cdk2 in High Five cells was approximately 10-fold greater than in Sf9 cells.

Cells were lysed in 10 ml 20 mM Tris-base, 10 mM NaCl, 1 mM EDTA, 1 mM DTT, 1 mM PMSF, 5 % glycerol, pH adjusted to 7.5, containing 50 mM NaF, 0.5 mM sodium orthovanadate, 8 mM β-glycerophosphate per culture dish. Cdk2 was purified from the soluble fraction of the cell lysate with HiTrap SP and Q columns (Pharmacia) equilibrated in 20 mM Tris-base, 10 mM NaCl, 1 mM EDTA, 1 mM DTT, 5 % glycerol, pH adjusted to 7.5. Cdk2 was present in the SP and Q flowthroughs. Final purification was by affinity chromatography using ATP-agarose (with an 11-atom spacer made up of adipic acid dihydrazide was used; Sigma A-6888) equilibrated in 20 mM Tris-base, 10 mM NaCl, 1 mM EDTA, 1 mM DTT, 5 % glycerol, pH 7.5. Cdk2 was eluted from ATP-agarose using a linear NaCl gradient in buffer. The yield per culture dish ranged from 0.1-0.5 mg. Cdk2 was dialysed against 20

mM Tris-base, 10 mM NaCl, 1 mM EDTA, 1 mM DTT, 5 % glycerol, pH 7.5. Cdk2 was divided into 1-ml aliquots in microcentrifuge tubes, frozen with liquid nitrogen, and stored at –70 °C.

The primary sequence of Cdk2 was analyzed for proteinase cleavage sites using the program PeptideMass (http://www.expasy.ch/tools/peptide-mass.html). Glu-C was determined to be the most useful for determining the phosphorylation state of Cdk2. Therefore, Cdk2 was digested by Glu-C. To prepare for proteinase digestion, Cdk2 (1 mg) was dialyzed against H_2O, lyophilized, resuspended in 20 µl acetonitrile and brought to a total volume of 200 µl with 25 mM ammonium carbonate pH 7.8. Endoproteinase Glu-C (Boehringer Mannheim 1420399) was added at a Glu-C:Cdk2 molar ratio of approximately 1:50 for 6 hours at room temperature. The proteinase reaction mixture was lyophilized and analyzed by MALDI-TOF mass spectrometry with a PerCeptive-Biosystems Voyager DE Pro by Dr. Phillip W. Ryan (Colorado State University's Macromolecular Resources Facility). The matrix used was α-cyano-hydroxycinnamic acid.

Viable viral expansions would not occur in High Five cells. Therefore Sf9 cells grown in Grace's Supplemented Medium (GibcoBRL 11605-094) were used for viral expansions. The optimal volume of virus for expression was determined empirically by testing a range of volumes from 10 µl to 1 ml per 8 ml culture. Typically, peak expression was found using 100 µl of expanded

viral stock. Viral stock was stable at 4 °C in a Grace's Medium supernatant of centrifuged infected Sf9 cells for at least 9 months.

2.1.f p21 Expression and Purification

Human p21 was expressed using the plasmid pET3a-p21 (gift of J. W. Harper; Harper et al., 1993). One ml of overnight culture was diluted into 1 L of LB medium containing 50 mg/L ampicillin. The 1 L culture was incubated for 24 hours at 37 °C; induction with IPTG was not necessary. The cell culture was centrifuged in the Beckman JS-4.2 rotor for 30 minutes at 4.2 krpm and 4 °C. The cell pellet was resuspended in 20 ml 20 mM Tris-base, 1 mM EDTA, pH7.5. The cells were lysed by sonication five times for 15 seconds. The lysate was centrifuged using a Beckman JA20 rotor centrifuged for 30 minutes at 15 krpm, 4 °C.

The resulting pellet was resuspended by sonication in 20 ml of 6 M urea, 20 mM Tris-base, 1 mM EDTA, 1 mM DTT, 1 mM PMSF, pH 7.5. The resuspended insoluble fraction was centrifuged at 15 krpm and 4 °C for 10 minutes. The supernatant for the insoluble fraction was loaded onto a 10-ml DEAE Fast Flow (Pharmacia) (1.5 cm diameter) in 4 M urea, 20 mM Tris-base, 1 mM EDTA, 1 mM DTT, pH 7.5. The flow-through and five volumes of buffer were collected and loaded onto a SP HiTrap column pre-equilibrated in the same buffer. The column was washed with buffer until the flow-through contaminants were eluted, as detected by absorbance at 280 nm. p21 was eluted with the same buffer with a linear gradient of 0-1 M NaCl over 200 ml

collected in 10-ml fractions. Peak fractions were determined by SDS-PAGE using 16 % gels. Peak fractions were pooled and dialyzed (SpectraPor MWCO 2 kDa) against 4 L of 5 % (v/v) acetic acid.

Final p21 purification was by reversed-phase C_4 HPLC using linear 0.1 %/minute acetonitrile/water gradients containing 0.1 % TFA. p21 was stored as a lyophilized powder and yields ranged from 5-10 mg/L. Expected and observed masses from electrospray mass spectrometry agreed to within 0.02 % (expected mass, with Met 1 processing and no post-translational modifications 17987.8 Da; observed 17991.8 Da).

2.1.g Manual Synthesis of the p21 PCNA Binding Domain

A peptide corresponding to the PCNA-binding domain of human p21 (residues 137-163) was synthesized using manual solid-phase Boc chemistry at the 0.25 mmol scale (Schnolzer et al., 1992).

0.373 g MBHA resin was swelled in 10 ml DMF for 10 minutes. 0.359 g HBTU and 1 mmol of the first C-terminal amino acid (Boc-lysine; 0.415 g) were mixed with 2.5 ml DMF and 0.3 ml DIEA in a test tube. The mixture was sonicated until clear. After two minutes, the resin and amino acid solution were mixed with shaking in a peptide reaction vessel for 40 minutes for the first amino acid and 12 minutes for subsequent amino acids. The resin was rinsed with 5 x 10 ml aliquots of DMF. Coupling was confirmed with the Kaiser ninhydrin test (Kaiser et al., 1970) or chloranil test for proline

(Christensen, 1979). If the test was positive, coupling of the same amino acid was repeated. If the test was negative then the Boc group was removed with TFA (2 rounds of 6 ml TFA for 2 minutes in duplicate), and the next round of coupling would begin.

The single His(DNP) residue was deprotected in the fume hood with approximately 5 ml thiophenol (strong stench) and rinsed with approximately 200 ml DMF, until the residual stench was largely absent. The resin was sequentially rinsed with 50 ml CH_2Cl_2, 50 ml diethyl ether, and 50 ml methanol. The resin was desiccated under vacuum overnight to remove residual solvents. The peptide was cleaved from the resin by HF cleavage in an HF reaction apparatus (Stewart and Young, 1984) in an HF-approved fume hood using 10 ml HF per g of dried resin and 1 ml anisole per g of dried resin. The resin was resuspended with diethyl ether and placed in a fritted glass funnel equipped with an aspirator side arm flask. The resin-peptide mixture under gentle vacuum was dried to a sandy consistency. The peptide was eluted from the resin with 5 % (v/v) acetic acid in water solution. Elution continued until the filtered liquid was no longer foaming, indicating all the peptide had eluted. The eluted peptide fraction was lyophilized.

Purification was by reversed-phase C_{18} HPLC using a linear 0.1 %/minute acetonitrile/water gradient containing 0.1% TFA and the peptide eluted at approximately 22 % acetonitrile. The peptide was stored as a lyophilized powder with a yield of approximately 100 mg. The identity of the peptide was

confirmed with MALDI mass spectrometry (expected mass 3398.9 Da; observed 3398.4 Da).

2.1.h Staurosporine

Staurosporine (listed as >98% pure by HPLC; Sigma S4400) was used as supplied. The concentration of the staurosporine stock solution was determined with NMR spectroscopy. Equal volumes of solutions of staurosporine in methanol and tyrosine in water were mixed and analyzed by ^{1}H NMR spectroscopy. The concentration of the tyrosine stock solution was determined on a 40 µl aliquot dissolved in 800 µl of 6 M GuHCl with an absorbance of 0.245 at 276 nm using an extinction coefficient of 1450 M^{-1} cm^{-1} at 25 °C (Edelhoch, 1967). 1D ^{1}H NMR spectra were collected with a Varian Unity Inova spectrometer operating at 400.1 MHz for ^{1}H. A recycle delay of 10 s was used. The staurosporine resonance at 9.25 ppm was set to an intensity of two based on the total integral of the ^{1}H spectrum of staurosporine. The intensities of the Tyr H^{δ} and H^{ε} resonances were then measured by integration to obtain the molar ratio of staurosporine to tyrosine, and hence the concentration of the staurosporine stock solution.

2.1.i Concentration Determinations

Concentrations of protein stock solutions were determined by absorbance at 280 nm 25 °C with a Beckman DU640 spectrometer. Spectra were recorded of aliquots from stock solutions dissolved in 6 M guanidine-HCl, 10 mM sodium phosphate, pH 6.5 (Edelhoch, 1967). Guanidine-HCl concentrations

were determined by refractive index versus 10 mM sodium phosphate, pH 6.5 (Pace, 1986). Extinction coefficients at 280 nm of 38,830, 13,940, 14,650 and 35,560 M^{-1} cm^{-1} for cyclin A, p21, PCNA and Cdk2, respectively, were used (Edelhoch, 1967). Protein solutions were sufficiently concentrated that the absorbance at 280 nm was in the range 0.1 to 0.4. Absorbance above 325 nm was negligible (<0.02), and so spectra were not corrected for light scattering (Figure 2.2).

2.1.j Kinase Assays

Cyclin A-Cdk2 activity was assayed by quantifying histone H1 phosphorylation (modified from Connell-Crowley et al., 1993). Assays were performed at pH 7.5 in 25 mM HEPES, 50 mM NaCl, 5 mM $MgCl_2$. Reactions contained 10 μg calf thymus histone H1 (Gibco BRL 13221-015) as determined by absorbance using an extinction coefficient at 280 nm of 3840 M^{-1} cm^{-1} in 6 M GuHCl (Edelhoch, 1967; Pace, 1986), 2.5 μCi [γ-^{33}P] adenosine triphosphate, 250 nM cyclin A-Cdk2 and the indicated quantities of staurosporine, p21 and PCNA. The phosphorylation reaction was incubated for 20 minutes at 30 °C, analyzed with denaturing (SDS) polyacrylamide gel electrophoresis, and the extent of histone H1 phosphorylation quantified with a Molecular Dynamics PhosphorImager. Reactions were performed at least three times with reproducible results.

2.1.k Sedimentation Equilibrium of PCNA and the p21 PCNA-Binding Domain

Sedimentation equilibrium was performed at 5 °C with a Beckman XL-I analytical ultracentrifuge. PCNA and PCNA with an equimolar quantity of the p21 PCNA-binding domain alone were dialyzed overnight at 4 °C against the reference buffer (20 mM Tris, 150 mM NaCl, pH 7.5). Initial loading concentrations in the range 17-42 μM were used. Data were collected at 15, 20, and 22.5 krpm using 12 mm pathlength six-sector centerpieces and an An-60Ti rotor. Data were analyzed with ORIGIN (Beckman Instruments). The data were accounted for by an ideal single species model, based on the random distribution of residuals (Figures 2.2 and 2.3). A solvent density of 1.01 g/ml and partial molar volumes of 0.738 and 0.737 for PCNA and PCNA with the p21 PCNA-binding domain respectively were calculated as described elsewhere (Laue et al., 1992).

2.2 RESULTS

2.2.a Protein Characterization

Denaturing (SDS) polyacrylamide gel electrophoresis analysis indicates the cyclin A, Cdk2, p21 and PCNA, used for this study, are essentially free of contaminating proteins (Figure 2.1). In particular, Cdk2 is free of any potential Cdk inhibitors derived from the insect-cell expression system. UV absorbance spectra do not exhibit significant light scattering at 360 nm (Figure 2.2).

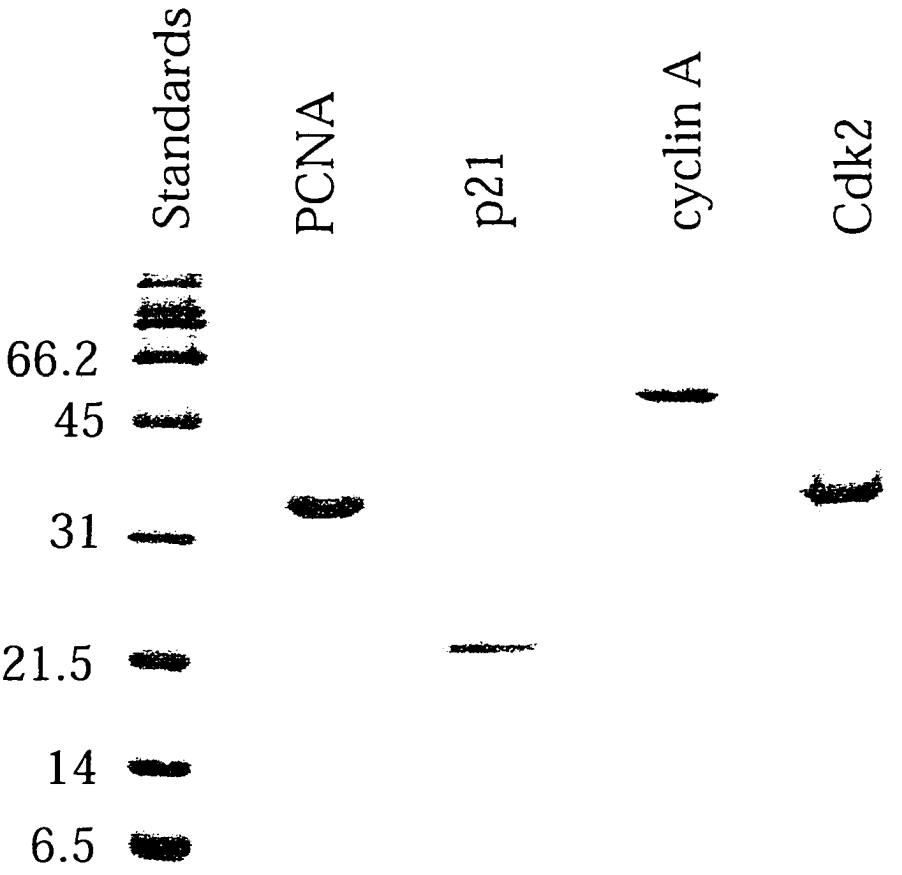

Figure 2.1. SDS-PAGE of PCNA, p21, cyclin A, and Cdk2
Denaturing (SDS) polyacrylamide gel stained with Coomassie-blue showing the purity of PCNA, p21, cyclin A and Cdk2 with approximately 5-10 μg of protein loaded per gel. The first lane contains molecular mass standards labeled in kDa. Some minor contaminants are present.

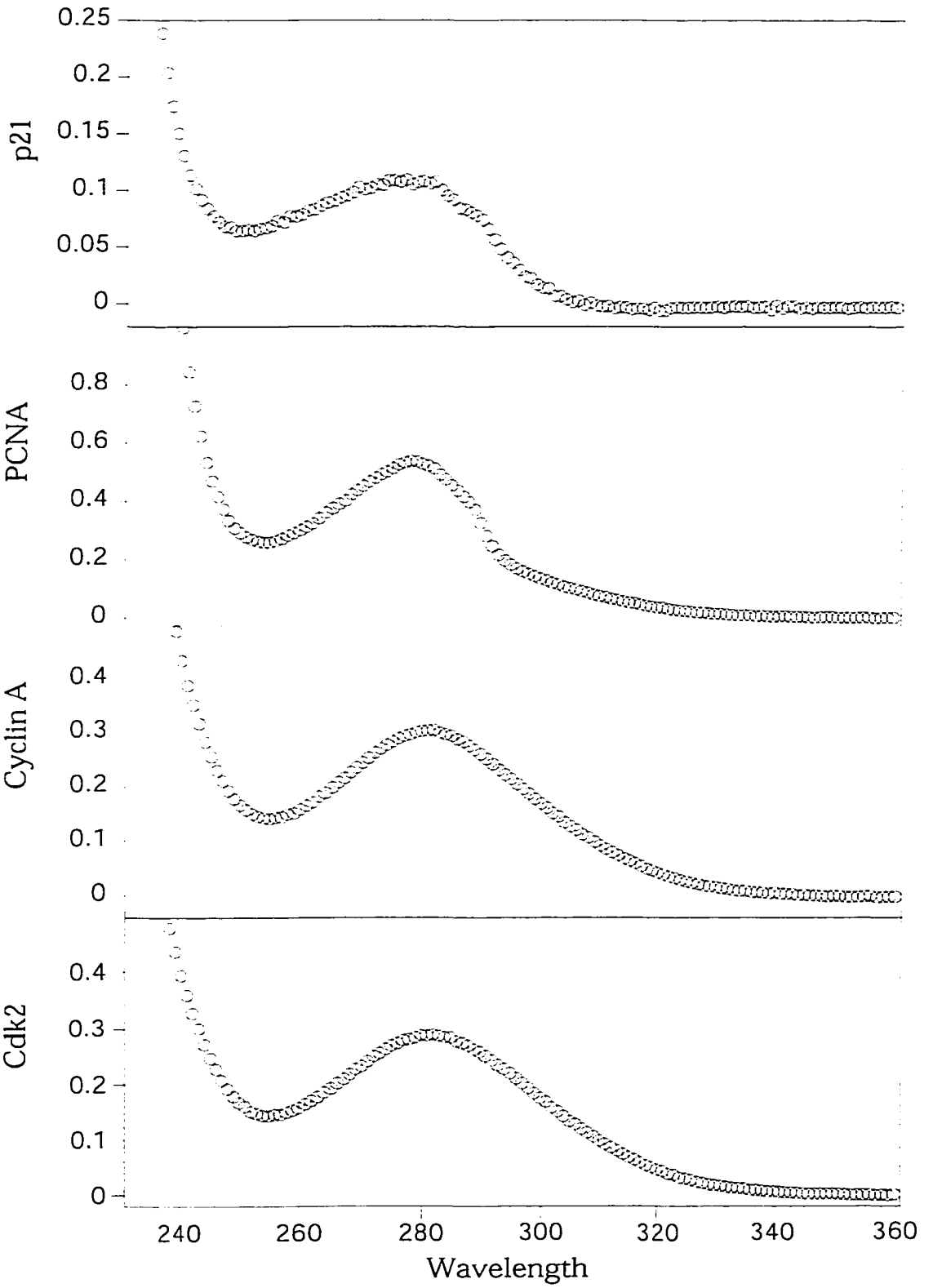

Figure 2.2. Absorbance spectra of p21, PCNA, cyclin A, Cdk2
Concentrations of p21, PCNA, cyclin A, and Cdk2 were determined by absorbance in denaturing conditions (Edelhoch, 1967).

The PCNA used here forms a trimer as shown by sedimentation equilibrium (expected molecular mass of the PCNA trimer 86.3 kDa; observed 84.4±2 kDa), as expected if correctly folded (Gulbis et al., 1996) (Figure 2.3). The PCNA trimer is functional for binding three molecules of a peptide corresponding to the PCNA-binding domain of human p21 (residues 137-163), as shown by sedimentation equilibrium (expected molecular mass of the trimeric PCNA-p21 peptide complex 96.5 kDa; observed 92.8±2 kDa) (Figure 2.4).

The phosphorylation state of Cdk2 was determined by MALDI mass spectrometry analysis of the protease products generated by Glu-C. If Thr14 and Tyr15 were not phosphorylated, then a peptide product of mass 1755.9 Da, corresponding to residues 13-28 would be expected. If Thr160 was not phosphorylated, then a peptide product of mass 2589.4 Da, corresponding to residues 139-162, would be expected. Phosphorylation would increase the expected masses by 77.96 Da per phosphate group. Peptides of masses 1757 and 2591 Da were observed, indicating that the Cdk2 was not phosphorylated at any of the potential sites. In addition, the observation of these (and other) Glu-C digest products confirms the identity of Cdk2 (Table 2.1).

2.2.b Analytical Ultracentrifugation

The technique originally used to study the stoichiometry of the p21-inhibited cyclin A-Cdk2 complex was analytical ultracentrifugation. The resulting data

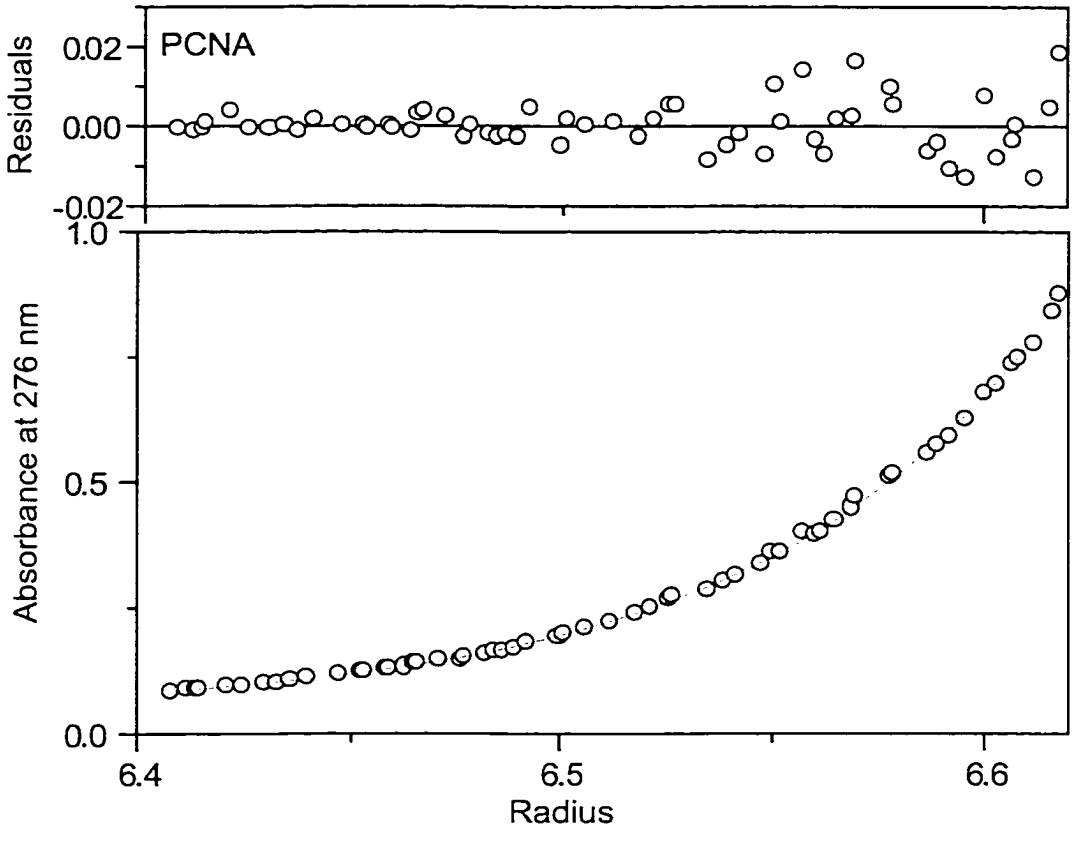

Figure 2.3. Sedimentation Equilibrium of PCNA
Sedimentation equilibrium analysis of PCNA. The data shown are from 25 μM concentration and an angular velocity of 20 krpm with a variance of 3.53.

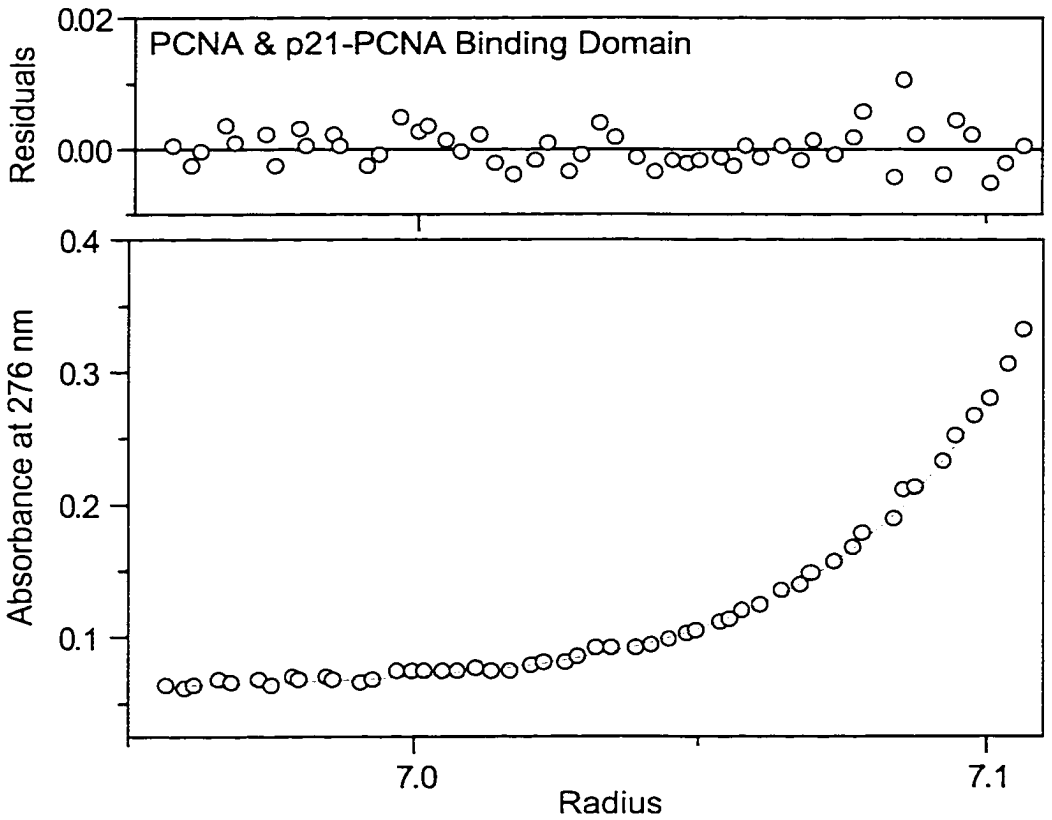

Figure 2.4. Sedimentation Equilibrium of PCNA with the p21-PCNA Binding Domain

Sedimentation equilibrium analysis of PCNA with the p21-PCNA binding domain in equimolar ratio. The data shown are from the 17 μM concentration and an angular velocity of 20 krpm with a variance of 1.01.

is summarized in Appendix A. Full-length p21, p57, and cyclin A all aggregated during ultracentrifugation. This aggregation occurred when centrifuged alone and with other proteins in the complex, indicating that this not a satisfactory method for studying these complexes.

Residues	Expected Mass (Da)	Measured Mass (Da)
82-138	6581.583	6583.84
258-316	6564.375	6570.38
139-162	2589.394	2591.27
58-73	1855.044	1853.2
13-28	1755.939	1757.65
29-40	1384.852	1386.06
163-172	1233.663	1230.85
74-81	1025.567	1016.71
43-51	929.505	930.298
74-138	7588.132	7585.98
209-257	5704.930	5665.23
13-40	3121.773	3123.13
58-81	2861.592	2872.24
52-73	2538.465	2526.72
29-42	1614.942	1616.35
43-57	1612.927	1616.35
3-12	1191.637	1192.47
29-51	2525.430	2527.84
13-51	4262.351	4264.85

Table 2.1. MALDI Mass Spectrometry for Glu-C Digestion of Cdk2

Peaks of molecular masses below 1000 Da were ignored; therefore some residues were detected via incomplete digestion products ranging from 1 to 3 missed cleavages.

Reed and co-workers reported similar sedimentation experiments to those we were attempting (Hengst et al., 1998). Their results suggested that p21 binds to cyclin A-Cdk2 in a 1:1 manner. These published results were consistent with the sedimentation equilibrium studies described here, yet our data (and arguably that of Hengst et al.) were too ambiguous to publish. Our data showed that, at relatively low angular velocity (20 krpm), p21 appeared monomeric (observed molecular mass approximately 22600 Da; expected molecular mass 18119 Da). Increasing the angular velocity (25-40 krpm) would decrease the observed molecular mass and decrease the apparent total protein concentration in the cell. At low angular velocity (6 krpm) cyclin A-Cdk2-p21 exhibited an apparent stoichiometry of 1:1 was present, with residuals suggestive of aggregation. At lower concentrations but higher angular velocities (8 and 10 krpm), the apparent mass continued to increase towards apparent p21:cyclin A-Cdk2 stoichiometries in excess of 3:1, with residuals suggesting aggregation. These results strongly suggested that aggregation was occurring. Contrary to standard practice with sedimentation equilibrium experiments, Hengst et al. (1998) published no buffer conditions, only one loading concentration, and a single unusually low angular velocity of 17 krpm for p21, 10 krpm for cyclin A-Cdk2, and 9 krpm for p21-cyclin A-Cdk2. Thus, the results are not conclusive. Therefore, activity assays above the K_d for binding of p21 with cyclin A-Cdk2 were used instead.

2.2.c Cyclin A-Cdk2 activity

It is important to know the activity of cyclin A-Cdk2 and how stable that activity is over time, since the apparent stoichiometry of inhibition by p21 will depend on the fraction of active complexes. The cyclin A and Cdk2 used here form a complex, since the two proteins co-elute as the complex from HiTrap SP at a lower ionic strength than either cyclin A or Cdk2 alone. To quantify the degree of cyclin A and Cdk2 association under conditions of the histone H1 phosphorylation assays, kinase activity was measured as the mole fractions of cyclin A and Cdk2 were varied. Cdk2 exhibits increased activity when bound to cyclin A in a 1:1 complex. Therefore, an equimolar solution of cyclin A and Cdk2 will exhibit maximal activity only if both proteins are (equally) active for forming a 1:1 functional complex. In contrast, maximal activity will be seen at an unequal molar ratio if either cyclin A or Cdk2 are only partially viable for formation of a functional complex due to, for example, protein misfolding. Co-purifying enzymes that phosphorylate histone H1 are essentially absent, since cyclin A alone or Cdk2 alone do not exhibit histone H1 kinase activity (Figure 2.5). We find that, for our cyclin A and Cdk2 preparations, the extent of histone H1 phosphorylation is maximal when Cdk2 and cyclin A are present in equimolar ratios (Figure 2.5). This result indicates that the Cdk2 and cyclin A used here are essentially equally functional for formation of the cyclin A-Cdk2 complex.

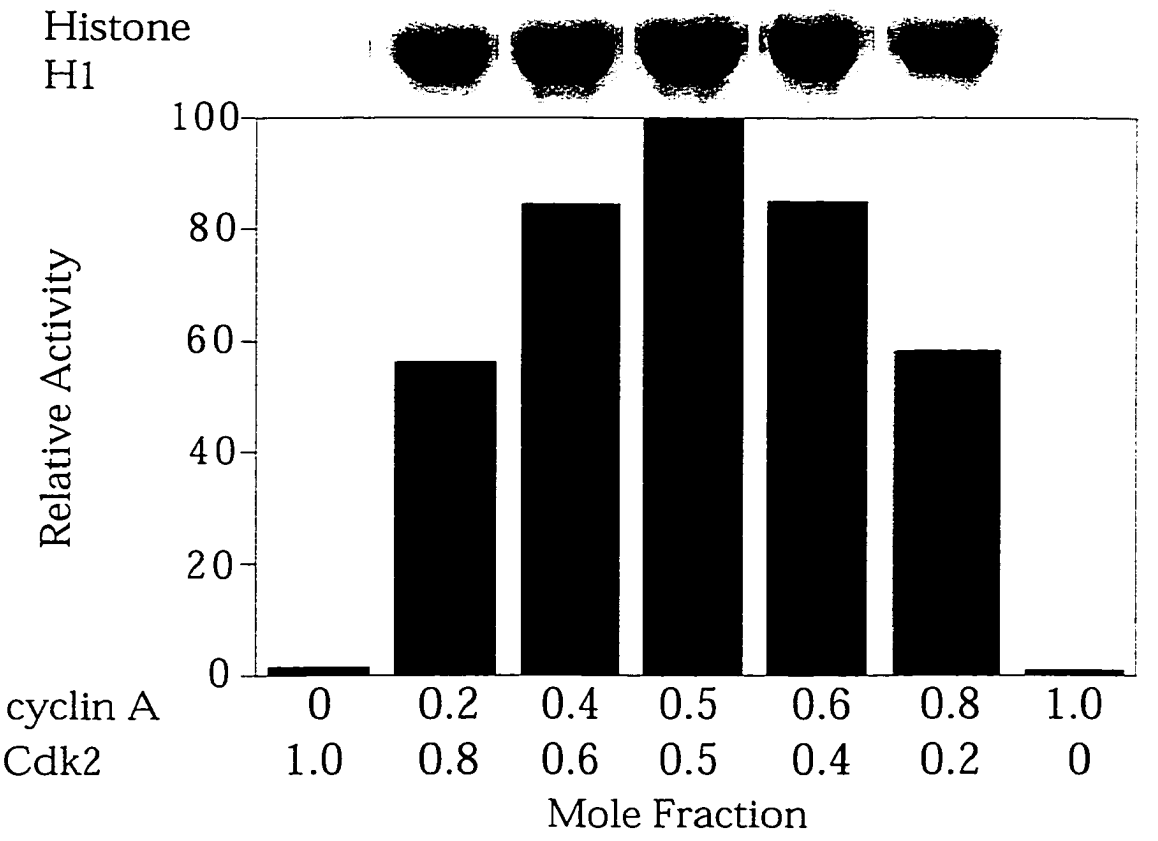

Figure 2.5. Plot of Cyclin A-Cdk2 Activity
Cyclin A and Cdk2 exhibit maximal activity when mixed in an equimolar ratio, indicating that the cyclin A and Cdk2 are equally functional for formation of a 1:1 complex. Neither cyclin A alone nor Cdk2 alone exhibit measurable phosphorylation activity. Due to either product inhibition or substrate depletion the activities do not directly correspond to percentage of active enzyme.

The activity of cyclin A-Cdk2 over time and at differing concentrations is also an important factor in determining the apparent stoichiometry of p21 inhibition. To determine activity over time, Selwyn's test of enzyme inactivation was performed (Selwyn, 1965). This test follows the extent of a reaction as a function of product (F(*p*)) versus specific initial total enzyme concentrations (e_0) with time (t):

$$e_0t = F(p)$$

Cyclin A-Cdk2 concentrations of 250, 125, and 62.5 nM were tested at relative times equal to an e_0t of 15, 30, and 60 minutes for 250 nM with an e_0t point for 62.5 μM of 7.5 minutes relative to 250 nM. Data sets were normalized to the earliest e_0t for each experiment, 250 and 125 μM normalized to 100 % at 15 minutes relative to 250 nM and 62.5 was normalized to 50 % at 7.5 minutes relative to 250 nM (Figure 2.6). The results suggest that cyclin A-Cdk2 activity was essentially equivalent at least 8 hours at 62.5 nM, 4 hours at 125 nM, and 2 hours at 250 nM.

The data shown in Figure 2.5 indicate that cyclin A and Cdk2 are equally active for assembly, but do not establish that the cyclin A-Cdk2 used here is fully active as a kinase. Therefore, cyclin A-Cdk2 activity was calibrated with staurosporine (Figure 2.7A). Staurosporine is a potent kinase inhibitor (IC_{50} is in the low nanomolar range) that binds cyclin A-Cdk2 (Lawrie et al., 1997). The crystal structure of the cyclin A-Cdk2-staurosporine complex shows that staurosporine binds Cdk2 in the ATP binding site with a 1:1 stoichiometry (Lawrie et al., 1997).

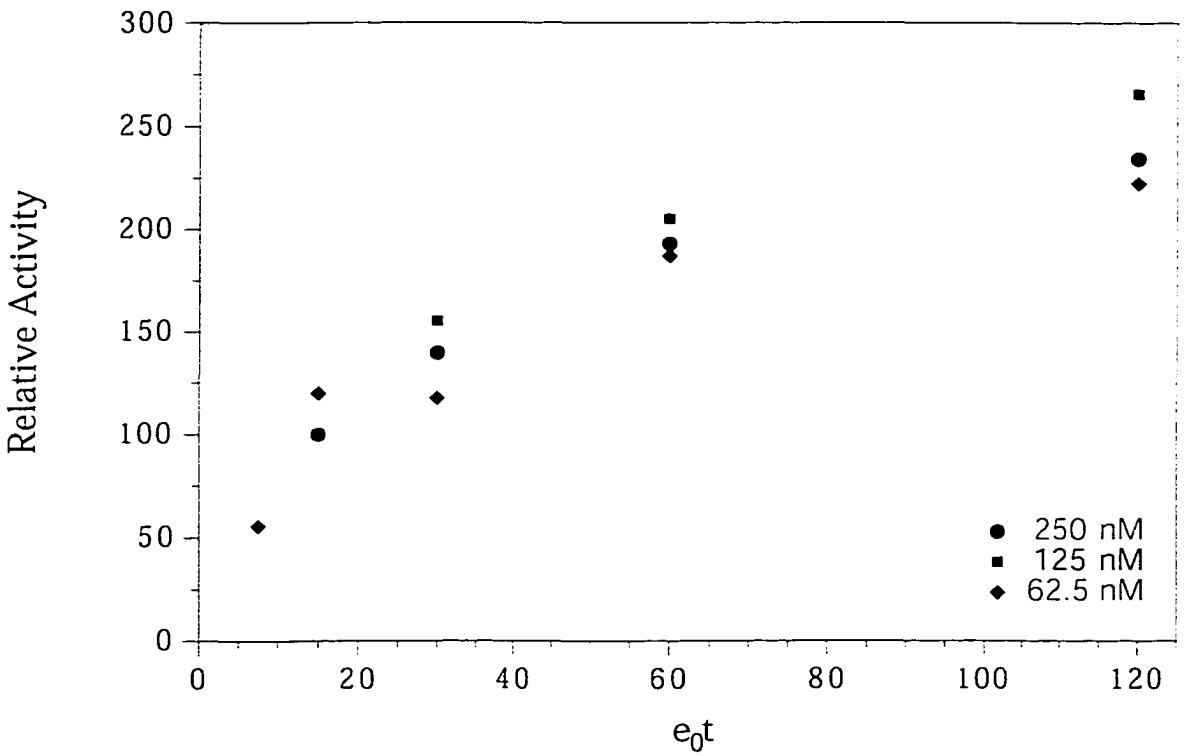

Figure 2.6. Selwyn's Test of Enzyme Inactivation
Cyclin A-Cdk2 concentrations of 250 nM and 125 nM were normalized to 100 % at a relative e_0t of 15 minutes and 62.5 nM was normalized to 50% at e_0t of 7.5 minutes.

A

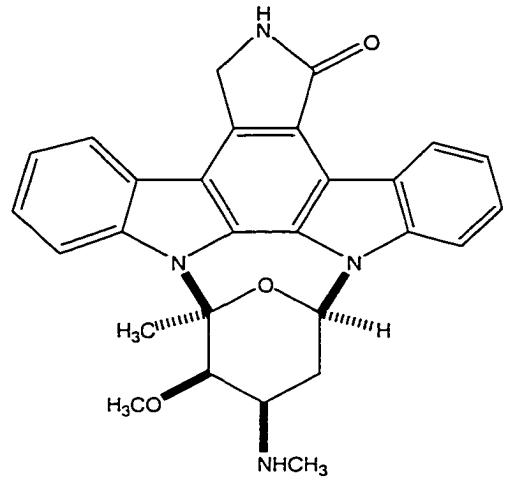

B

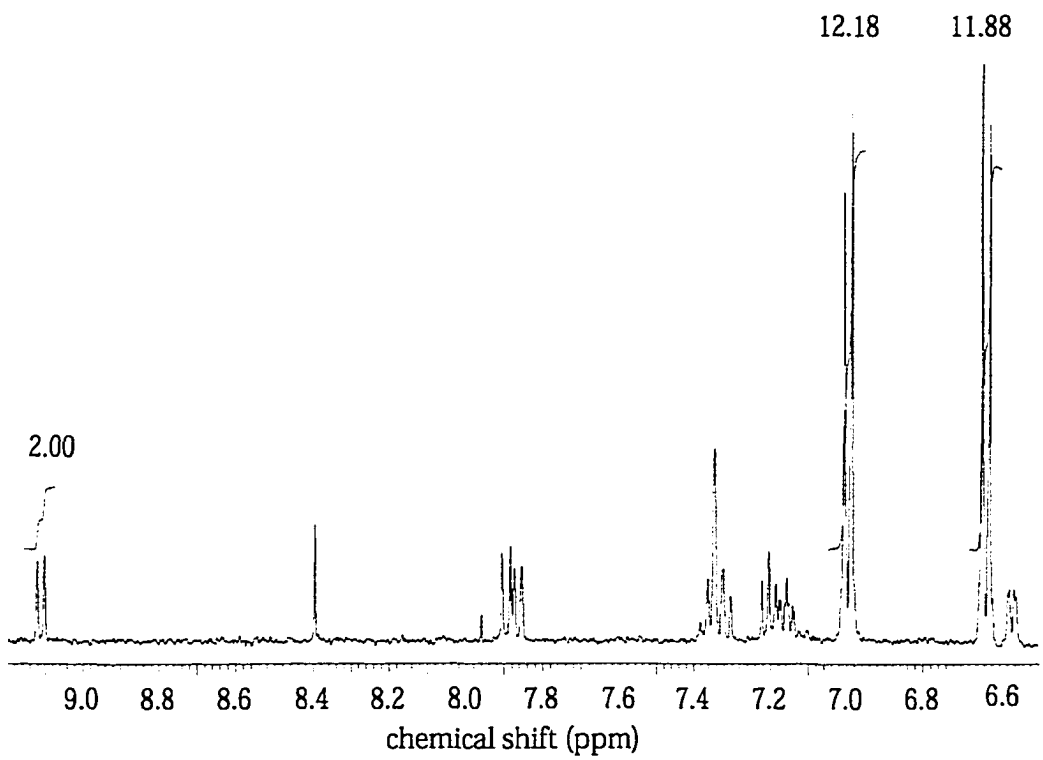

Figure 2.7. Staurosporine Structure & Concentration Determination
A. Staurosporine structure as determined by crystallography (Furusaki et al., 1982).
B. Region of the 400 mHz one-dimensional ^1H NMR spectrum used to determine the concentration of the staurosporine stock solution. Comparison of the integrated intensity of the staurosporine resonance at 9.25 ppm with the integrated intensities of the H^{δ} and H^{ε} resonances of tyrosine of known concentration yields the staurosporine concentration.

If cyclin A-Cdk2 were partially active, then staurosporine would fully inhibit cyclin A-Cdk2 at molar ratios of staurosporine to cyclin A-Cdk2 of less than one at the concentrations used here. This approach assumes that the staurosporine is essentially fully active as a Cdk2 inhibitor, which is reasonable given the chemical nature of staurosporine and that bind tightly to cyclin A-Cdk2 (Figure 2.7A). Staurosporine concentration was determined with NMR spectroscopy (Figure 2.7B). This "single-point" measurement yields an apparent extinction coefficient at 292 nm for staurosporine in methanol of 3.1 x 10^3 M^{-1} cm^{-1}. Cyclin A-Cdk2 activity was monitored in the presence of staurosporine at known molar ratios (Figure 2.8). The activity of cyclin A-Cdk2 decreased with added staurosporine concentration until the molar ratio of staurosporine to cyclin A-Cdk2 was 1:1 (Figure 2.8). This result indicates that the cyclin A-Cdk2 complex is approximately 90% active for histone H1 phosphorylation.

2.2.d Cyclin A-Cdk2 Inhibition by p21

The extent of histone H1 phosphorylation by cyclin A-Cdk2 was measured as the molar ratio of p21 to cyclin A-Cdk2 was varied from 0.1 to 4 (Figure 2.9A). The activity of cyclin A-Cdk2 is reduced by approximately 90 % at a 1:1 molar ratio (Figure 2.9A). This result was independent of the order of addition of the three proteins (Figure 2.9B). Thus, p21 inhibits the cyclin A-Cdk2 complex with a 1:1 stoichiometry. Because cyclin A-Cdk2 is approximately 90 % active (Figure 2.8), the inhibition stoichiometry of 1:1

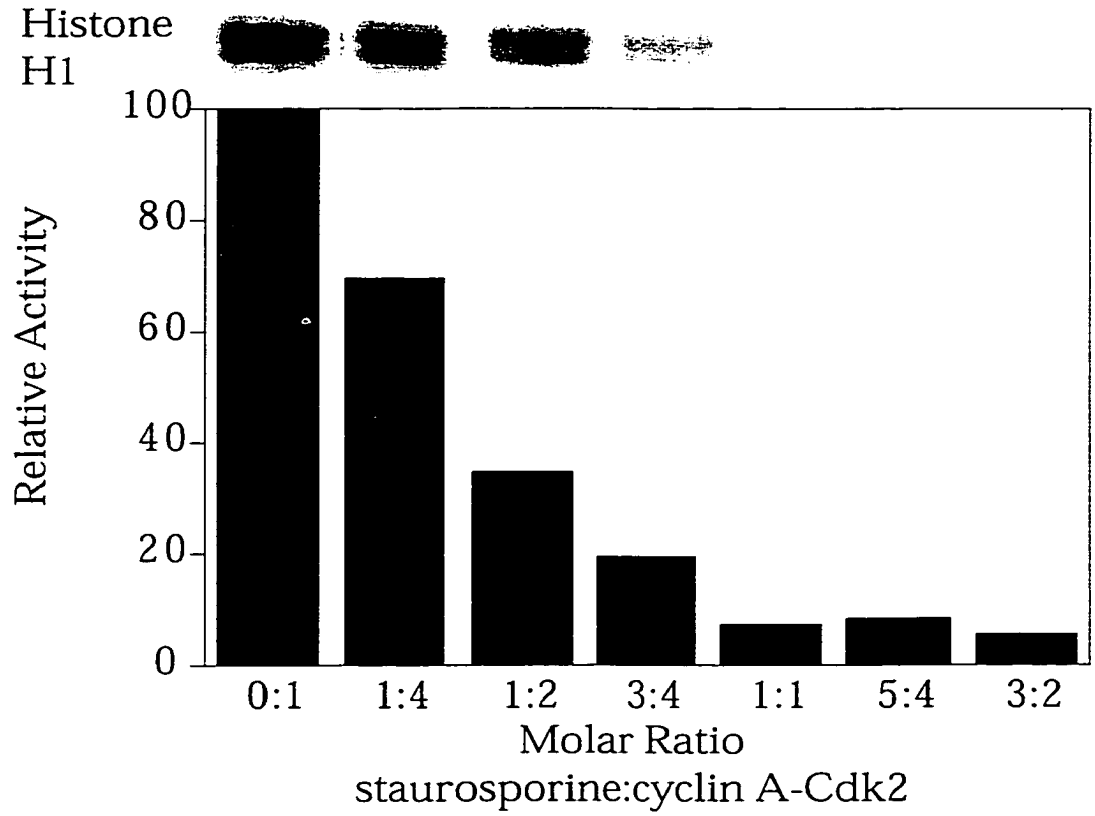

Figure 2.8. Cyclin A-Cdk2 Inhibition by Staurosporine
The decrease in cyclin A-Cdk2 activity with the increasing molar ratio of staurosporine (IC_{50} is in the low nm range) indicates that cyclin A-Cdk2 is approximately 90% active.

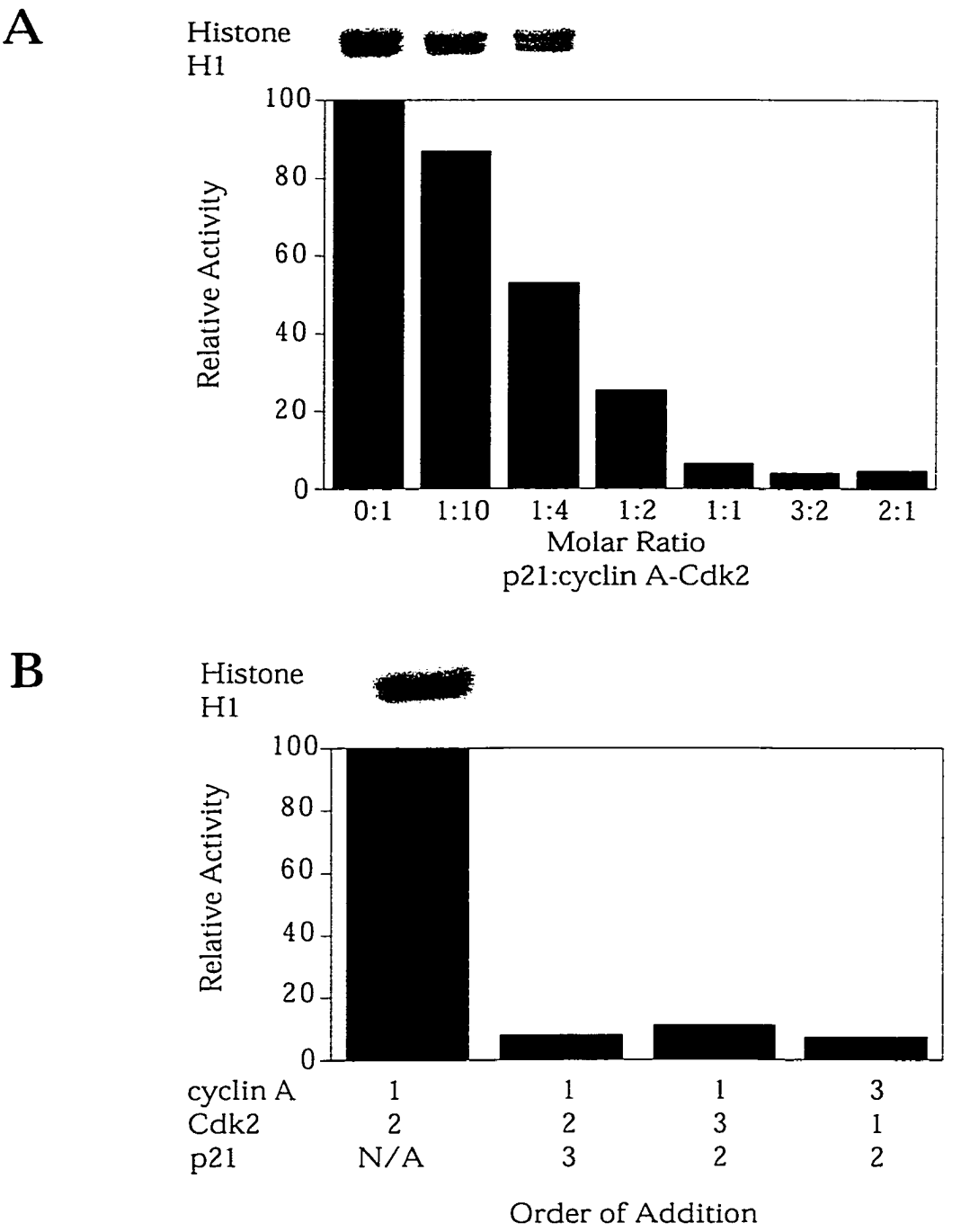

Figure 2.9. p21 Inhibition of Cyclin A-Cdk2

A. Cyclin A-Cdk2 inhibition by p21. The decrease in cyclin A-Cdk2 activity with the increasing molar ratio of p21 indicates that cyclin A-Cdk2 is effectively inhibited by an equimolar ratio of p21.

B. Inhibition of cyclin A-Cdk2 by p21 is unaffected by the order of addition of the proteins.

does reflect a different true stoichiometry, that was not the resulting of cyclin A-Cdk2 being partially active. We note that if p21 were substantially inactive, then the apparent stoichiometry would exceed 1:1.

2.2.e Effects of PCNA

Cyclin-Cdk complexes, including cyclin A-Cdk2, are associated with PCNA *in vivo*. PCNA does not affect phosphorylation of histone H1 by cyclin A-Cdk2 (Figure 2.10A). PCNA exists as a trimer, and each subunit is able to bind a peptide derived from p21 (Figures 2.3 and 2.4). It is conceivable that PCNA associated with cyclin-Cdk complexes has the potential to sequester p21 and so moderate Cdk inhibition by p21. However, titration of an equimolar solution of p21 and cyclin A-Cdk2 with PCNA did not relieve inhibition of the Cdk2 activity (Figure 2.10B). The order of addition of the proteins did not modify this result (Figure 2.10C). Thus, PCNA does not moderate the inhibitory effect of p21 on cyclin A-Cdk2.

2.3 DISCUSSION

Cell-cycle progression is regulated in part by the catalytic activity of cyclin-dependent kinases (Morgan, 1997). In turn, Cdk activity must be tightly regulated to ensure orderly cell division and growth. One mechanism for negatively controlling Cdk activity is provided by p21. p21 inhibits Cdk activity, and p21 overexpression results in cell-cycle arrest (El-Deiry et al., 1993; Gu et al., 1993; Harper et al., 1993; Xiong et al., 1993).

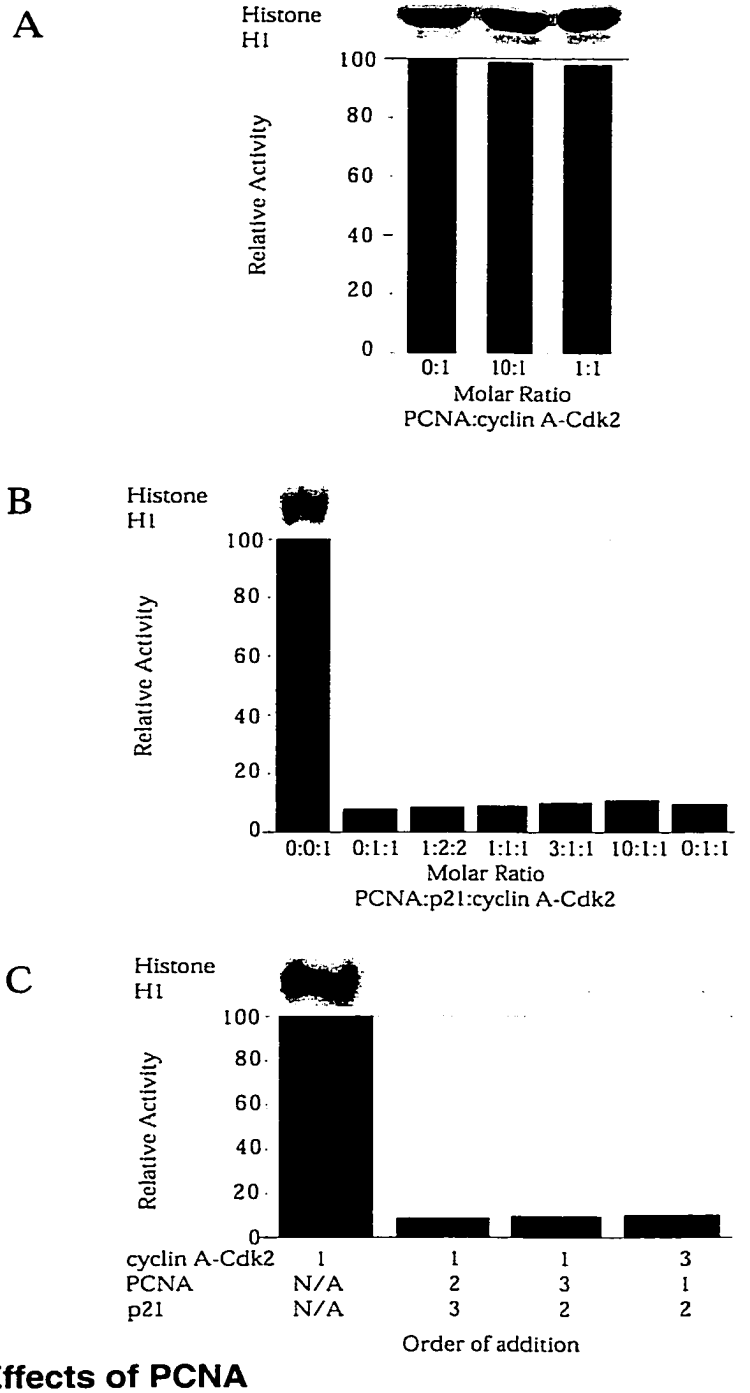

Figure 2.10. Effects of PCNA

A. Addition of PCNA does not moderate cyclin A-Cdk2 activity.

B. Addition of PCNA does not moderate cyclin A-Cdk2 inhibition by p21.

C. The negligible effect of PCNA on p21 inhibition of cyclin A-Cdk2 is unaffected by the order of addition of the proteins.

One proposal for the mechanism of Cdk2 inhibition by p21 is that p21-containing cyclin A-Cdk2 complexes are active, and that kinase activity is inhibited only when multiple molecules are bound to cyclin A-Cdk2 (Zhang et al., 1994a; Zhang et al., 1994b; Harper et al., 1995). It has been suggested that a requirement for inhibition by multiple p21 molecules would result in a buffer mechanism for p21 in which Cdk activity is sensitive to small changes in p21 levels (Harper et al., 1995). Alternatively, it has been suggested that p21 may play a positive role in Cdk activation by acting as an assembly factor for cyclin-Cdk complexes at low stoichiometric ratios and only as an inhibitor at high stoichiometric ratios (Zhang et al., 1994a; LaBaer et al., 1997; Cheng et al., 1999).

The requirement for multiple p21 molecules for Cdk inhibition can be evaluated directly by determining the stoichiometry of the inhibited cyclin-Cdk-p21 complex. Prior determinations of the stoichiometry of p21 inhibition of cyclin A-Cdk2 are, however, somewhat uncertain since neither protein concentrations nor activity were known with accuracy (Zhang et al., 1994a; Zhang et al., 1994b; Harper et al., 1995; Cai and Dynlacht, 1998; Hengst et al., 1998). Here, using purified, full-length proteins, we find that cyclin A-Cdk2 complexes of known concentration that have been calibrated for activity are inhibited effectively by a single p21 molecule. Moreover, the same stoichiometry is observed in the presence of the p21-binding protein PCNA. In addition, these results are unaffected by the order of addition of

the individual proteins. Although other proteins may moderate p21 activity *in vivo* (Funk and Galloway, 1998) and cyclin-Cdk complexes other than cyclin A-Cdk2 may require multiple p21 molecules for inhibition or use p21 as an assembly factor (Zhang et al., 1994a; LaBaer et al., 1997; Cheng et al., 1999), our results indicate that a single bound molecule of p21 is sufficient to inhibit cyclin A-Cdk2.

Cyclin A-Cdk2 retains some activity in the presence of excess p21, in accord with previous studies (Cai and Dynlacht, 1998; Hengst and Reed, 1998). The presence of equimolar p21 abolishes approximately 90% of cyclin A-Cdk2 activity, and addition of p21 above a 1:1 molar ratio leads to a further slight decrease in activity. The essentially undetectable kinase activity of Cdk2 or cyclin A alone suggests that the residual activity of cyclin A-Cdk2 in the presence of p21 does not result from a low level of insect kinase from the High Five cells that co-purified with Cdk2. Complete inhibition is not to be expected on thermodynamic grounds until the concentration of p21 is in excess such that cyclin A-Cdk2 is fully bound by p21. For 99% complex formation, the free p21 concentration must be 99-fold greater than the dissociation constant (Creighton, 1993). It is to be expected therefore, that cyclin A-Cdk2 exhibits a low level of kinase activity in the presence of equimolar p21.

The N-terminal cyclin-Cdk inhibition domain of p21 is 44% identical in primary sequence to the corresponding domain of $p27^{Kip1}$ (Figure 1.4) (Polyak et al., 1994). The crystal structure of the Cdk-inhibition domain of p27 (residues 22-106) bound to a truncated form of human cyclin A (residues 173-432) and full-length human Cdk2 phosphorylated at Thr160 shows that p27 can inhibit cyclin A-Cdk2 with a 1:1 stoichiometry (Figure 1.3D) (Russo et al., 1996a). Given the sequence homology of the Cdk-inhibition domains of p21 and p27 and the common stoichiometry of inhibition, it seems likely that p21 disrupts Cdk activity in a manner similar to that seen in the crystal structure of the p27-inhibited cyclin A-Cdk2 complex.

Chapter 3

Contribution of Local α-Helix Formation in the Intrinsically Disordered Cyclin A-Cdk2 Inhibitor $p27^{Kip1}$

This chapter describes a collaboration project. Dr. Ewa Bienkiewicz performed the mutagenesis, protein purification, NMR, and CD on p27ID and point mutants (Figures 3.3, 3.4, and 3.5). My contributions included the production, purification, and CD of the p27-Cdk binding domain and the kinase-inhibition assays (Figures 3.2, 3.5, 3.6, 3.7, and 3.8).

3.0 INTRODUCTION

$p27^{Kip1}$ belongs to the p21 family of cyclin-dependent kinase (Cdk) inhibitors (Figure 1.4). p27 induces G1 arrest and is implicated in numerous processes involving cellular growth and differentiation (Polyak et al., 1994; Toyoshima and Hunter, 1994; Chellappan et al., 1998). For example, p27-deficient mice are 20-40% larger than normal and exhibit abnormalities such as hyperplasia, female infertility and pituitary tumors.

The p21 family of proteins has a modular structure with the conserved Cdk-inhibition domain located at the N-terminus (Figure 3.1B) (Polyak et al., 1994; Toyoshima and Hunter, 1994; Chellappan et al., 1998). The crystal structure of the human p27 Cdk-inhibition domain (residues 22-106) bound to human cyclin A-Cdk2 gives mechanistic insights to how p27 inhibits cyclin A-Cdk2 (Figure 3.1A) (Russo et al., 1996a). In the crystal structure, the p27 inhibition domain is in an extended structure over the surface of cyclin A-Cdk2. A highly conserved N-terminal motif (LFG) binds in a pocket of cyclin A. The C-terminal region binds the active site of Cdk2 and remodels the Cdk2 structure.

The p27 inhibition domain when bound to cyclin A-Cdk2 forms both an α-helix that makes contacts with both cyclin A and Cdk2 and a 3_{10} helix that bind the active site of Cdk2 (Figures 1.3C and 3.1A). Circular dichroism (CD) spectroscopy shows this helical content is mostly absent in the

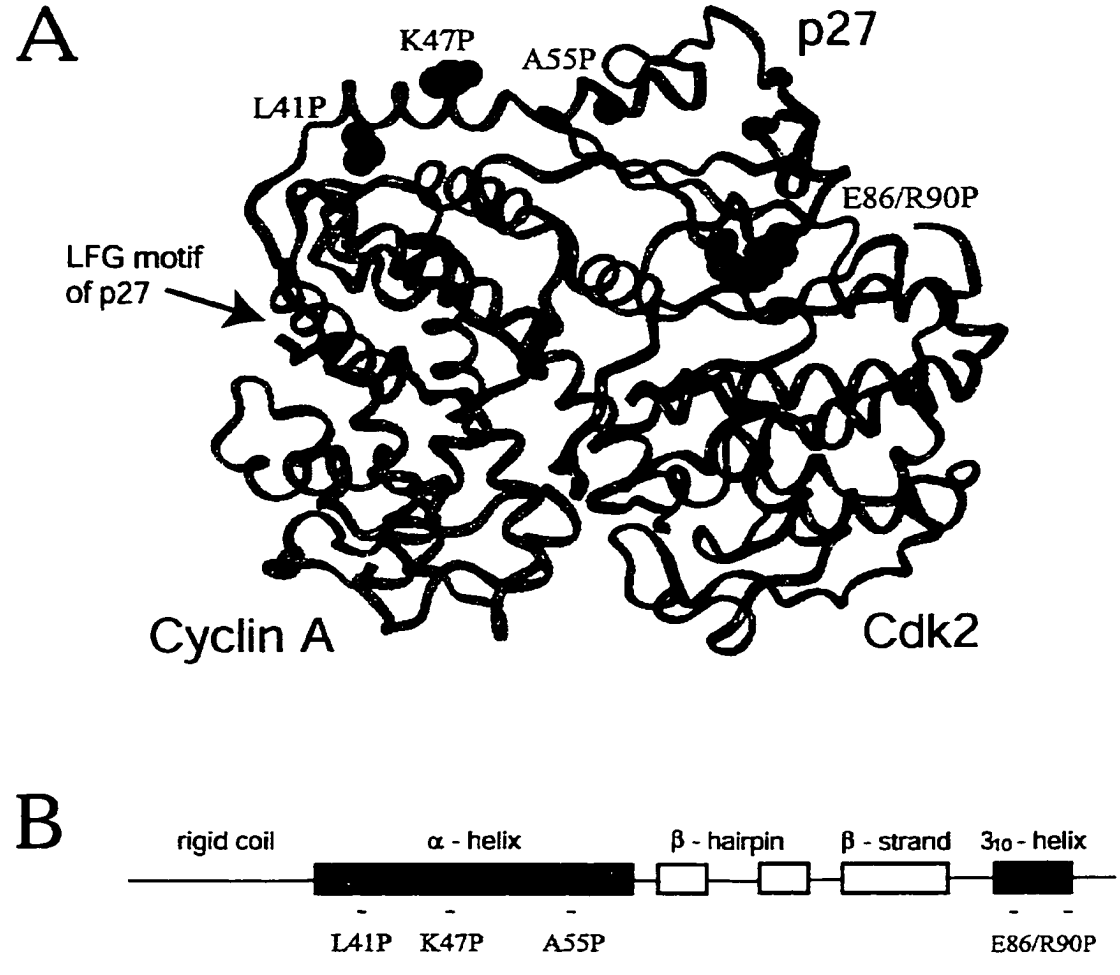

Figure 3.1. p27 Bound to cyclin A-Cdk2 and Domain Structure
A. The p27 inhibition domain has a well-ordered conformation in the crystal structure of the p27-inhibited cyclin A-Cdk2 complex (Russo et al., 1996a).

B. Schematic representation of the secondary structure of p27 Cdk-inhibition domain when bound to cyclin A-Cdk2.

unbound inhibitor at 30 °C. At lower temperature, however, some helical formation is observed. Using proline mutagenesis, the region containing helical propensity found by CD, was mapped to the same region as that of the α-helix from the crystal structure. As determined by both proline and alanine mutagenesis, we conclude that significant disruption and stabilization of this helical region has small functional effects.

3.1 METHODS

3.1.a Protein Expression, Purification and Mutagenesis

p27ID (corresponding to residues 22-97 of human p27 with an additional N-terminal Gly-Ser-His-Met) and p27ID mutants were expressed as His-tag fusion proteins in *Escherichia coli* strain BL21 (DE3) and purified using His-bind resin (Novagen 69670) by Dr. E. A. Bienkiewicz. The His-tag sequence was cleaved with thrombin prior to final purification by C_{18} HPLC. p27ID mutants were prepared using the QuikChange protocol (Stratagene).

The p27-Cdk binding domain ($p27_{63-97}$) was prepared by digestion of purified p27ID with endoproteinase AspN (Sigma P3303) in 25 mM ammonium carbonate, 5 % acetonitrile (v/v), pH 7.8. Three product peaks were purified by reversed phase C_4 HPLC using linear 1 %/minute acetonitrile/water gradients containing 0.1 % TFA. The three purified products were analyzed with MALDI mass spectrometry. The second peak was found to be within 2 Da of the expected fragment mass of 4246 Da.

Human cyclin A and Cdk2 were prepared as described in sections 2.1.a and 2.1.c (Adkins and Lumb, 2000).

The identity of all proteins was confirmed with MALDI mass spectrometry, with expected and observed masses agreeing to within 1 Da, with the exception of Cdk2, which was confirmed by Glu-C digest with MALDI mass spectrometry of resulting fragments (Section 2.2.c).

3.1.b Phosphorylation Assays

Cyclin A-Cdk2 activity was assayed by quantifying histone H1 phosphorylation at 15 and 30 °C as described previously in section 2.1.h (Adkins and Lumb, 2000), except reactions contained 50 nM cyclin A-Cdk2. The extent of inhibition was used as a measure of the extent of binding in a nonlinear least squares fit to calculate K_d values, assuming a 1:1 binding stoichiometry. This fit used the following equation, where K_a is the association constant, [A] is the enzyme concentration, E_f is the value of the reaction when the enzyme is fully occupied with inhibitor, and E_u is the value of the reaction when the enzyme is unoccupied with inhibitor.

$$y = \left(\frac{K_a[A]}{1 + K_a[A]}(E_f - E_u)\right) + E_u$$

3.1.c Biophysical Methods

Dr. E. A. Bienkiewicz collected all the CD spectra on Jasco J720 and Aviv 62DS spectrometers, with the exception of $p27_{63\text{-}97}$ (Cdk2-binding domain),

which I collected. Samples contained 50 or 100 μM protein in 25 mM HEPES, 50 mM NaCl, 5 mM $MgCl_2$, 1 mM DTT, pH 7.5, with the exception of $p27_{63-97}$, which contained 10 μM protein. Protein concentrations were determined by absorbance in 6 M GuHCl, 150 mM NaCl, pH 6.5 using extinction coefficients at 280 nm of 15,220 M^{-1} cm^{-1} and 9530 M^{-1} cm^{-1} for p27ID (and mutants) and Cdk2-binding domain, respectively (Edelhoch, 1967). Helix content (f_H) was estimated from $[\theta]_{222}$ using f_H= -($[\theta]_{222}$ + 2340)/30,300 (Chen et al., 1972) or using CDPro (Sreerama et al., 2000; Sreerama and Woody, 2000).

Drs. E. A. Bienkiewicz and K. J. Lumb collected the NMR data with a Varian Unity Inova operating at 500.1 MHz for ^1H as described previously (Campbell et al., 2000). Gradient-enhanced DQF-COSY spectra were acquired at 35 °C on 1 mM p27ID in 10 mM sodium phosphate, 10 mM DTT, pH 4.4. Steady-state ^1H-^{15}N NOE values were measured at 30 °C on 1 mM p27ID in kinase buffer (25 mM HEPES, 50 mM NaCl, 5 mM $MgCl_2$, pH 4.4) containing 1 mM DTT.

3.2 RESULTS AND DISCUSSION

3.2.a Intrinsic Structural Disorder of the p27 Cdk-Inhibition Domain

p27ID corresponds to residues 22 to 97 of human p27. This region of p27 has an ordered structure when bound to cyclin A-Cdk2 (Figure 3.1A). p27ID effectively inhibits histone H1 phosphorylation by cyclin A-Cdk2 that is >90 % active (calibrated with staurosporine; section 2.2.c). Approximately 90 %

inhibition of cyclin A-Cdk2 is observed in the presence of equimolar p27ID (Figure 3.2), indicating that p27ID inhibits cyclin A-Cdk2 with a 1:1 stoichiometry (c.f. Figure 2.9), in accord with the crystallography results (Figure 3.1A). If p27ID were substantially inactive, then the apparent molar ratio of p27ID to cyclin A-Cdk2 for essentially complete inhibition would exceed 1:1.

At the same temperature (30 °C) as the cyclin A-Cdk2 inhibition assay, the CD spectrum of p27ID is reminiscent of an unfolded protein (Figure 3.3). The minimum at 204 nm is indicative of an unfolded conformation, and the weak negative shoulder at 222 nm indicates the absence of significant amounts of helix or β-strand. All except three H^{α} resonances fall within 4.0-4.5 ppm, and the H^{N} chemical shifts fall within 7.9-8.5 ppm, which correspond to the values expected for unfolded proteins (Wishart and Sykes, 1994). The ^{1}H-^{15}N NOE is negative (-1 to –3.9) for each resolved amide crosspeak in the HSQC spectrum, indicating that the p27ID main chain is highly flexible with motion on a time scale characteristic of unfolded proteins (Cho et al., 1996). CD spectra of p27ID collected under NMR and kinase-assay conditions were essentially identical. The spectroscopic data collectively indicate that the p27 Cdk-inhibition domain is intrinsically disordered in isolation under conditions where the domain is an effective Cdk2 inhibitor. Similar behavior is exhibited by the related Cdk inhibitor p21 (Kriwacki et al., 1996). Since p27 is folded when bound to cyclin A-Cdk2 (Figure 3.1A), p27 binding is coupled with folding.

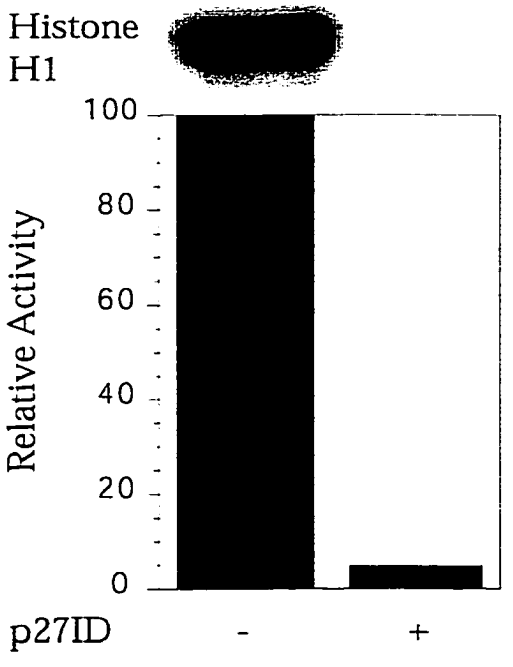

Figure 3.2. p27ID Activity Assay
A. An equimolar ratio of p27ID inhibits histone H1 phosphorylation by cyclin A-Cdk2.

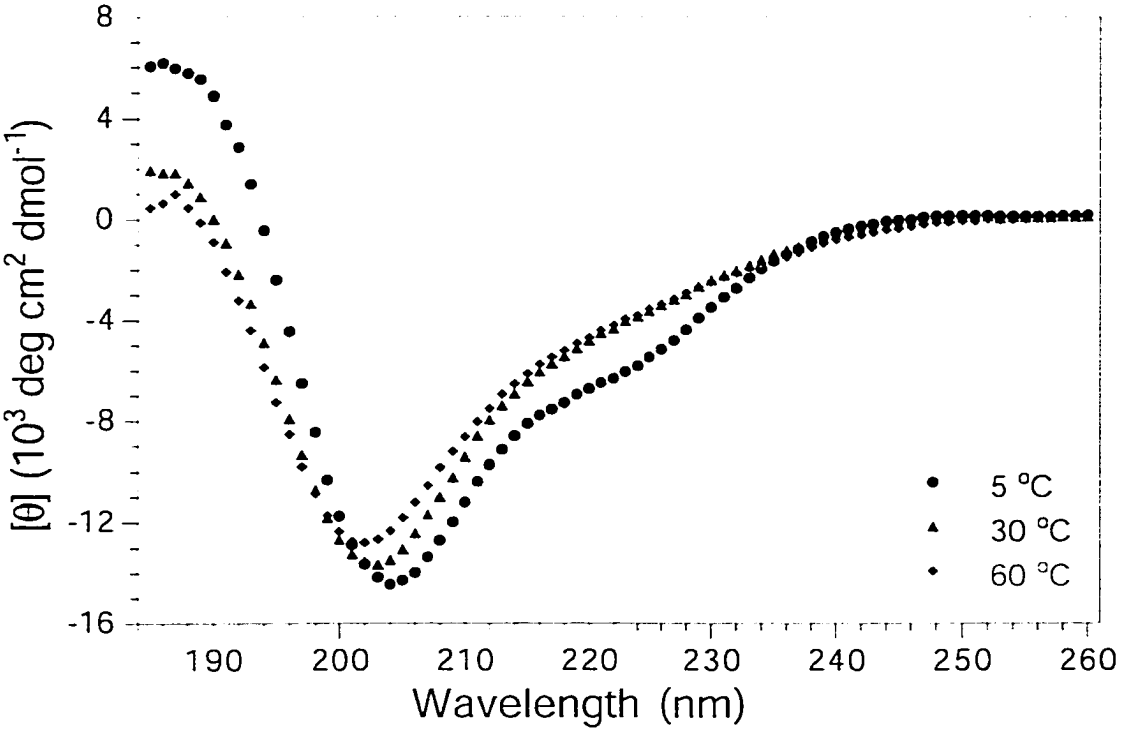

Figure 3.3. Circular Dichroism Spectra of p27ID
CD spectra of p27ID (100 μM) in kinase-assay buffer (25 mM HEPES, 50 mM NaCl, 5 mM $MgCl_2$, pH 7.5) containing 1 mM DTT. The CD spectra at 30 and 60 °C are characteristic of an unfolded protein. At 5 °C, the CD spectrum indicates the presence of helix. The CD spectrum of p27ID at 5 °C is independent of pH (4 to 7.5) and concentration (20 μM to 1 mM). Data were collected by Dr. E. A. Bienkiewicz.

3.2.b Helix Formation in the p27 Cdk-Inhibition Domain

While intrinsically disordered at 30 °C and above, p27ID becomes partially helical at lower temperature, as indicated by CD spectroscopy (Figure 3.3). The helix content at 5 °C is estimated to be between 10 or 16 % from $[\theta]_{222}$ and CDPro (Table 3.1), (Chen et al., 1972; Sreerama et al., 2000; Sreerama and Woody, 2000), which is less than expected based on the crystal structure of the p27-inhibited cyclin A-Cdk2 complex (33 %). The temperature dependence of the CD signal at 222 nm indicates that the helix is only marginally stable (Figure 3.4C). Thus, although intrinsically disordered at physiological temperature, p27ID exhibits an inherent propensity to adopt helical structure.

3.2.c Helix Localization by Proline-Mapping Mutagenesis

CD cannot provide information directly that allows us to determine if the helix observed at low temperature corresponds to the regions of p27 that adopt stable helices upon binding cyclin A-Cdk2. Although single proline residues can be accommodated in helices of folded proteins with some local distortion (Barlow and Thornton, 1988), proline greatly destabilized isolated helices (reviewed by Serrano, 2000). Proline mutations are therefore expected to disrupt helix formation and alter the CD spectrum in the unbound p27 Cdk-inhibition domain if placed in regions that adopt helical conformations, but to have little or no effect on helix content, as measured by CD, if placed in unfolded regions.

p27ID	Temp (°C)	$[\theta]_{222}$ % Helix	CDPro % Helix	CDPro % Strand	CDPro % Turn	CDPro % Unord
WT	5	9.9	16.3	19	16.0	49.0
	30	5.2	8.4	21.8	16.0	53.3
L41P	5	4.4	8.1	20.1	15	56.9
	30	3.2	7.3	20.1	14.2	58
K47P	5	-0.2	4.6	19.4	13.5	62.0
	30	1.2	6.4	19.8	13.2	59.6
A55P	5	-0.2	5.0	19.4	13.1	61.6
	30	1.7	6.3	19.7	13.5	59.6
E86/R90P	5	10.4	17.0	19.3	16.6	47.0
	30	5.3	8.9	23.8	17.2	50.2
$p27_{63-97}$	5	-10.2	0.2	23.0	25.9	50.9

Table 3.1. Secondary structure content of p27ID, p27ID mutants, and $p27_{63-97}$ Dr. E. A. Bienkiewicz performed the analysis for p27ID and p27ID mutants and I performed the analysis for $p27_{63-97}$.

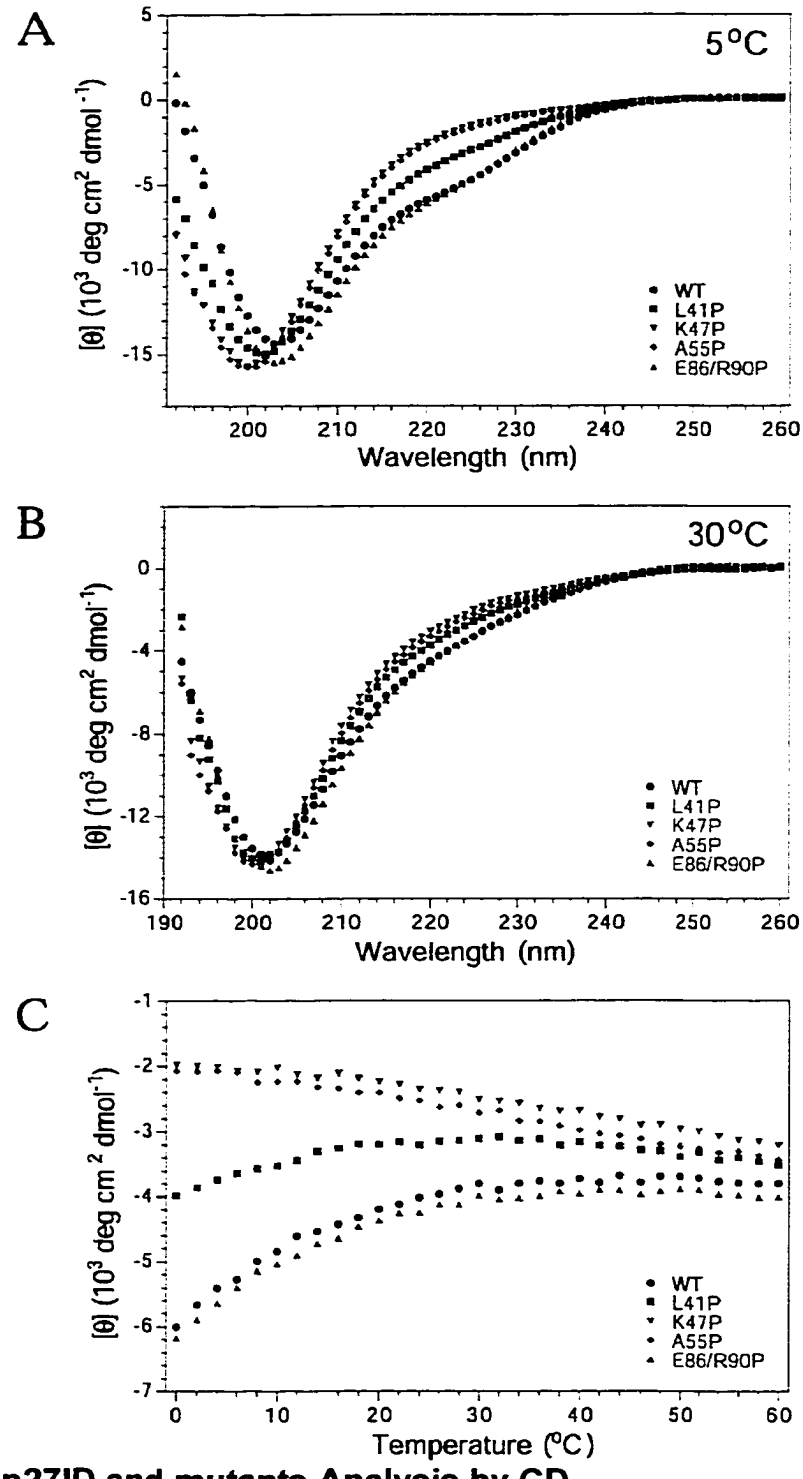

Figure 3.4. p27ID and mutants Analysis by CD

A. CD spectra of p27ID and the proline mutants at 5 °C.

B. CD spectra of p27ID and the proline mutants at 30 °C.

C. Temperature dependence of $[\theta]_{222}$ of p27ID and the proline mutants. Data collected by Dr. E. A. Bienkiewicz.

p27 forms two helical regions upon binding cyclin A-Cdk2: an α-helix comprising residues 38 to 59, and a 3_{10} helix comprising residues 85-90 (Figure 3.1B). Three sites in the α-helix (Leu 41, Lys 47 and Ala 55) were chosen for the high helical propensity of the wild-type amino acid (Serrano, 2000). The Lys 47 and Ala 55 side chains project away from cyclin A-Cdk2, whereas Leu 41 forms part of the binding interface with cyclin A (Figure 3.1A). The three aromatic residues at the center of the 3_{10} helix were not changed, since mutation of aromatic residues can affect the far-UV region of the CD spectrum regardless of any change in secondary structure (Woody and Dunker, 1996). Instead, Glu 86 and Arg 90 were mutated together to proline to disrupt main chain hydrogen bonding within the 3_{10} helix. If either the α or 3_{10} helices are partially populated at low temperature, then the proline mutations would be expected to destabilize the helix and decrease the helical component of the CD spectrum.

Proline substitutions in the region of p27 that adopts α-helix upon binding cyclin A-Cdk2 diminish the helix content of unbound p27ID as observed by the disappearance of the 222 nm shoulder in the CD spectra (Figure 3.4A). Helix formation at 5 °C in the K47P and A55P mutants is essentially abolished, as judged by the decrease in the amplitude of the CD signal at 222 nm (Figure 3.4A), and the temperature dependence of the CD signal at 222 nm (Figure 3.4B), which is typical of unfolded or extended structures (Woody, 1992). The L41P mutation is less destabilizing and reduces the helix content approximately two-fold at 5 °C (Figure 3.3A), consistent with its

position in the first turn of the helix. The proline substitutions in the region that adopts the 3_{10} helix did not affect significantly the CD spectrum at 5 °C (Figure 3.4A) or the thermal stability of the helix (Figure 3.4C). These results map the marginally stable helix observed with CD at low temperature to the vicinity of p27 that forms the α-helix upon binding cyclin A-Cdk2. At 30 °C, the CD signal at 222 nm (indicative of helix formation) is slightly less negative for the L41P, K47P and A55P mutants, suggesting that the helix is present to some extent in the wild-type domain even at 30 °C (Figure 3.4B). In contrast, the 3_{10} helix does not appear to be present in the isolated p27 Cdk-inhibition domain even at low temperature.

3.2.d Analysis of 3_{10} Helix by Deletion Mapping

The absence of 3_{10} helix or helical propensity is further shown by analysis of the CD spectrum taken at 5 °C of a deletion mutant of p27 corresponding to residues 63-97 ($p27_{63-97}$) (Figure 3.5). CD spectra of this domain indicate a positive band at approximately 224 nm and strong negative band at approximately 198 nm. These characteristics are highly indicative of a largely unstructured domain or poly-proline II conformation (Woody, 1992). Analysis by Selcon3 of the CDPro software package (Sreerama and Woody, 2000) indicates that total helix content is less than 1 %, while unordered or random conformation is estimated to be greater than 50 %. It is concluded that there is no intrinsic local propensity to form the 3_{10} helix.

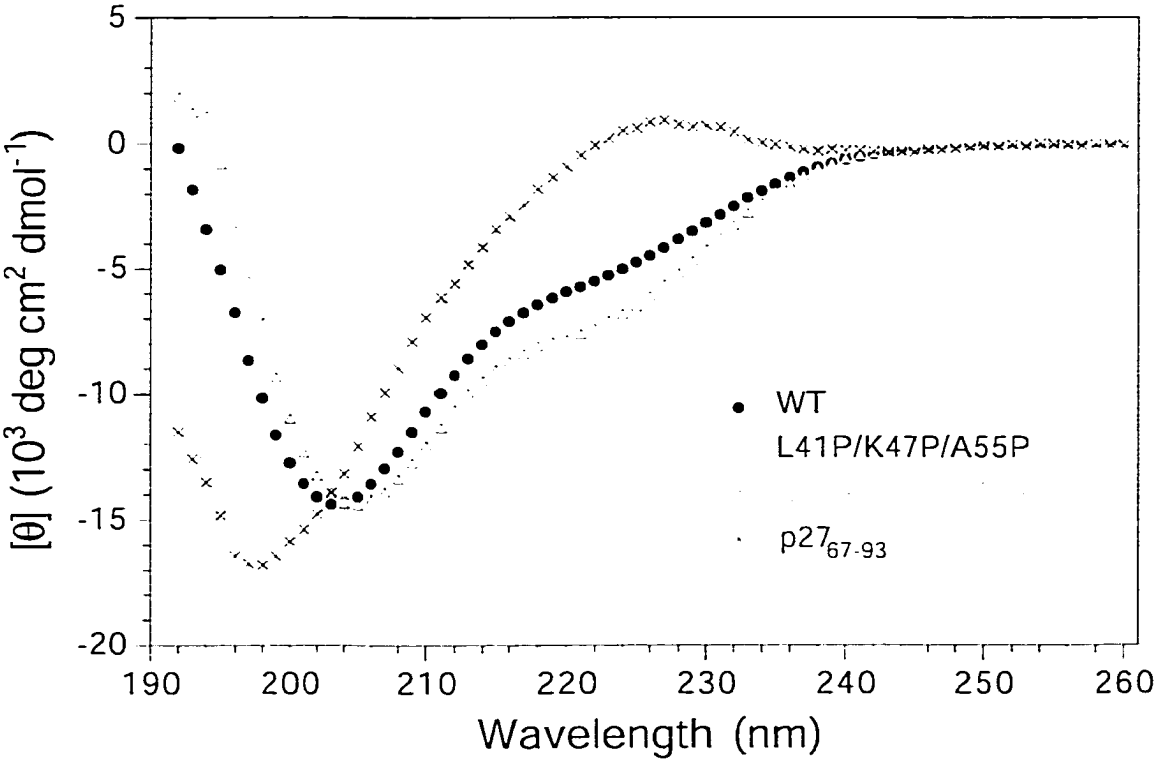

Figure 3.5. CD analysis p27ID with Triple Mutants and Cdk-Binding Domain

Circular dichroism spectra of p27ID, E40A/D44A/K47A, L41P/K47P/A55P, and the Cdk-binding domain at 5 °C. I collected the data for the Cdk-binding domain, residues 63-97 and Dr. Ewa Bienkiewicz collected the data for the remaining proteins.

3.2.e Contribution of Helical Propensity to Cdk Inhibition

If the incipient α-helix of p27 contributes significantly to the specificity of the interaction between p27 and cyclin A-Cdk2, then the ability of the L41P, K47P and A55P mutants to inhibit cyclin A-Cdk2 would be expected to be compromised. Dissociation constants (K_d) were determined with cyclin A-Cdk2 inhibition assays (Figure 3.6). p27ID binds cyclin A-Cdk2 with a K_d of 8 ± 2 nM at 30 °C. The L41P mutant, which contains approximately half of the helix in unbound wild-type domain, binds with a very similar affinity (K_d = 9 ± 1 nM). The K47P and A55P mutants, in which helix formation is essentially abolished, bind with lower affinities (16 ± 3 and 13 ± 2 nM, respectively). At lower temperature, where the helix is more populated, the K_d values for p27ID and K47P at 15 °C are 8 ± 1 nM and 10 ± 2 nM, respectively. Thus some correlation exists between loss of helix and increase in K_d, but the differences are very small in free energy terms ($\Delta\Delta G°$ = 0.1 to 0.4 ± 0.1 kcal mol^{-1}) compared to the free energy of binding ($\Delta G°$ = -11.5 kcal mol^{-1} for p27ID).

The E86P/R90P double mutation did not reduce the helix content of unbound p27ID, but did increase the K_d to 14 ± 2 nM ($\Delta\Delta G°$ = 0.4 ± 0.1 kcal/mol compared to p27ID). Since the helix content is unperturbed by the E86P/R90P mutations, the change in affinity likely reflects disruption of the quaternary contacts between the mutated residues of p27ID and Cdk2, including hydrogen bonds involving Arg 90 of p27 and Gln 131 and Asn 132 of Cdk2 (Russo et al., 1996a).

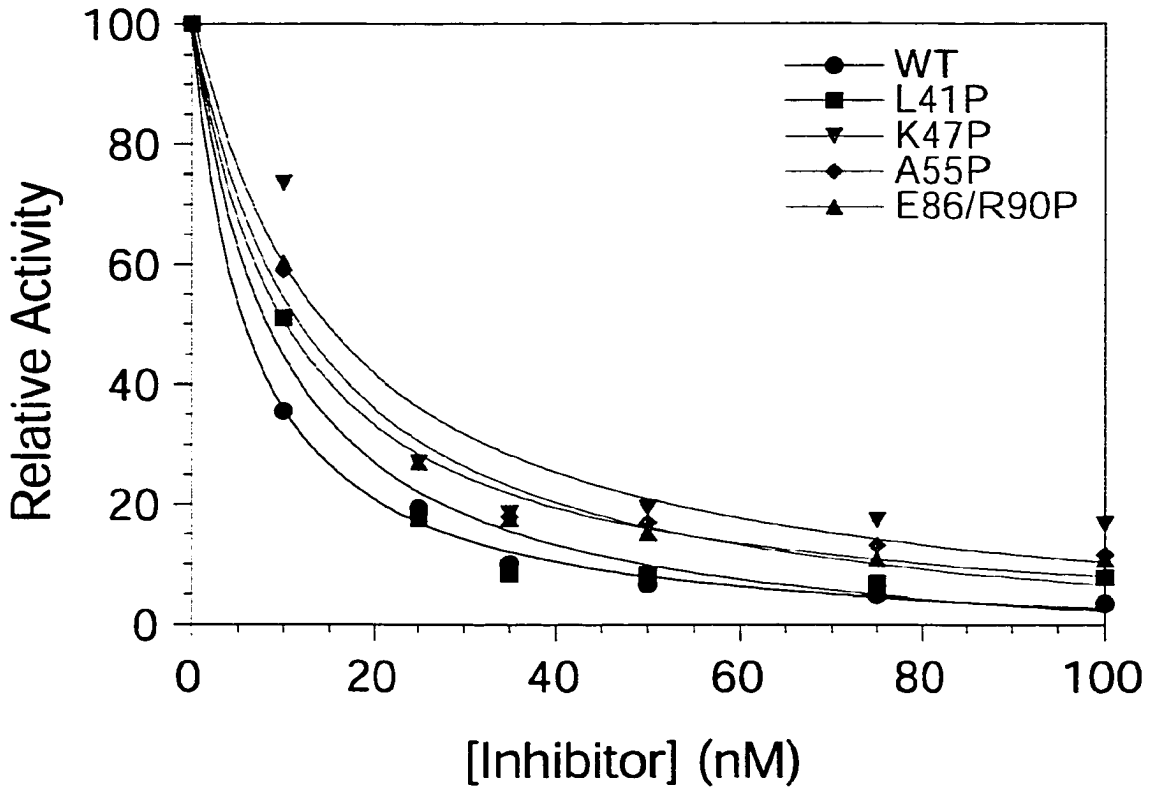

Figure 3.6. K_d Determinations from Cyclin A-Cdk2 Inhibition Assays

K_d determinations of wild-type p27ID and single and double proline mutants of p27ID.

Deletion of the LFG (Leu31-Phe32-Gly33) cyclin-binding motif of p27 reduces the ability of p27 to inhibit cyclin A-Cdk2 by 10^3-fold (Polyak et al., 1994). $p27_{63-97}$, a peptide corresponding to just the Cdk2-binding domain of p27 (residues 63-97), is also unable to inhibit cyclin A-Cdk2 under the conditions used here (Figure 3.7). This result highlights the need for an intact p27-cyclin A binding interface, in accord with previous studies (Polyak et al., 1994; Russo et al., 1996; Schulman et al., 1998). Moreover, binding to cyclin A alone but not to Cdk2 would be insufficient on structural grounds to inhibit Cdk activity (Russo et al., 1996a). It seems likely, therefore, that the binding hot spots involving the LFG and Cdk-binding motifs of p27 are preserved at least approximately in the proline mutants.

3.2.f Increasing Predicted α-Helix

Prediction of secondary structural elements can be difficult in the context of a native globular protein (reviewed by Honig, 1999). p27ID and mutants appear to be largely unstructured at 30 °C and monomeric by sedimentation equilibrium (data collected by Dr. E. A. Bienkiewicz and not shown); therefore any helix is largely isolated. The computer program AGADIR (Munoz et al., 1996; Munoz and Serrano, 1997) is useful for making predictions about formation of helices in isolated monomeric peptides (Figure 3.8A). To further study the role of α-helix in the function of p27ID, two more mutants were designed using AGADIR. One mutant incorporates the three mutants that have already been shown to disrupt α-helix content at 5 °C, L41P/K47P/A55P, to completely eliminate any predicted α-helix (Figure

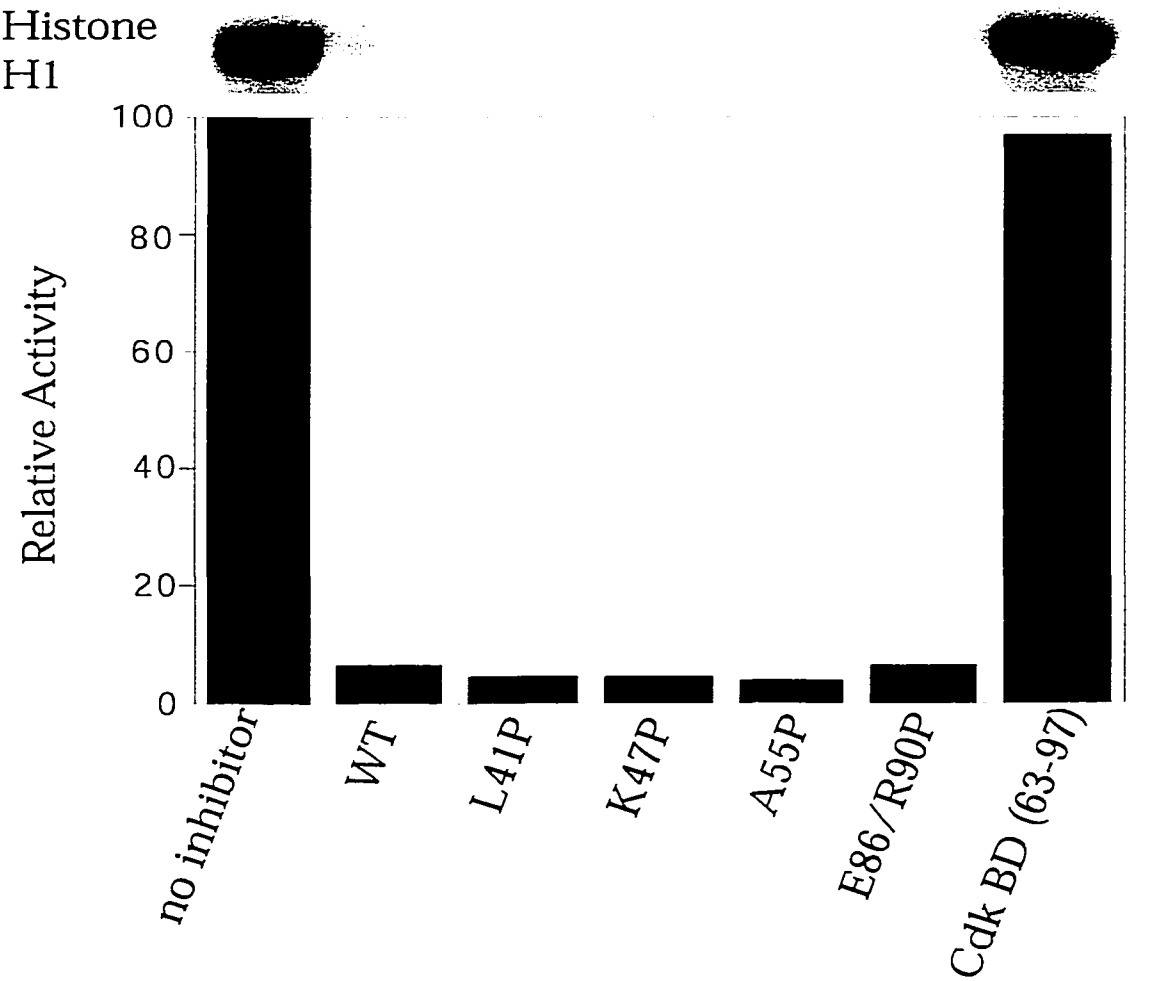

Figure 3.7. p27 Cdk Binding Domain Activity Comparison
Comparisons of p27 single and double proline mutants with the p27 Cdk-binding domain (residues 63-97) at a 1:1 stoichiometric ratio.

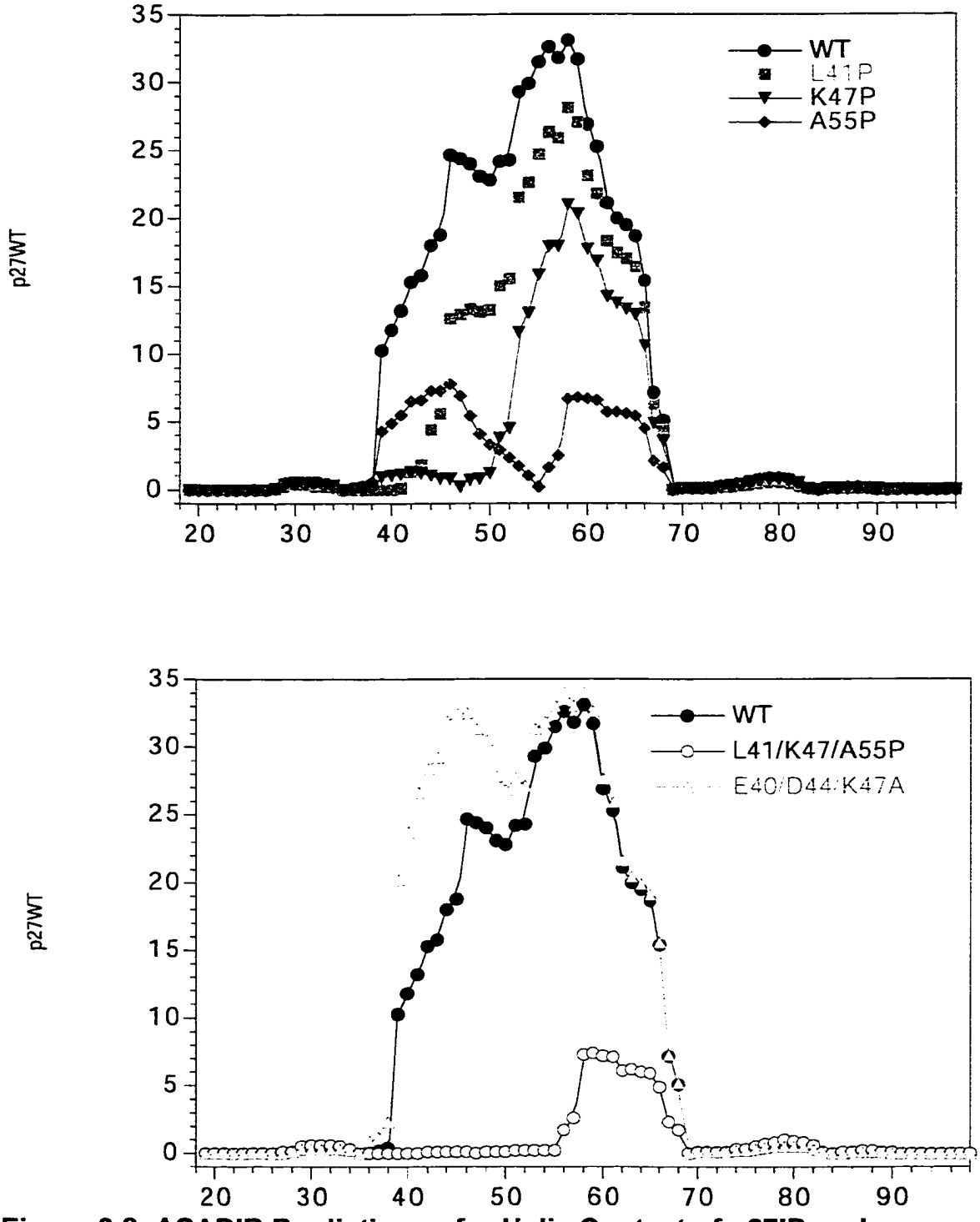

Figure 3.8. AGADIR Predictions of α-Helix Content of p27ID and Mutants

A. AGADIR helix predictions of p27ID wild-type and single proline mutants. E86/R90P is not shown because it is completely superimposed by wild-type p27ID.

B. AGADIR helix predictions of p27ID wild-type, L41P/K47P/A55P, and E40A/D44A/K47A.

3.8B). The triple-proline mutant does have reduced helical content at 5 °C as compared to the low levels of α-helix from the A55P and K47P mutants (Figure 3.5). The triple-alanine mutant (E40A/D44A/K47A) has mutations in residues not making side chain contacts with cyclin A or Cdk2 to alanine, a strong helix promoter (Serrano, 2000). E40A/D44A/K47A is predicted to have an increased α-helix content by as much as 50 % over p27ID (Figure 3.5). E40/D44/K47 does have an observed increase in α-helix by CD. The propensity for these residues to adopt a more rigid helix may give interesting insight to the role of this helix in the inhibition function. One group has actually suggested the helix may play a steric role in resistance to inhibition by p27 with a viral cyclin, which would be disruptive to the normal location of the helix (Card et al., 2000). The triple alanine mutant may have a similar effect with cyclin A, due to increase helicity.

The K_d determinations for E40A/D44A/K47A were anomalous using the standard kinase assay conditions. A one-hour equilibration time was needed before adding ATP to the kinase mixture. The activity of the E40A/D44A/K47A mutant is similar to the wild type p27ID when the longer equilibration time is used (Figure 3.9). The K_d for E40A/D44A/K47A is 12.5 nM ± 3 nM ($\Delta\Delta G^\circ = 0.3 \pm 0.1$ kcal mol^{-1} compared to p27ID). After observing that disrupted helix is somewhat detrimental to the binding of p27ID to cyclin A-Cdk2, it is notable that increasing the helical propensity is also marginally detrimental.

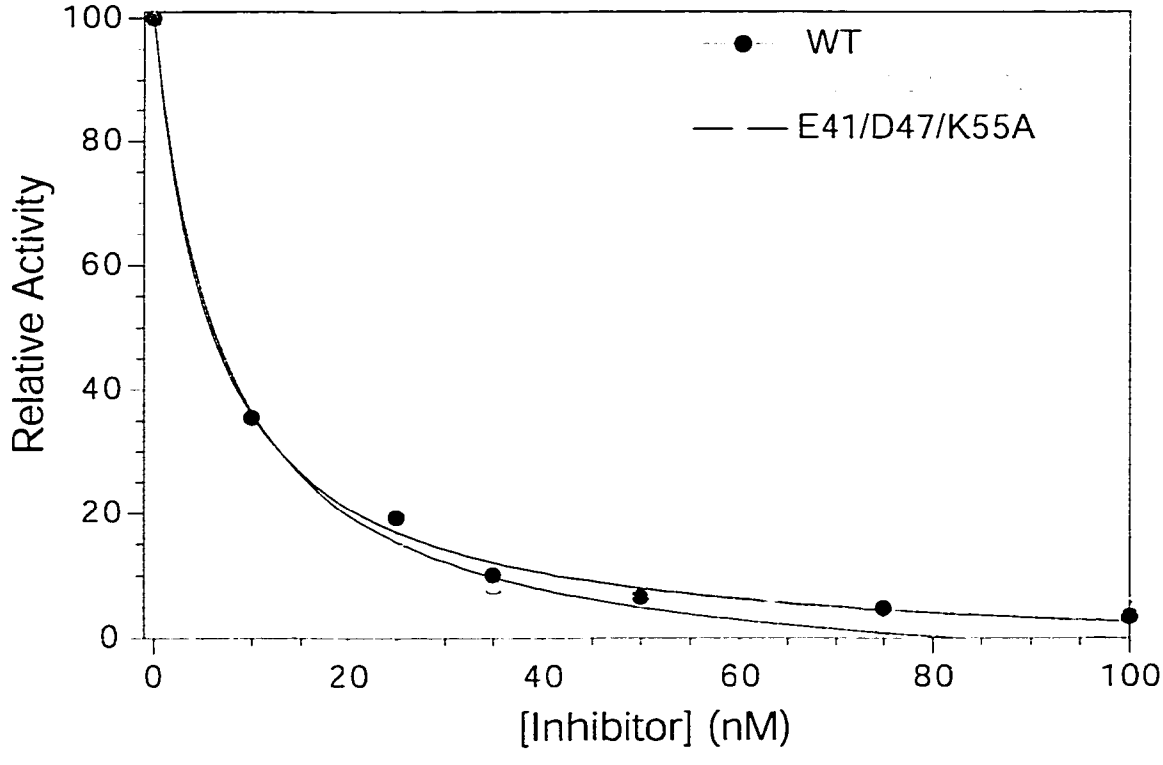

Figure 3.9. K_d Determinations of p27ID wild-type, L41P/K47P/A55P, and E40A/D44A/K47A

3.2.g Coupled Folding and Binding of p27

A significant number of biologically active proteins involved in diverse cellular processes, such as the cell cycle, gene expression and translation have disordered structures that undergo a protein-folding disorder-order transition upon binding target proteins or nucleic acids (reviewed in Wright and Dyson, 1999; Williamson, 2000). Molecular recognition by such proteins is analogous to protein folding in that a very large number of possible conformations converge to a single, well-defined structure. During protein folding, any property of the denatured state that biases the conformational search towards the native structure, such as local helix formation, might be expected to be a key element of folding. Indeed, mutations in native helices that increase helical propensities have been shown in several proteins (i.e., CheY, ADA2h, acylphosphatase, and the GCN4 leucine zipper) to increase the stability of the native state (Munoz et al., 1996; Viguera et al., 1996; Taddei et al., 2000; Zitzewitz et al., 2000).

The inhibition domain of p27 is intrinsically disordered at physiological temperatures. However, the domain exhibits a marked propensity for marginally stable helical structure, revealed by proline-mapping mutagenesis at low temperature, which corresponds to the stable α-helix induced upon binding cyclin A-Cdk2. This marginally stable helix may contribute to the assembly of the p27-inhibited cyclin A-Cdk2 complex by reducing either the entropy penalty or the complexity of the conformational search that the

otherwise disordered p27 inhibition domain experiences in order to adopt the correct structure that endows recognition specificity. However, disruption of the incipient helix in the unbound inhibitor affects only marginally the stability of the p27-cyclin A-Cdk2 complex, but complete disruption does have an impact on stability.

3.3 CONCLUSIONS

We conclude that non-local (quaternary) contacts between p27 and cyclin A-Cdk2 are more important energetically than pre-existing local (helical) interactions in unbound p27 in determining the free energy of assembly of the p27-cyclin A-Cdk2 complex.

Several protein folding mechanisms have been proposed with differing emphasis on the role of local and non-local interactions (Fersht, 1997; Baldwin and Rose, 1999; Arai and Kuwajima, 2000; Bilsel and Matthews, 2000). For p27, the mechanism of coupled folding and binding is more akin to a protein folding mechanism in which the context of non-local tertiary or quaternary interactions is likely more significant in energetic terms than local (secondary) structure formation in dictating protein structure (Lumb et al., 1994; Minor and Kim, 1996; Fersht, 1997).

Increasing and decreasing helix propensity appears to subtly disrupt p27ID function. This disruption may be caused by a stiffening of helical regions of

this protein, as alluded to before; steric hindrance is considered one reason why a viral cyclin replacing cyclin A appears to be resistant to p27 inhibition (Card et al., 2000). Crystal structures of the cyclin A-Cdk2 complex in the absence and presence of p27ID (Figure 3.10) suggests that the structure of cyclin A is mostly unchanged by the binding of p27ID, but Cdk2 undergoes significant changes in the β-sheet domain and a subtle shift of the α-helix domain (Russo et al., 1996a; Card et al., 2000). A possible two-stage mechanism of inhibition could involve initial binding by p27ID to cyclin A and then folding of the α-helix and β-turns of p27ID with a concurrent adjustment of the Cdk2 β-sheet and α-helical lobes. Future studies could use NMR and fluorescence to determine if either the cyclin A portions or the Cdk2 portions are occupied first during binding.

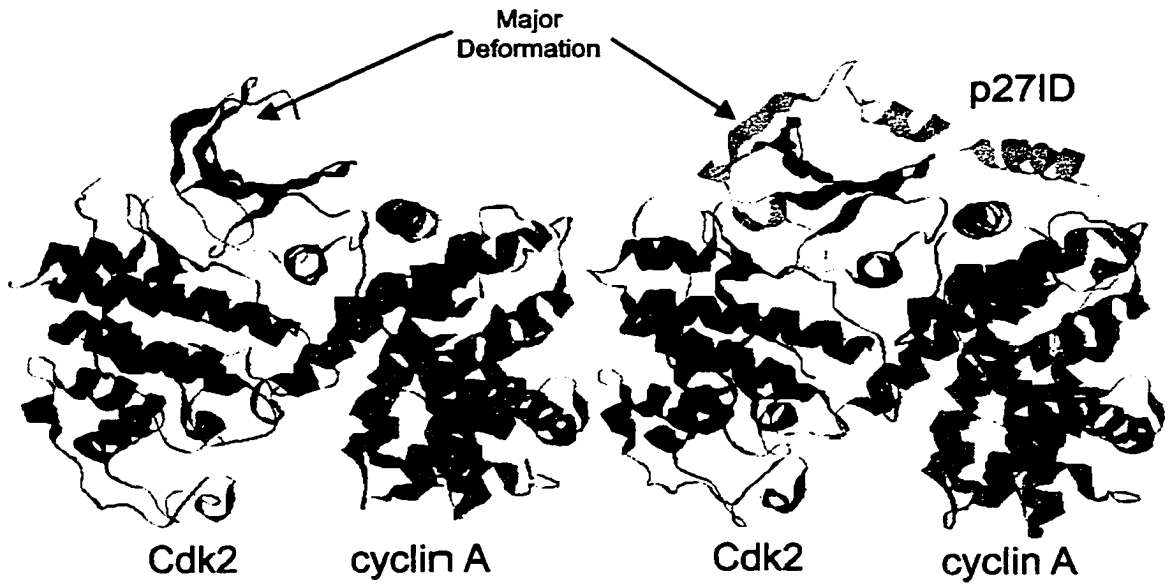

Figure 3.10. Comparison of Crystal Structure of Cyclin A-Cdk2 with and without p27ID

Chapter 4
Structure-Function Analysis of the Intrinsically Disordered Cdk-Inhibitor $p57^{Kip2}$

4.0 INTRODUCTION

The p21 family of Cdk-inhibitors includes p21, p27, and p57. These proteins share a common N-terminal Cdk-inhibition domain (Figure 1.4). When over-expressed, any of these proteins can arrest cells in G1 phase of the cell cycle (Morgan, 1997).

p57 (Lee et al., 1995; Matsuoka et al., 1995) contains the N-terminal Cdk-inhibition domain (Figure 1.4). The C-terminal region of p57 contains a QT domain that is defined by degenerate repeats of the type EPVEEQXX and is homologous with the p27 C-terminal QT domain (Matsuoka et al., 1995). The C-terminal of p57 also contains a PCNA binding domain and a nuclear localization sequence (Watanabe et al., 1998). The internal region of p57 is made up of proline-alanine-proline-alanine (PAPA) repeats (Matsuoka et al., 1995). This sequence diversity makes p57 the most diverse member of the p21 family of Cdk inhibitors.

The chromosomal location of p57 (11p15) is linked to Beckwith-Weidemann syndrome and Wilms' Tumor (Hatada et al., 1996; Matsuoka et al., 1996; Reid et al., 1996). The Cdk-inhibition function and the linkage to human diseases have focused research towards the *in vivo* role of p57 (section 1.3.c).

While full-length p57 has been extensively characterized using molecular biology techniques, the domain has yet to be defined in structural terms. We

show here that full-length p57 and the N-terminal inhibition domain of human p57 (Figure 1.4), although functionally active, are essentially devoid of the stable helical or β-sheet structure typical of globular proteins. We conclude that p57 contains an intrinsically disordered yet biologically active inhibition domain.

4.1 METHODS

4.1.a p57 Mutagenesis, Expression, and Purification

A plasmid encoding human p57 without the His-tag, p-hp57, was made by cassette mutagenesis of pRSET-His-p57, a vector for N-terminally His-tagged human p57 (gift of J. W. Harper). Human p57 was expressed in *Escherichia coli* strain BL21 (DE3) pLysS using p-hp57. One ml of overnight culture was diluted into 1 L LB medium containing 50 mg/L ampicillin and 35 mg/L chloramphenicol. The 1 L culture was incubated at 37 °C until the optical density at 600 nm measured 1.0 and then induced with 0.5 mM IPTG. The cells were harvested by centrifugation at 4.2 krpm in a Beckman JS-4.2 rotor at 4 °C for 30 minutes. The cell pellet was resuspended in 20 mM Tris-base, 1 mM EDTA, 1 mM DTT, 1 mM PMSF, pH 7.5. The cells were lysed by sonication and centrifuged at 15 krpm using a Beckman JA20 rotor at 4 °C for 25 minutes. The soluble and insoluble fractions were analyzed by 12 % SDS-PAGE and p57 was found approximately evenly split between both fractions. The soluble fraction was found to be the most reliable fraction for purification. Therefore, the soluble fraction was dialyzed (SpectraPor MWCO

25 kDa) at 4 °C overnight against 10 mM Tris-base, 10 mM NaCl, 1 mM EDTA, 1 mM DTT, 5 % glycerol, pH 7.5.

The dialysate was loaded onto a 5 ml HiTrap Q column (Pharmacia) at 4 °C pre-equilibrated in 10 mM Tris-base, 10 mM NaCl, 1 mM EDTA, 1 mM DTT, 5 % glycerol, pH 7.5. The resulting flow-through was loaded onto a 5-ml HiTrap SP column equilibrated with 10 mM Tris-base, 10 mM NaCl, 1 mM EDTA, 1 mM DTT, 5 % glycerol, pH 7.5 at 4 °C. p57 was eluted from the SP column with a linear gradient of 0.2-1 M NaCl over 100 ml, collecting 10-ml fractions. p57-containing fractions were identified by SDS-PAGE using 12 % gels and pooled.

Final p57 purification was by reversed-phase C_{18} HPLC using a linear acetonitrile/water gradient containing 0.1 % TFA. Pure p21 was stored as a lyophilized powder and the yield ranged from 0.5-1 mg/L. The samples submitted mass spectrometry were 0.2 mg of the above lyophilized powder. MALDI mass spectrometry results were inconclusive because the mass was in a range bracketing 32 kDa (32370 ± 630 Da); the expected mass was 32177 Da. Electrospray mass spectrometry was unable to measure the mass of the sample. p57, like full-length p21 and full-length p27, is poorly soluble (<10 μM). It was concluded that this protein was p57 since the expected mass was in the right range by mass spectrometry, the protein migrated as expected by SDS-PAGE at 57 kDa as observed by others (Lee et al., 1995; Matsuoka et al., 1995), and the protein inhibited cyclin A-Cdk2.

4.1.b p57-ID6 Mutagenesis, Expression, and Purification

Initially, PCR mutagenesis was used to amplify the DNA encoding the inhibition domain (residues 26-98) plus some residues N- and C-terminal of the inhibition domain (i.e. residues 1-106) from pRSET-His-p57 for subcloning into pET-based vectors. This fragment was resistant to PCR amplification, and when a clone was made it was found to contain multiple mutations. Hence, the restriction sites available in pRSET-His-p57 and p-hp57 were analyzed and *Kas I* restriction sites were found useful for a different cloning approach (Figure 4.1). Cassette mutagenesis using *Kas I* restriction sites was performed on p-hp57. A stop codon (TAG) was placed in the coding sequence 24 base pairs 3' from the coding sequence of the inhibition domain. The vector was designed with subsequent sub-cloning in mind. Using a *BamHI* digestion, then an *Nde I* digestion, the inhibition domain could be further sub-cloned into other vectors. Using an *Nde I*-only digestion followed by ligation resulted in an expression vector for the p57 QT domain. This versatile parent vector was called p-hp57-ID1.

p57-ID1 was expressed, purified with difficulty, and found to have very poor solubility (<5 μM 95 °C for 1 minute and <1 μM without heating), measured by UV absorbance. Cassette mutagenesis of p-hp57-ID1 was performed removing the first 23 residues from the expressed inhibition domain, making the N-terminal more similar to that of the p27-inhibition domain. p-hp57-ID2 did not express well in any *E. coli* BL21 (DE3) strains. In an effort to make a p57 inhibition domain that could be purified in low-expression conditions, the

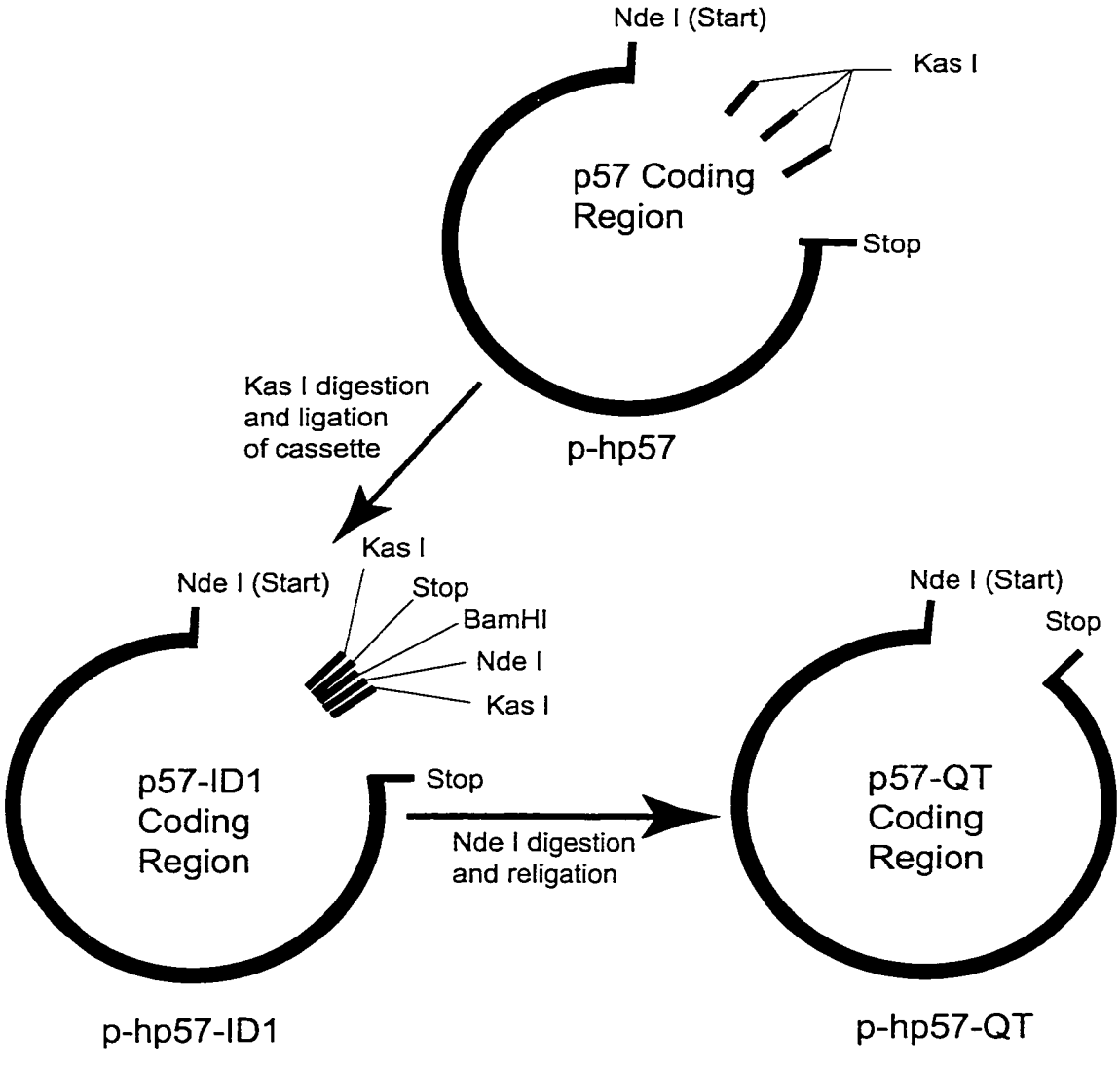

Figure 4.1. Design of p57-ID1 Expressin Vector
Designed primarily to make a p57-Inhibition domain expression vector, the design also made a QT expression vector possible.

coding sequence for p57-ID2 was sub-cloned into pET15b to introduce the N-terminal His-tag sequence. Similar to full-length p57, expressed p57-ID3 was distributed approximately evenly between soluble and insoluble fractions. Thrombin cleavage of the His-tag was poor and made subsequent HPLC difficult because the cleaved and uncleaved peptides had overlapping elution profiles. Solubility was approximately 10 μM. Poor cleavage and solubility encouraged more sub-cloning steps (Figure 4.2). The final expression vector used here was pET15b-p57-ID6 (Figure 4.2). This p57-ID6 (residues 26–98) is soluble to approximately 50 μM; while not as soluble as the homologous p27ID it does represent a better than 50-fold increase in solubility over p57-ID1.

p57-ID6 was expressed using the plasmid pET15b-p57ID6. One ml of overnight culture of pT7-PCNA-transformed *Escherichia coli* strain BL21(DE3) was used per 1 L LB medium containing 50 mg/L ampicillin. Six 1-L cultures were incubated at 37 °C until the optical density at 600 nm was 0.6 and were then induced with 0.5 mM IPTG at 37 °C for 3 hours. The cells were harvested by centrifugation in a Beckman JS-4.2 rotor at 4 °C for 30 minutes. Each cell pellet was resuspended in 10 ml His-bind buffer (5 mM imidazole, 500 mM NaCl, 20 mM Tris-HCl, pH 7.9). The cells were lysed by sonication and centrifuged at 15 krpm using a Beckman JA20 rotor at 4 °C for 25 minutes. The soluble fraction was loaded onto a 10-ml His-bind resin column (1.5 cm diameter) at 4 °C charged with 50 mM $NiSO_4$ and

```
p57-ID1 MSDASLRSTSTMERLVARGTFPVLVRTSACRSLFGPVDHEELSRELQARLAELNAEDQNRWDYDFQQDMPLRGP
p57-ID2                         MLVRTSACRSLFGPVDHEELSRELQARLAELNAEDQNRWDYDFQQDMPLRGP
p57-ID3   MGSSHHHHHHSSGLVPRGSHMLVRTSACRSLFGPVDHEELSRELQARLAELNAEDQNRWDYDFQQDMPLRGP
p57-ID4                               MTSACRSLFGPVDHEELSRELQARLAELNAEDQNRWDYDFQQDMPLRGP
p57-ID6      MGSSHHHHHHSSGLVPRGSHMTSACRSLFGPVDHEELSRELQARLAELNAEDQNRWDYDFQQDMPLRGP
p27-ID   MGSSHHHHHHSSGLVPRGSHMEHPKPSACRNLFGPVDHEELTRDLEKHCRDMEEASQRKWNFDFQNHKPLEGK
```

			Sol.	Expr.
p57-ID1	GRLQWTEVDSDSVPAFYRETVQVGRCRLLLAP	p57 residues 1 -106	1 μM	Poor
p57-ID2	GRLQWTEVDSDSVPAFYRETVQVGRCRLLLAP	p57 residues 23-106	n/a	Poor
p57-ID3	GRLQWTEVDSDSVPAFYRETVQVGRCRLLLAP	p57 residues 23-106+ His-Tag	10 μM	Low
p57-ID4	GRLQWTEVDSDSVPAFYRETVQVG	p57 residues 26-97	n/a	Low
p57-ID6	GRLQWTEVDSDSVPAFYRETVQVG	p57 residues 26-97 + His-Tag	50 μM	Good
p27-ID	YEWQEVEKGSLPEFY	p27 residues 22-88 + His-Tag	100 μM	Excellent

Figure 4.2. p57-Inhibition Domains
Early attempts at making a functional isolated p57-inhibition domain used a larger number of relative residues than the homologous p27-inhibition domain. The final p57-inhibition domain represents overall a very similar number of residues as compared to p27ID. The last two columns give estimates of solubility and expression levels.

equilibrated in His-bind buffer. The column was washed with 50-ml His-bind buffer, followed by a 50 ml wash with His-wash buffer (60 mM imidazole, 500 mM NaCl, 20 mM Tris-HCl, pH 7.9). p57-ID6 was eluted with 50 ml His-elute buffer (1 M imidazole, 500 mM NaCl, 20 mM Tris-HCl, pH 7.9). EDTA was added to a final concentration of 50 mM to the eluted fraction to chelate Ni^{2+} before adding 50 mM DTT to reduce disulfide bonds. The eluted fraction was dialysed (Spectrapor 2 kDa MWCO) at 4 °C overnight against 4 L thrombin cleavage buffer (150 mM NaCl, 2.5 mM $CaCl_2$, 20 mM Tris-HCl, pH 8.4).

40 units of thrombin (Novagen 69671) were added to the dialysate and incubated for 24 hours. His-tag cleavage was confirmed with SDS-PAGE with 16 % gels. Final purification of p57-ID6 was by reversed-phase C_{18} HPLC using linear acetonitrile/water gradients containing 0.1 % TFA. Pure p57-ID6 was stored as a lyophilized powder. The expected mass for p57-ID6 was 8896 Da and the mass observed by MALDI mass spectrometry was 8895 Da. Yield was approximately 3 mg/L.

4.1.c Phosphorylation Assays

Cyclin A-Cdk2 activity was assayed by quantifying histone H1 phosphorylation at 30 °C as described in section 2.1.h, except reactions contained 50 nM cyclin A-Cdk2. The extent of inhibition was used as a measure of the extent of binding in a nonlinear least squares fit to calculate K_d values assuming a 1:1 binding stoichiometry. This fit used the following

equation, where K_a is the association constant, [A] is the ligand concentration, E_f is the extent of the reaction when the enzyme is fully occupied with inhibitor, and E_u is the extent of the reaction when the enzyme is unoccupied with inhibitor.

$$y = (\frac{K_a[A]}{1 + K_a[A]}(E_f - E_u)) + E_u$$

4.1.d Biophysical Methods

CD spectra were collected on Jasco J720 and Aviv 62DS spectrometers. Samples contained 10 μM protein in 10 mM sodium phosphate, 50 mM NaCl, 1 mM DTT, pH 7.0. Protein concentrations were determined by absorbance in 6 M GuHCl, 150 mM NaCl, pH 6.5 using extinction coefficients at 280 nm of 13940 M^{-1} cm^{-1} and 14440 M^{-1} cm^{-1} for p57-ID6 and p57, respectively (Edelhoch, 1967). Helix content was estimated from f_H =-($[\theta]_{222}$ + 2340)/30,300 where f_H is fraction of helix (Chen et al., 1972) or using CDPro (Sreerama et al., 2000; Sreerama and Woody, 2000).

Sedimentation equilibrium experiments were performed with a Beckman XL-I. Data were collected at 5 °C and 280 nm at rotor speeds of 40 and 48 krpm on samples of total p57-ID6 concentrations of approximately 50 μM, 30 μM, and 15 μM. Samples were dialyzed against 10 mM sodium phosphate, 150 mM NaCl, 1 mM DTT, pH 7.0. A solvent density of 1.01 g ml^{-1} and a partial molar volume of 0.704 was calculated as described elsewhere (Laue et al.,

1992) and adjusted for temperature (McRorie and Voelker, 1993). Data sets were fit by non-linear least squares analysis to a single-species model using ORIGIN (Beckman Instruments).

4.1.e Gel Filtration Chromatography

The Stokes's radius of p57-ID6 at 4 °C was determined by gel filtration (Siegel and Monty, 1966) on Sephacryl S-100 (1.6 X 60 cm) (Pharmacia 17-1165-01) equilibrated in 10 mM sodium phosphate, 150 mM NaCl, 1 mM DTT, pH 7.5. The separation range for globular proteins on this column was 1-100 kDa with a flow rate of 0.1-0.5 ml/minute. The flow rate used here was 0.2 ml/minute. The column was calibrated with bovine RNase A, bovine chymotrypsinogen A, hen ovalbumin, bovine serum albumin, and Blue Dextran 2000.

4.2 RESULTS

4.2.a Activity and K_d of p57 and p57-ID6

The inhibition activity of full-length p57 is similar to p27ID, with a slightly lower K_d value of 16 ± 2 nM (Figure 4.3). The kinase assays for p57-ID6 were not inhibiting to completion at lower concentration with the typical 10 minute pre-equilibration time. Increasing that time to 1 hour prior to adding ATP gave results more in line with the full-length K_d determinations. The p57-ID6 inhibitor has a K_d value of 12.5 ± 2 nM and binds with an apparent 1:1 stoichiometry (Figure 4.3).

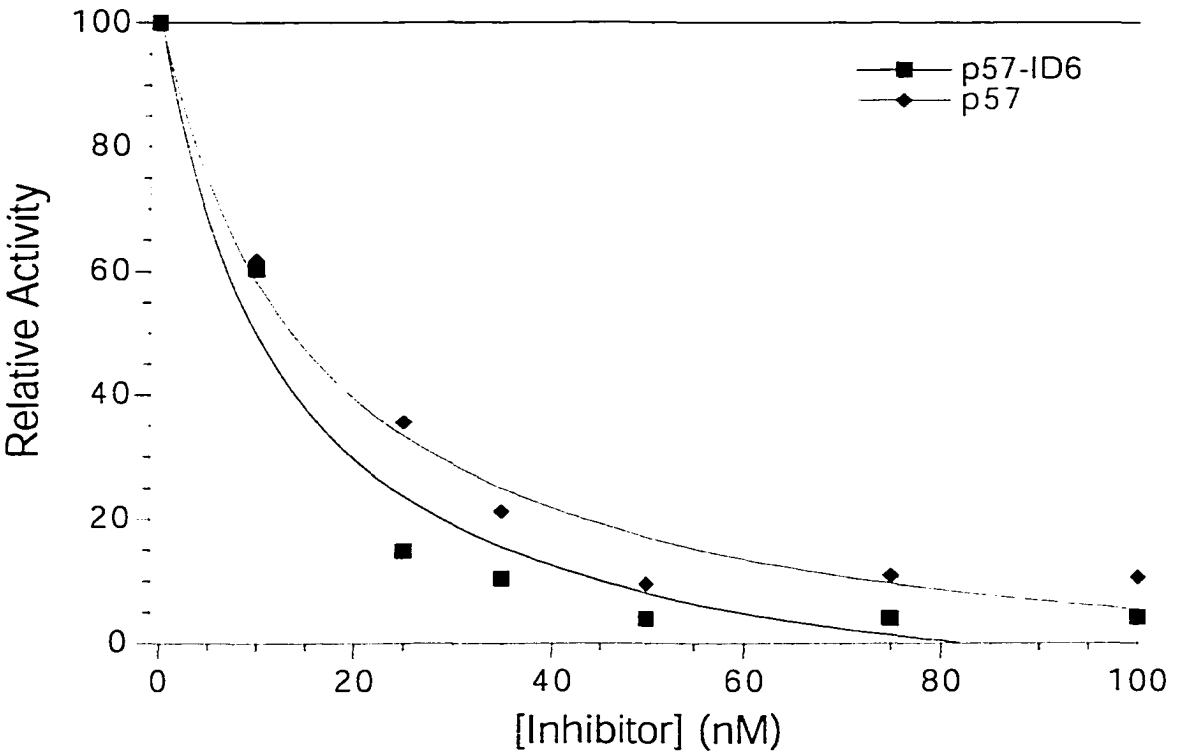

Figure 4.3. p57 and p57–ID6 K_d Determinations
p57 and p57–ID6 K_d determinations from cyclin A-Cdk2 inhibition assays.

4.2.b Secondary Structure Content of p57 and p57-ID6

The CD spectra of p57 and p57-ID6 are highly similar to those of p21 (Kriwacki et al., 1996) and p27ID (Figure 3.3). In contrast to the predictions by AGADIR, p57 and p57-ID6 (Figure 4.1) do not exhibit any significant increase in α-helix versus that measured for p27 or p21. Full-length p57 (Figure 4.4B) at 5 °C appears to have very little contribution to over all helix content from the C-terminal residues (99-316) absent in p57-ID6 (Figure 4.5B). Analysis by the Selcon3 program of the CDPro package (Sreerama et al., 2000; Sreerama and Woody, 2000) estimates a total helix content of approximately 11 % and strand/turn content to be approximately 57 % for p57, corresponding to approximately 34 residues of helix and 180 residues of turn/strand. The Selcon3 estimate of total helix is approximately 18 % and strand/turn is approximately 43 % for p57-ID6, corresponding to approximately 13 residues of helix and 31 residues of strand. Hence, strand and turn predominate the C-terminal of p57 while the N-terminal region has a higher average relative helix content. The region of helical content would probably map largely to the regions of p57-ID6 that are homologous to p27ID and have localized regions of helical propensity (section 3.2.c).

4.2.c Thermal stability of the secondary structures of p57 and p57-ID6

One of the early methods used to solubilize full-length p57 and some inhibition domain mutants was to heat to 95 °C for 1 minute. Others have

used this technique over prolonged incubation times for p21 and p27, and the inhibition activity was reported to be stable (Hengst and Reed 1996; Polak et al. 1994). This tended to increase solubility by approximately 50 %. Increasing solubility by this method was undesirable because the highest solubility was highly variable and resulted in anomalous concentration determinations. Making a saturated solution and clarifying the sample by microcentrifugation at 14 krpm (Eppendorf Centrifuge 5415C) for 10 minutes resulted in more reliable maximum solubilities (approximately 10 μM for p57 and 50 μM for p57-ID6).

Thermal denaturation of p57 suggests that it undergoes a structural change at higher temperatures that is not completely reversible upon cooling (Figure 4.4A). p57-ID6 also shows a change in the secondary structure upon heating and cooling (Figure 4.5A). Usually, a lack of thermal reversibility would suggest that a protein was not returning to its "native" state. Even accounting for a slight baseline shift some changes in the shape of the CD spectrum are occurring that may or may not be significant to function or over-all "disorder". In this case, the native state is "natively" unfolded.

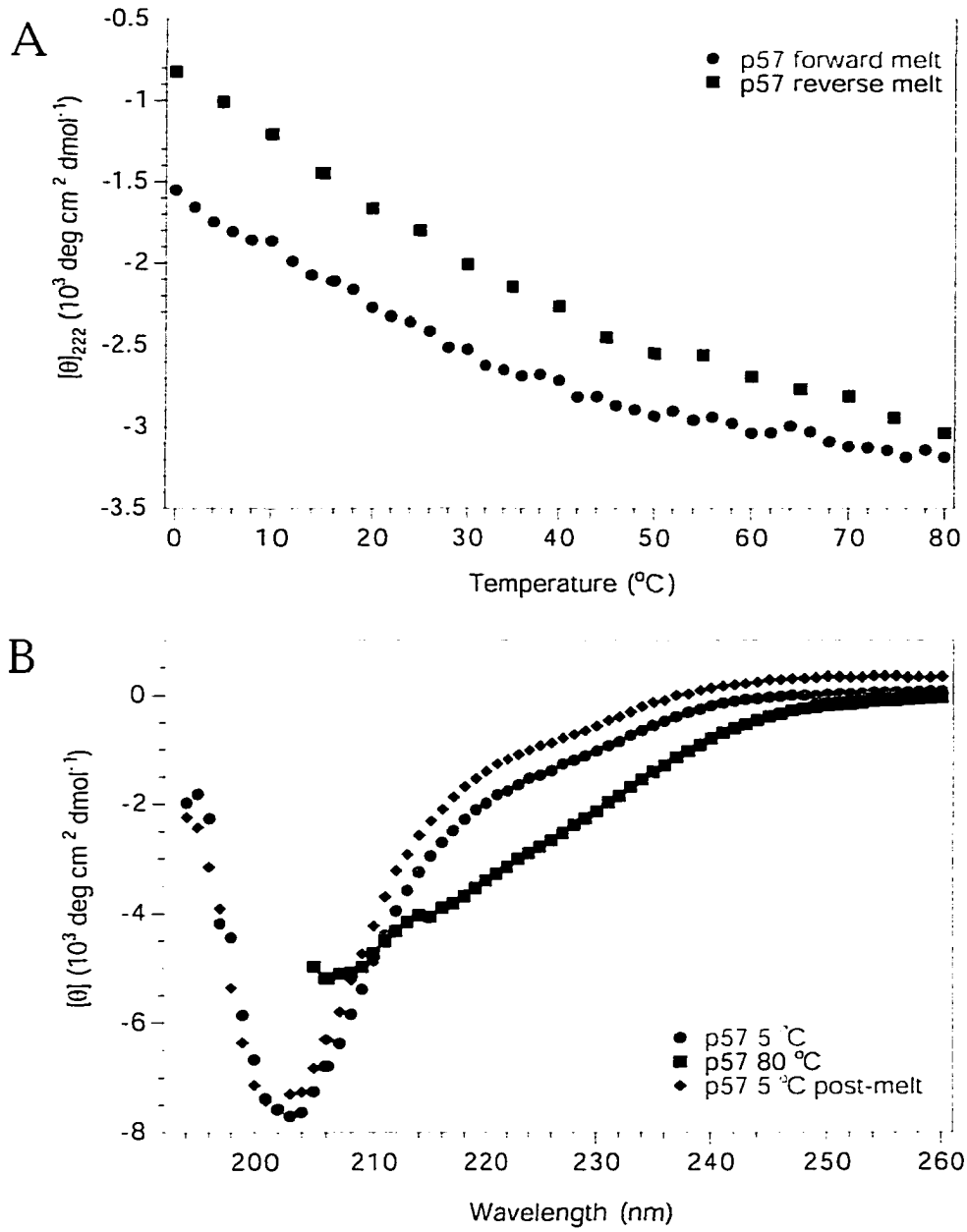

Figure 4.4. CD analysis of p57
A. Forward and reverse temperature melts of p57.
B. Wavelength CD spectra of p57 at 5 °C, 80 °C, and 5 °C after forward and reverse melts.

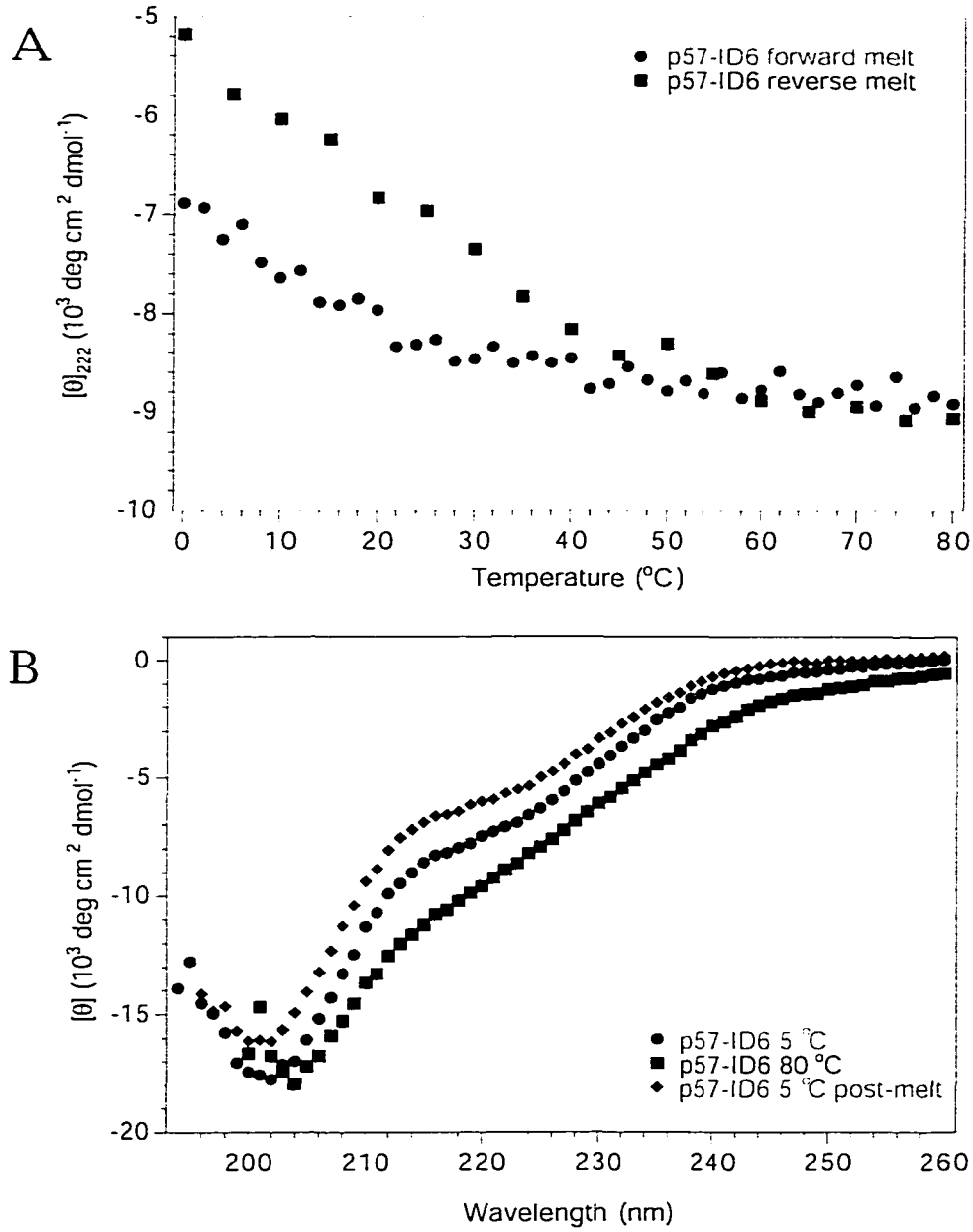

Figure 4.5. CD analysis of p57-ID6
A. Forward and reverse temperature melts of p57-ID6.
B. Wavelength CD spectra of p57-ID6 at 5 °C, 80 °C, and 5 °C after forward and reverse melts.

4.2.d Sedimentation Equilibrium of the p57-Inhibition Domain

The p57 inhibition domain was studied by sedimentation equilibrium (Figure 4.6). The observed molecular mass (10,066.6 Da ± 487 Da) was between 10 and 15 % higher than the expected molecular mass (8896.7 Da) with good residuals and variance of fit (Figure 4.6). p27ID and mutants display similarly high apparent molecular mass (data collected by Dr. E. A. Bienkiewicz and not shown). The inhibition domains of p27 and p57 may have anomalous partial specific volumes ($\bar{v}$), since these domains are "natively unfolded" and therefore unlikely to be hydrated in the same manner as a globular protein (Laue et al., 1992).

Denaturing proteins in guanidine-HCl or urea tends to either maintain the non-denatured $\bar{v}$ or to lower it, and in some cases this reduction is dramatic (Lee and Timasheff, 1974; Prakash and Timasheff, 1981). This could account for the discrepancy in molecular mass by sedimentation equilibrium. While these inhibition domains are not in denaturant, it is likely the hydration state of this family of Cdk inhibitors causes a reduction in $\bar{v}$ from the typical calculated value, in this case a change from about 0.71 to 0.68 would be ideal and not unreasonable for denatured protiens. Sedimentation equilibrium experiments in H_2O and D_2O could be used to determine the experimental $\bar{v}$ for these proteins (McRorie and Voelker, 1993).

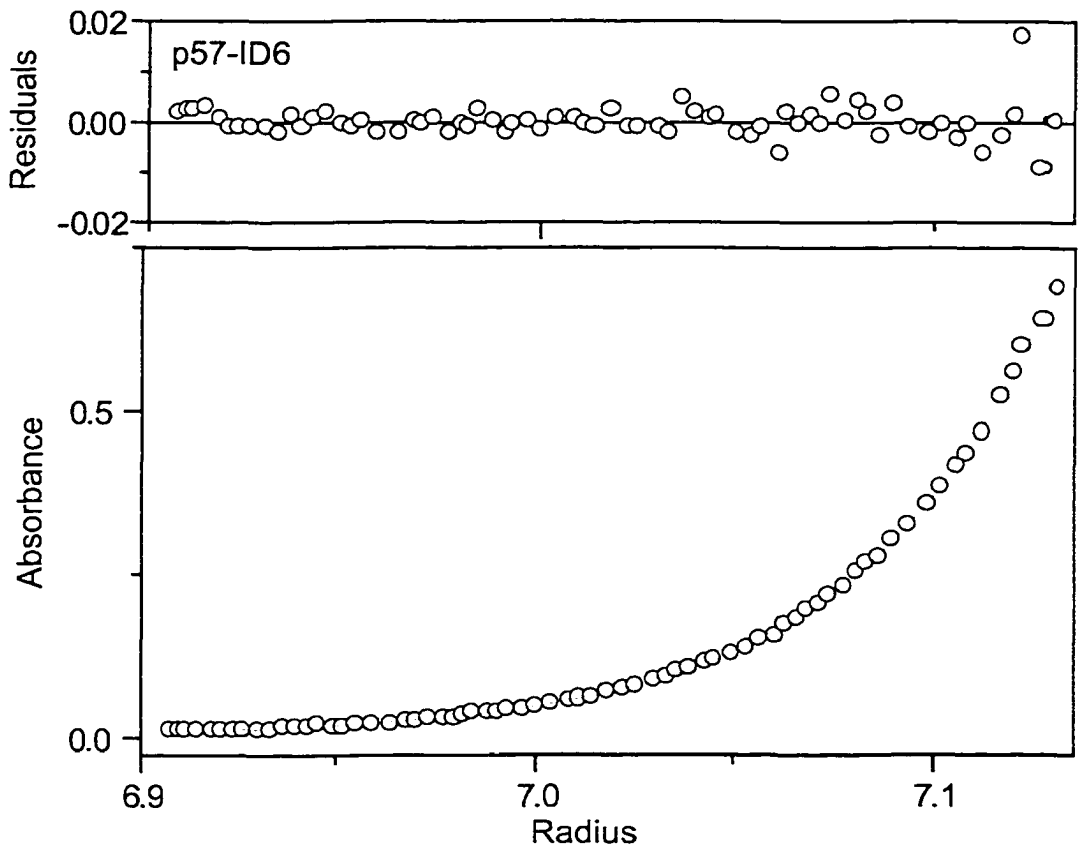

Figure 4.6. Sedimentation equilibrium analysis of p57-ID6
The data shown are from the 50 μM concentration cell and an angular velocity of 48 krpm with a variance of 0.842

4.2.e Stokes' Radius of p57-ID6

An apparent Stokes' radius of 24.1 Å for p57-ID6 was obtained using gel filtration (Figure 4.7). Results from sedimentation equilibrium studies indicate that p57-ID6 is monomeric (Figure 4.6). The expected Stokes' radius for a monomeric globular protein of equivalent molecular mass would be 12.8 Å. Because this protein is unfolded, the Stokes' radius probably reflects an ensemble of structures that are nearly twice that of a single compact globular fold.

4.3 DISCUSSION

p21 has been characterized as a "natively unfolded" protein (Kriwacki et al., 1996). The closely-related protein p57 has been shown here by spectroscopic and hydrodynamic data collectively indicating that it is largely unfolded.

Understanding the nature of natively unfolded proteins may eventually give structural proteomics researchers the ability to determine which protein structures to solve and early information on how to approach those structure determinations. Using predictive tools, like AGADIR, to determine proteins with similar sequences, but with properties for aggregation can further clarify where efforts should be concentrated. As an example, an AGADIR comparison between peptides of the inhibition domains of p21, p27, and p57

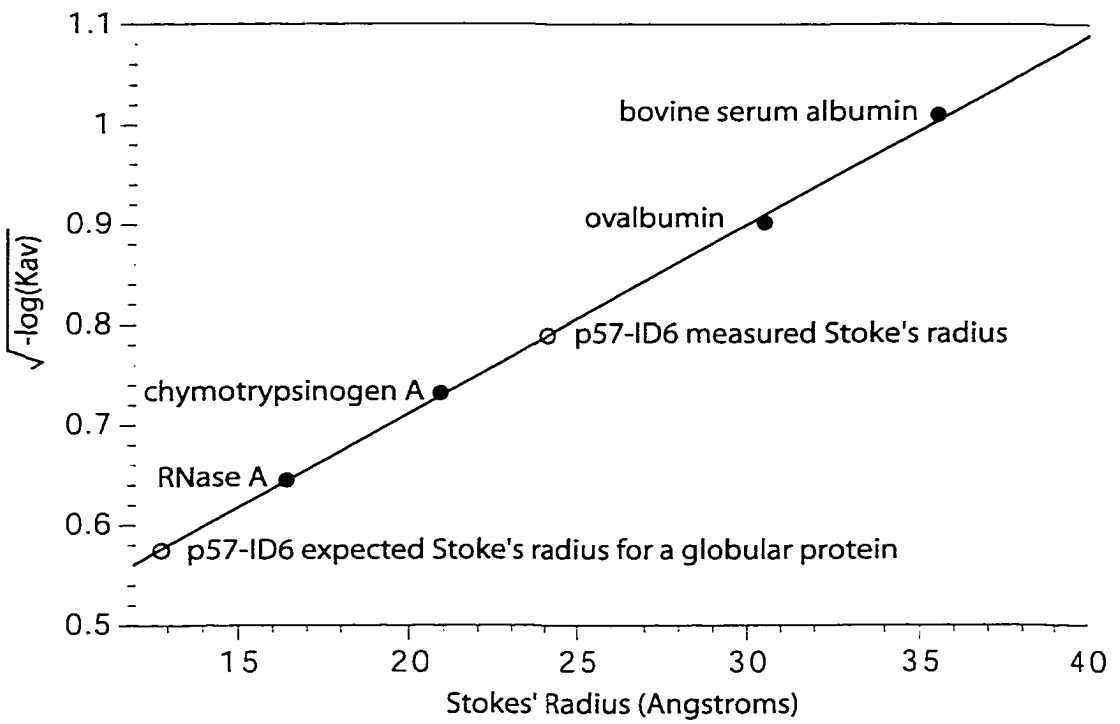

Figure 4.7. Stokes' Radius of p57-ID6

shows that p57 is predicted to have the highest helical content at approximately 53 % in one region (Figure 4.8). The monomeric inhibition domain does not have an increased tendency towards helicity when measured by CD, but the helix propensity could have some function in p57's tendency to aggregate (West et al., 1999; Rochet and Lansbury, 2000). Therefore, a complete understanding of the extended nature of a entire family of "natively unfolded" proteins could help in the design of methods for further study and prediction of these types of proteins.

A stacked plot of the number of amino acids for the complete sequences of p21, p27, and p57 was made. On a different stacked plot the relatvie tendencies toward order and disorder (Xie et al., 1998) have been compiled for each amino acid using only those propensities that were not considered complex (i.e., not easily classified as only order/disorder promoting). This plot included the individual amino acids and the groupings of those amino acids *including aromatics, hydrophobic, most flexible, least flexible, etc.* (Xie et al., 1998). These plots together give a qualitative analysis of the tendency or propensity toward order ("-" correlation) and disorder ("+" correlation) (Figure 4.9). This qualitative analysis does correlate with the p21 family of proteins being typical "natively unfolded" proteins. This method of analyzing proteins for being ordered and disordered was designed to complement or parallel a separate algorithm utilizing a neural network trained with ordered and disordered protein data sets (Dunker et al., 1998; Garner et al., 1998; Romero et al., 1998; Romero et al., 2001).

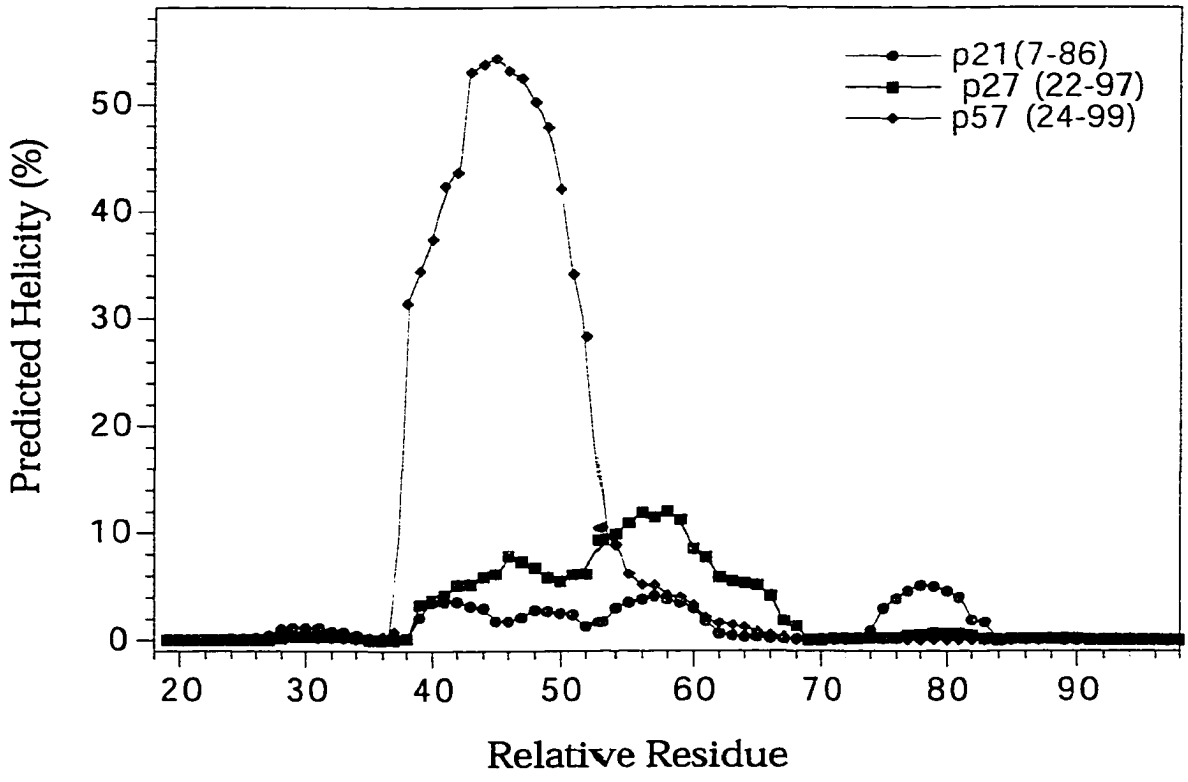

Figure 4.8. AGADIR Analysis of p21, p27, and p57 Inhibition Domains
Residue alignments are relative to the p27 sequence.

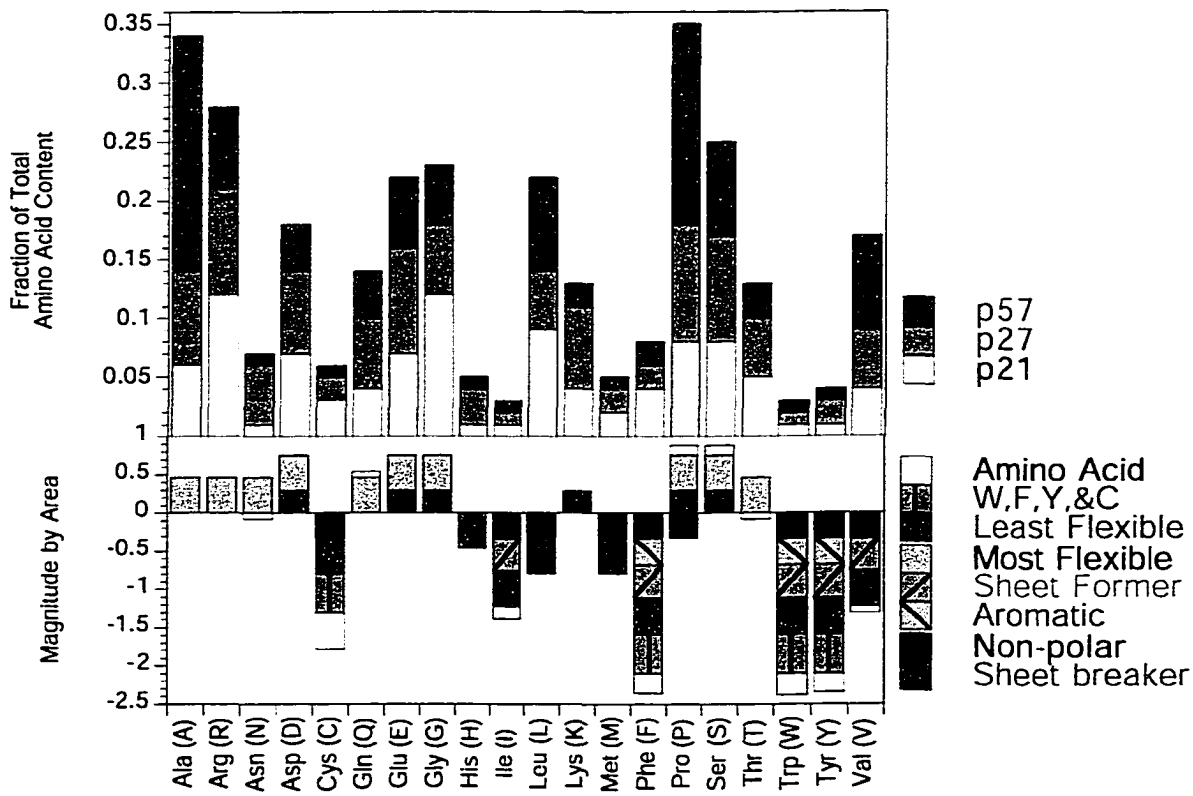

Figure 4.9. p21, p27, and p57 Amino Acid Content and Tendencies Toward Order and Disorder

The tendencies toward order ("-" correlation) and disorder ("+" correlation) have been compiled for each amino acid using the propensities that were not considered complex (Xie et al., 1998).

Analysis of p21, p27, and p57 using this PONDR (http://disorder.chem.wsu.edu/PONDR/PONDR.htm) predicted p21 to be largely structured, but p27 and p57 to be largely unstructured. Considering the correlation using order or disorder promoting amino acid propensities, the lack of correlation with p21 using the neural network method was unexpected. Neural networks for use in determining ordered or disordered proteins do not provide any functional information for their results. This lack of functional information and correlation with a known disordered protein means the neural network method of predicting protein order or disorder has not matured to be an important tool for prediction of proteins not analyzed by structural means.

The N-terminal domain of p21, p27, and p57 have been studied by different methods, and all are shown to be largely disordered in the unbound state. Future studies could characterize the extended confirmations and the functional the roles of the QT domains of p27 and p57, and the PAPA repeats of p57. Such analyses would further our knowledge of this family of "natively unfolded" proteins and may lead to a more general understanding of how "natively unfolded" proteins function.

APPENDIX A

Summary of Sedimentation Equilibrium Stoichiometry Experiments of p21 and p57

Protein(s)	Angular Velocity (krpm)	Temp. (K)	Meas. M_r	Expected M_r	Abs. (nm)	Instr[1]
cyclin A	18	293	46 kDa	49 kDa	280	XL-A
cyclin A	25	293	40 kDa	49 kDa	280	XL-A
cyclin A	32	293	16 kDa	49 kDa	280	XL-A
p57	18	293	26 kDa	32 kDa	230	XL-A
p57	25	293	22 kDa	32 kDa	230	XL-A
p57	32	293	16 kDa	32 kDa	230	XL-A
cyclin A-p57	18	293	37 kDa	81 kDa	230	XL-A
cyclin A-p57	25	293	27 kDa	81 kDa	230	XL-A
cyclin A-p57	32	293	20 kDa	81 kDa	230	XL-A
Cdk2	20	293	36 kDa	34 kDa	280	XL-A
Cdk2	30	293	25 kDa	34 kDa	280	XL-A
Cdk2	40	293	19 kDa	34 kDa	280	XL-A
cyclin A-Cdk2	20	293	76 kDa	82 kDa	280	XL-A
cyclin A-Cdk2	30	293	77 kDa	82 kDa	280	XL-A
p21	30	293	6.5 kDa	18 kDa	230	XL-A
p21	30	293	13.5 kDa	18 kDa	230	XL-A
p21	30	293	14 kDa	18 kDa	230	XL-A

p21-Cyclin A-Cdk2	6	293	109 kDa	102 kDa	280	XL-A
p21-Cyclin A-Cdk2	8	293	121 kDa	102 kDa	280	XL-A
p21-Cyclin A-Cdk2	10	293	140 kDa	102 kDa	280	XL-A
p21	40	293	15 kDa	18 kDa	230	XL-I
p21	40	293	14 kDa	18 kDa	230	XL-I
p21	40	293	14 kDa	18 kDa	230	XL-I
cyclin A-Cdk2	40	293	54 kDa	84 kDa	230	XL-I
cyclin A-Cdk2	40	293	46 kDa	84 kDa	230	XL-I
cyclin A-Cdk2	40	293	45 kDa	84 kDa	230	XL-I
cyclin A-Cdk2	40	293	45 kDa	84 kDa	230	XL-I
cyclin A-Cdk2	20	293	75 kDa	84 kDa	230	XL-I
cyclin A-Cdk2	20	293	82 kDa	84 kDa	230	XL-I
mini-cyclin A	15	283	34 kDa	30 kDa	230	XL-I
mini-cyclin A	20	283	82 kDa	30 kDa	230	XL-I
mini-cyclin A	20	283	28 kDa	30 kDa	230	XL-I
mini-cyclin A	30	283	24 kDa	30 kDa	230	XL-I
mini-cyclin A	30	283	30 kDa	30 kDa	230	XL-I
mini-cyclin A	40	283	17 kDa	30 kDa	230	XL-I
mini-cyclin A	20	283	227 kDa	30 kDa	230	XL-I
mini-cyclin A	20	283	154 kDa	30 kDa	230	XL-I

mini-cyclin A	20	283	174 kDa	30 kDa	230	XL-I
Cdk2	20	283	61 kDa	36 kDa	230	XL-I
Cdk2	20	283	93 kDa	36 kDa	230	XL-I
Cdk2	30	283	41 kDa	36 kDa	230	XL-I
Cdk2	30	283	40 kDa	36 kDa	230	XL-I
Cdk2	30	283	52 kDa	36 kDa	230	XL-I
Cdk2	40	283	35 kDa	36 kDa	230	XL-I
Cdk2	40	283	34 kDa	36 kDa	230	XL-I
Cdk2	40	283	38 kDa	36 kDa	230	XL-I
p21	20	283	23 kDa	18 kDa	230	XL-I
p21	20	283	18 kDa	18 kDa	230	XL-I
p21	20	283	26 kDa	18 kDa	230	XL-I
p21	30	283	21 kDa	18 kDa	230	XL-I
p21	30	283	13 kDa	18 kDa	230	XL-I
p21	30	283	10 kDa	18 kDa	230	XL-I
p21	40	283	14 kDa	18 kDa	230	XL-I
p21	40	283	8 kDa	18 kDa	230	XL-I
p21	40	283	5 kDa	18 kDa	230	XL-I
mini-cyclin A/Cdk2	15	278	62 kDa	65 kDa	230	XL-I
mini-cyclin A/Cdk2	15	278	65 kDa	65 kDa	230	XL-I
mini-cyclin A/Cdk2	15	278	68 kDa	65 kDa	230	XL-I

mini-cyclin A/Cdk2	22.5	278	68 kDa	65 kDa	230	XL-I
mini-cyclin A/Cdk2	22.5	278	64 kDa	65 kDa	230	XL-I
mini-cyclin A/Cdk2	22.5	278	68 kDa	65 kDa	230	XL-I
mini-cyclin A/Cdk2	30	278	70 kDa	65 kDa	230	XL-I
mini-cyclin A/Cdk2	30	278	66 kDa	65 kDa	230	XL-I
mini-cyclin A/Cdk2	30	278	67 kDa	65 kDa	230	XL-I

[1]Two analytical ultracentrifuges were used in these experiments. Prior to the acquisition of the XL-I at CSU, we used the XL-A at the University of Colorado Health Sciences Center.

APPENDIX B

Biophysical Characterization of the 4-Helix Bundle of TFIIA

This work, together with the transcription data collected by R. Ogg and M. Robinson, was published in *Proteins* (Stargell et al., 2001).

B.0 INTRODUCTION

Initiation of transcription on a TATA-containing RNA polymerase II promoter is a complex process, involving a large number of interactions between multiple factors. These factors include TFIID, comprising the TATA-binding protein (TBP) and TBP-associated factor, TFIIA, TFIIB, TFIIE, TFIIF, TFIIH, and RNA polymerase II (Lemon and Tjian, 2000). An important step in initiation complex assembly is the recognition of the TATA element by TBP and the formation of a stable TBP-TATA complex. TFIIA binds both TBP and DNA directly, and at least part of the functional role of TFIIA is related to stabilization of the TBP-DNA interaction (Buratowski et al., 1988; Cortes et al., 1992; Lieberman and Berk, 1994; Ozer et al., 1994; Sun et al., 1994; Yokomori et al., 1994; Kobayashi et al., 1995). TFIIA has also been implicated in mediating the response to transcriptional activators (Lieberman and Berk, 1994; Ozer et al., 1994; Sun et al., 1994; Yokomori et al., 1994; Kobayashi et al., 1995), and in relieving the inhibitory effects of

transcriptional repressors (Meisterernst and Roeder, 1991; Meisterernst et al., 1991; Inostroza et al., 1992; Auble and Hahn, 1993; Merino et al., 1993; Kokubo et al., 1998; Liu et al., 1998).

TFIIA is highly conserved among eukaryotes both in primary sequence and function (DeJong and Roeder, 1993; Yokomori et al., 1994; Oya and Schulz, 2000). Yeast TFIIA is a heterodimer of two proteins encoded by the essential genes TOA1 and TOA2 (Ranish et al., 1992). The crystal structure of the yeast TBP-TFIIA-DNA complex (Geiger et al., 1996; Tan et al., 1996) reveals that the Toa1 and Toa2 subunits of TFIIA are tightly associated and contribute equally to a six-stranded β-sheet domain and a left-handed four-helix bundle (Figure B.1). The β-domain of TFIIA makes all the TBP and DNA contacts (Geiger et al., 1996; Tan et al., 1996). In contrast, the four-helix bundle domain of TFIIA projects away from the remainder of the complex in the crystal structure, and does not contact TBP or DNA.

To investigate the role of the four-helix bundle of TFIIA, a fusion protein (called 4HB) corresponding to the four-helix bundle, but not the β-sheet domain, was characterized. Spectroscopic analyses establish that the 4HB folds as a stable, helical structure. *In vivo* studies by R. Ogg and M. Robinson demonstrate that 4HB is sufficient for recruiting the remainder of the initiation complex when fused to a DNA-binding domain. We conclude that interactions with TFIIA involving the four-helix bundle, in addition, to

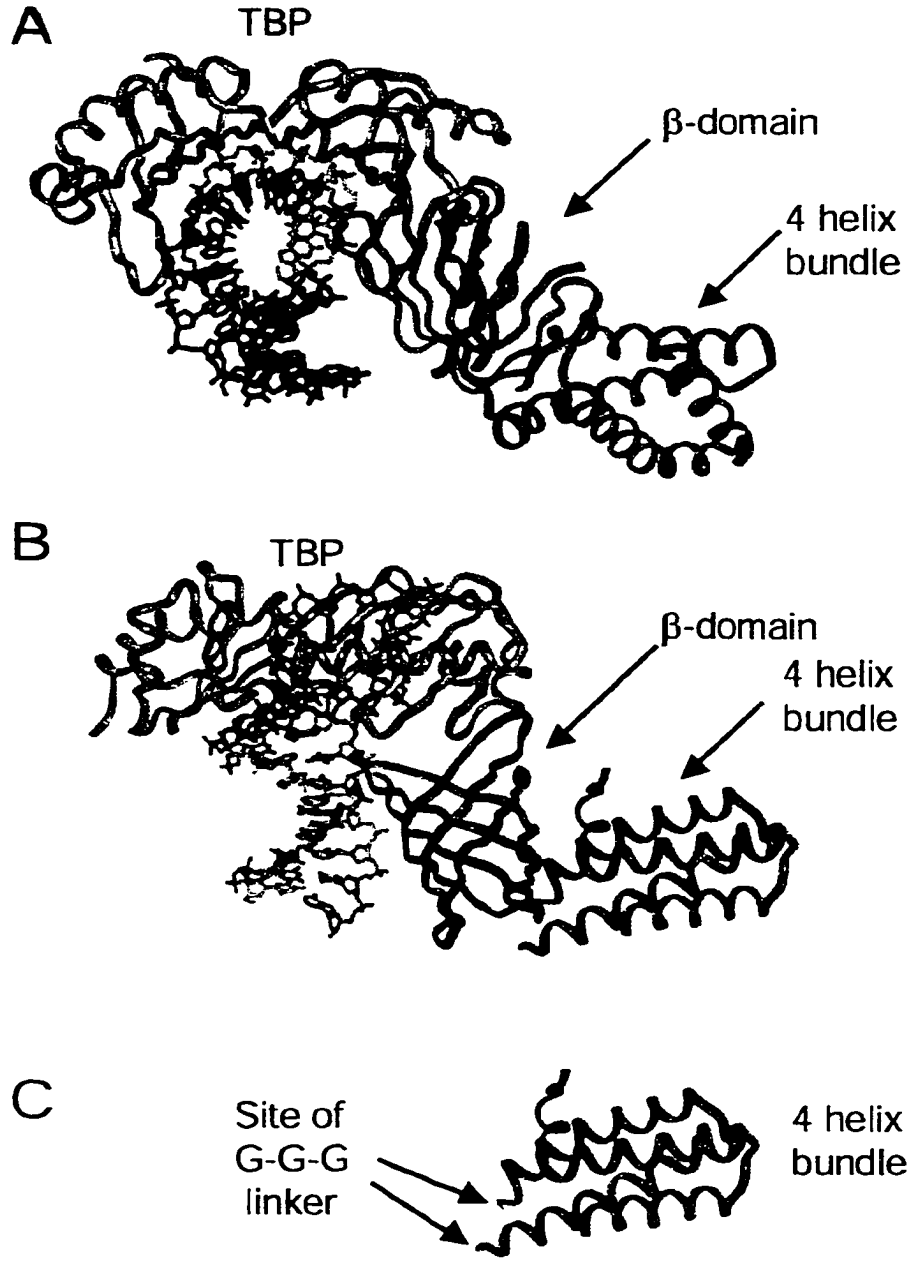

Figure B.1. Structure of the Yeast TFIIA-TBP-DNA Complex (Geiger et al., 1996; Tan et al., 1996)

A. Shown are TBP (gold ribbon), Toa1 (blue ribbon), Toa2 (red ribbon), and DNA (black ball and stick). Ternary complex viewed from the upstream region of DNA, with the TATA element perpendicular to the plane of the paper. The β-domain and the four-helix bundle of TFIIA are indicated.

B. Image A rotated 90°.

C. The region of TFIIA corresponding to 4HB.

those observed with TBP and DNA via the β-domain, play an important role in transcription initiation.

B.1 METHODS

B.1.a Circular Dichroism Spectroscopy

CD spectra were collected with a Jasco J720 spectrometer. Samples contained 10 μm 4HB in 10 mM sodium phosphate, 150 mM NaCl, 1 mM DTT, pH 7.0. 4HB concentration was determined by absorbance in 6 M GuHCl assuming an extinction coefficient at 276 nm of 18,050 M^{-1} cm^{-1} (Edelhoch, 1967). GuHCl concentration was determined by refractometry (Pace, 1986). Helix content was estimated from $[\theta]_{222}$ as described by Chen et al. (Chen et al., 1972).

B.1.b Analytical Ultracentrifugation

Sedimentation equilibrium and sedimentation velocity experiments were performed with a Beckman XL-I. Final sedimentation equilibrium analysis data were collected at 25 °C and 276 nm at rotor speeds of 30 and 40 krpm on samples of total 4HB concentration of approximately 14, 29, and 44 μM. Samples were dialyzed against the reference buffer (10 mM sodium phosphate, 150 mM NaCl, 1 mM DTT, pH 7.0). A solvent density of 1.01 g ml^{-1} and a partial molar volume of 0.722 ml g^{-1} were calculated for analysis (Laue et al., 1992). Data sets were fit to various models (i.e. single species, monomer-dimer, monomer-trimer, monomer-dimer-tetramer, and monomer-tetramer) using Origin (Beckman Instruments). Discrimination between the

various models was based on the distribution of residuals and the variance of fit.

B.2 RESULTS AND DISCUSSION

Circular Dichroism (CD) spectroscopy was used to characterize the secondary structure and stability of 4HB. The CD spectrum of 4HB contains double minima at 208 and 222 nm and a positive band at 190 nm (Figure B.2A), indicating that 4HB is highly helical (Woody, 1995). The helix content at 0 °C is 37 % estimated from $[\theta]_{222}$ (Chen et al., 1972). The helix content corresponds to 61 residues, which compares well with the 58 residues observed in helices in the crystal structure of TFIIA (Geiger et al., 1996; Tan et al., 1996). The midpoint of thermal denaturation (T_m) of 4HB exceeds 80 °C at neutral pH, and is approximately 70 °C in 2 M GuHCl, pH 7.0 (Figure B.2B).

Sedimentation equilibrium indicates that 4HB exists in a monomer-trimer equilibrium with an association constant of 4 x 10^4 M (Figure B.3A). 4HB is therefore 75 % and 90 % monomeric at concentrations of 5 and 1 μM, respectively (calculated using $K_a = (1-f)/3f^3c^2$ where K_a is the association constant, f is the monomer fraction and c is concentration).

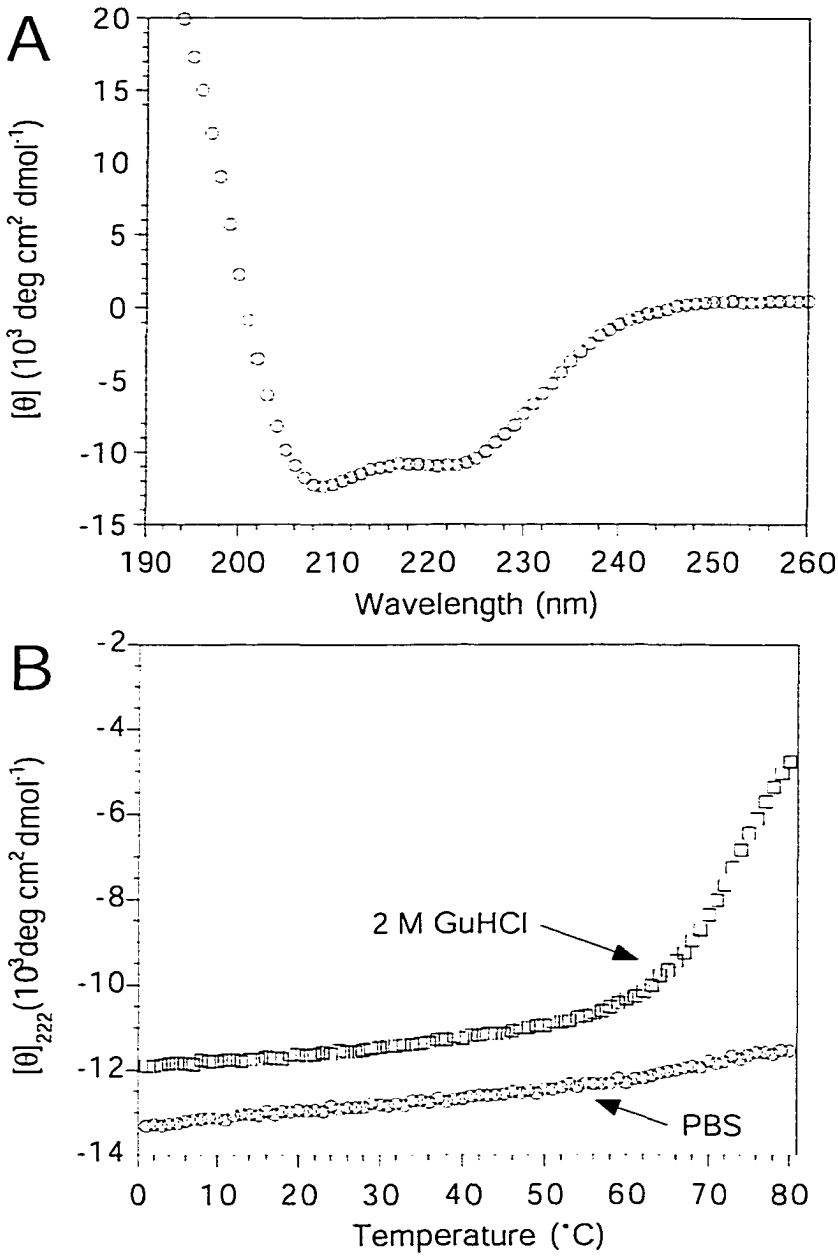

Figure B.2. 4HB folds as a Stable, Helical Monomer

A. CD wavelength spectrum of 4HB.

B. Temperature dependence of $[\theta]_{222}$ of 4HB (10 μM). The T_m of 4HB exceeds 80 °C and is approximately 70 °C in PBS containing 2 M GuHCl. The change in the folded baseline in the presence of GuHCl is reproducible.

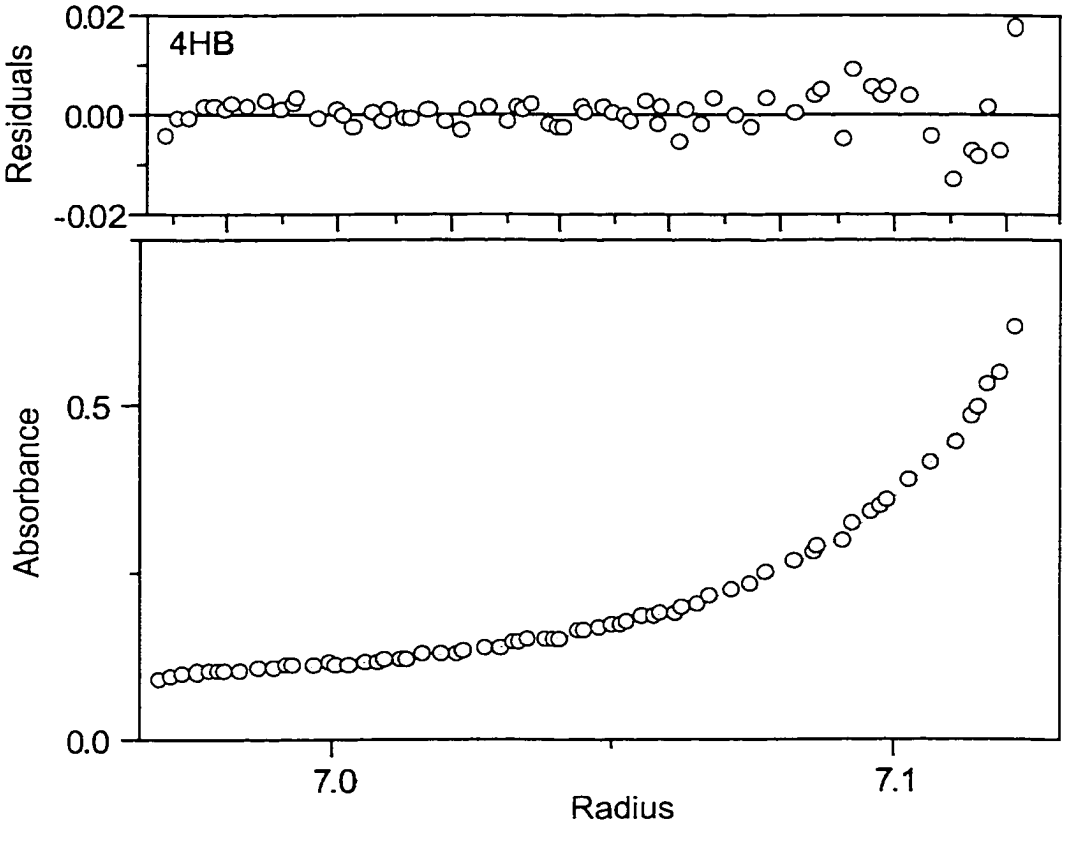

Figure B.3. Sedimentation Equilibrium of 4HB
Data shown are fit to monomer-trimer equilibrium. The variance is 0.84.

In vivo studies performed by R. C. Ogg, M. M. Robinson, Dr. L. A. Stargell showed, in artificial recruitment assays, that 4HB acts like a non-classical activator. This means that the role of the four-helix bundle domain of TFIIA in transcription is sensitive to promoter context for function and yet still has important interactions with the transcriptional machinery (Gaudreau et al., 1999; Nevado et al., 1999). Further, 4HB was analyzed for interactions related to oligomerization, i.e. recruitment of full-length TFIIA through dimerization. Two-hybrid analysis in yeast showed 4HB did not activate transcription through nucleating oligomerization. It was concluded that, in addition to making important contacts with TBP and DNA via the β-domain, TFIIA also makes additional specific contacts with the transcriptional machinery through the four-helix bundle domain.

References

Adkins, J. N. and Lumb, K. J. (2000). "Stoichiometry of cyclin A-cyclin-dependent kinase 2 inhibition by $p21^{Cip1/Waf1}$." *Biochemistry* **39**: 13925-30.

Alberts, B., Bray, D., Lewis, J., Raff, M., Roberts, K. and Watson, J. D. (1994). *Molecular Biology of the Cell.* New York, Garland Publishing, Inc.

Arai, M. and Kuwajima, K. (2000). "Role of the molten globule state in protein folding." *Adv Protein Chem* **53**: 209-82.

Auble, D. T. and Hahn, S. (1993). "An ATP-dependent inhibitor of TBP binding to DNA." *Genes Dev* **7**: 844-56.

Baldwin, R. L. and Rose, G. D. (1999). "Is protein folding hierarchic? I. Local structure and peptide folding." *Trends Biochem Sci* **24**: 26-33.

Ball, K. L., Lain, S., Fahraeus, R., Smythe, C. and Lane, D. P. (1997). "Cell-cycle arrest and inhibition of Cdk4 activity by small peptides based on the carboxy-terminal domain of $p21^{WAF1}$." *Curr Biol* **7**: 71-80.

Barlow, D. J. and Thornton, J. M. (1988). "Helix geometry in proteins." *J Mol Biol* **201**: 601-19.

Bienkiewicz, E. A., Adkins, J. N. and Lumb, K. J. (2001). "Contribution of local helix formation in the intrinsically disordered cell-cycle inhibitor $p27^{Kip1}$ to cyclin A-Cdk2 inhibition." *(submitted for publication).*

Bilsel, O. and Matthews, C. R. (2000). "Barriers in protein folding reactions." *Adv Protein Chem* **53**: 153-207.

Brotherton, D. H., Dhanaraj, V., Wick, S., Brizuela, L., Domaille, P. J., Volyanik, E., Xu, X., Parisini, E., Smith, B. O., Archer, S. J., Serrano, M., Brenner, S. L., Blundell, T. L. and Laue, E. D. (1998). "Crystal structure of the complex of the cyclin D-dependent kinase Cdk6 bound to the cell-cycle inhibitor $p19^{INK4d}$." *Nature* **395**: 244-50.

Brugarolas, J., Chandrasekaran, C., Gordon, J. I., Beach, D., Jacks, T. and Hannon, G. J. (1995). "Radiation-induced cell cycle arrest compromised by p21 deficiency." *Nature* **377**: 552-7.

Buratowski, S., Hahn, S., Sharp, P. A. and Guarente, L. (1988). "Function of a yeast TATA element-binding protein in a mammalian transcription system." *Nature* **334**: 37-42.

Cai, K. and Dynlacht, B. D. (1998). "Activity and nature of $p21^{WAF1}$ complexes during the cell cycle." *Proc Natl Acad Sci U S A* **95**: 12254-9.

Campbell, K. M., Terrell, A. R., Laybourn, P. J. and Lumb, K. J. (2000). "Intrinsic structural disorder of the C-terminal activation domain from the bZIP transcription factor Fos." *Biochemistry* **39**: 2708-13.

Card, G. L., Knowles, P., Laman, H., Jones, N. and McDonald, N. Q. (2000). "Crystal structure of a gamma-herpesvirus cyclin-Cdk complex." *EMBO J* **19**: 2877-88.

Carnero, A. and Hannon, G. J. (1998). "The INK4 family of CDK inhibitors." *Curr Top Microbiol Immunol* **227**: 43-55.

Chellappan, S. P., Giordano, A. and Fisher, P. B. (1998). "Role of cyclin-dependent kinases and their inhibitors in cellular differentiation and development." *Curr Top Microbiol Immunol* **227**: 57-103.

Chen, J., Jackson, P. K., Kirschner, M. W. and Dutta, A. (1995). "Separate domains of p21 involved in the inhibition of Cdk kinase and PCNA." *Nature* **374**: 386-8.

Chen, J., Peters, R., Saha, P., Lee, P., Theodoras, A., Pagano, M., Wagner, G. and Dutta, A. (1996). "A 39 amino acid fragment of the cell cycle regulator p21 is sufficient to bind PCNA and partially inhibit DNA replication in vivo." *Nucleic Acids Res* **24**: 1727-33.

Chen, Y. H., Yang, J. T. and Martinez, H. M. (1972). "Determination of the secondary structures of proteins by circular dichroism and optical rotatory dispersion." *Biochemistry* **11**: 4120-31.

Cheng, M., Olivier, P., Diehl, J. A., Fero, M., Roussel, M. F., Roberts, J. M. and Sherr, C. J. (1999). "The $p21^{Cip1}$ and $p27^{Kip1}$ CDK 'inhibitors' are essential activators of cyclin D-dependent kinases in murine fibroblasts." *EMBO J* **18**: 1571-83.

Cho, H. S., Liu, C. W., Damberger, F. F., Pelton, J. G., Nelson, H. C. and Wemmer, D. E. (1996). "Yeast heat shock transcription factor N-terminal activation domains are unstructured as probed by heteronuclear NMR spectroscopy." *Protein Sci* **5**: 262-9.

Christensen, T. (1979). *Peptides; structure and biological Function.* E. Gross and J. Meienhofer. Rockford, IL, Pierce Chemical Co.: 385-8.

Cole, R. D. (1989). "Purification and analysis of H1 histones." *Methods Enzymol* **170**: 524-32.

Cortes, P., Flores, O. and Reinberg, D. (1992). "Factors involved in specific transcription by mammalian RNA polymerase II: purification and analysis of transcription factor IIA and identification of transcription factor IIJ." *Mol Cell Biol* **12**: 413-21.

Creighton, T. E. (1993). *Proteins: Structures and molecular properties.* New York, W. H. Freeman and Company.

De Bondt, H. L., Rosenblatt, J., Jancarik, J., Jones, H. D., Morgan, D. O. and Kim, S. H. (1993). "Crystal structure of cyclin-dependent kinase 2." *Nature* **363**: 595-602.

DeJong, J. and Roeder, R. G. (1993). "A single cDNA, hTFIIA/alpha, encodes both the p35 and p19 subunits of human TFIIA." *Genes Dev* **7**: 2220-34.

Deng, C., Zhang, P., Harper, J. W., Elledge, S. J. and Leder, P. (1995). "Mice lacking $p21^{CIP1/WAF1}$ undergo normal development, but are defective in G1 checkpoint control." *Cell* **82**: 675-84.

Donehower, L. A., Harvey, M., Slagle, B. L., McArthur, M. J., Montgomery, C. A., Butel, J. S. and Bradley, A. (1992). "Mice deficient for p53 are developmentally normal but susceptible to spontaneous tumours." *Nature* **356**: 215-21.

Dunker, A. K., Garner, E., Guilliot, S., Romero, P., Albrecht, K., Hart, J., Obradovic, Z., Kissinger, C. and Villafranca, J. E. (1998). "Protein disorder and the evolution of molecular recognition: theory, predictions and observations." *Pac Symp Biocomput*: 473-84.

Dyer, M. A. and Cepko, C. L. (2000). "$p57^{Kip2}$ regulates progenitor cell proliferation and amacrine interneuron development in the mouse retina." *Development* **127**: 3593-605.

Edelhoch, H. (1967). "Spectroscopic determination of tryptophan and tyrosine in proteins." *Biochemistry* **6**: 1948-54.

El-Deiry, W. S. (1998). "p21/p53, cellular growth control and genomic integrity." *Curr Top Microbiol Immunol* **227**: 121-37.

El-Deiry, W. S., Tokino, T., Velculescu, V. E., Levy, D. B., Parsons, R., Trent, J. M., Lin, D., Mercer, W. E., Kinzler, K. W. and Vogelstein, B. (1993). "WAF1, a potential mediator of p53 tumor suppression." *Cell* **75**: 817-25.

Fero, M. L., Rivkin, M., Tasch, M., Porter, P., Carow, C. E., Firpo, E., Polyak, K., Tsai, L. H., Broudy, V., Perlmutter, R. M., Kaushansky, K. and

Roberts, J. M. (1996). "A syndrome of multiorgan hyperplasia with features of gigantism, tumorigenesis, and female sterility in $p27^{Kip1}$-deficient mice." *Cell* **85**: 733-44.

Fersht, A. R. (1997). "Nucleation mechanisms in protein folding." *Curr Opin Struct Biol* **7**: 3-9.

Fersht, A. R. (1999). *Structure and Mechanism in Protein Science.* New York, W. H. Freeman and Company.

Fisher, R. P. and Morgan, D. O. (1994). "A novel cyclin associates with MO15/CDK7 to form the CDK-activating kinase." *Cell* **78**: 713-24.

Fotedar, R., Fitzgerald, P., Rousselle, T., Cannella, D., Doree, M., Messier, H. and Fotedar, A. (1996). "p21 contains independent binding sites for cyclin and Cdk2: both sites are required to inhibit Cdk2 kinase activity." *Oncogene* **12**: 2155-64.

Funk, J. O. and Galloway, D. A. (1998). "Inhibiting CDK inhibitors: new lessons from DNA tumor viruses." *Trends Biochem Sci* **23**: 337-41.

Furusaki, A., Hashiba, N., Matsumoto, T., Hirano, A., Iwai, Y. and Omura, S. (1982). *Bull Chem Soc Jpn* **55**: 3681-5.

Gao, X., Chen, Y. Q., Wu, N., Grignon, D. J., Sakr, W., Porter, A. T. and Honn, K. V. (1995). "Somatic mutations of the WAF1/CIP1 gene in primary prostate cancer." *Oncogene* **11**: 1395-8.

Garner, E., Cannon, P., Romero, P., Obradovic, Z. and Dunker, A. K. (1998). "Predicting Disordered Regions from Amino Acid Sequence: Common Themes Despite Differing Structural Characterization." *Genome Inform Ser Workshop Genome Inform* **9**: 201-13.

Gaudreau, L., Keaveney, M., Nevado, J., Zaman, Z., Bryant, G. O., Struhl, K. and Ptashne, M. (1999). "Transcriptional activation by artificial recruitment in yeast is influenced by promoter architecture and downstream sequences." *Proc Natl Acad Sci U S A* **96**: 2668-73.

Geiger, J. H., Hahn, S., Lee, S. and Sigler, P. B. (1996). "Crystal structure of the yeast TFIIA/TBP/DNA complex." *Science* **272**: 830-6.

Gill, S. C. and von Hippel, P. H. (1989). "Calculation of protein extinction coefficients from amino acid sequence data." *Anal Biochem* **182**: 319-26.

Gu, Y., Turck, C. W. and Morgan, D. O. (1993). "Inhibition of CDK2 activity in vivo by an associated 20K regulatory subunit." *Nature* **366**: 707-10.

Gulbis, J. M., Kelman, Z., Hurwitz, J., O'Donnell, M. and Kuriyan, J. (1996). "Structure of the C-terminal region of $p21^{WAF1/CIP1}$ complexed with human PCNA." *Cell* **87**: 297-306.

Hadwiger, J. A., Wittenberg, C., Richardson, H. E., de Barros Lopes, M. and Reed, S. I. (1989). "A family of cyclin homologs that control the G1 phase in yeast." *Proc Natl Acad Sci U S A* **86**: 6255-9.

Harper, J. W., Adami, G. R., Wei, N., Keyomarsi, K. and Elledge, S. J. (1993). "The p21 Cdk-interacting protein Cip1 is a potent inhibitor of G1 cyclin- dependent kinases." *Cell* **75**: 805-16.

Harper, J. W. and Elledge, S. J. (1996). "Cdk inhibitors in development and cancer." *Curr Opin Genet Dev* **6**: 56-64.

Harper, J. W., Elledge, S. J., Keyomarsi, K., Dynlacht, B., Tsai, L. H., Zhang, P., Dobrowolski, S., Bai, C., Connell-Crowley, L., Swindell, E. and et al. (1995). "Inhibition of cyclin-dependent kinases by p21." *Mol Biol Cell* **6**: 387-400.

Hatada, I., Ohashi, H., Fukushima, Y., Kaneko, Y., Inoue, M., Komoto, Y., Okada, A., Ohishi, S., Nabetani, A., Morisaki, H., Nakayama, M., Niikawa, N. and Mukai, T. (1996). "An imprinted gene $p57^{KIP2}$ is mutated in Beckwith-Wiedemann syndrome." *Nat Genet* **14**: 171-3.

Heichman, K. A. and Roberts, J. M. (1994). "Rules to replicate by." *Cell* **79**: 557-62.

Hengst, L., Gopfert, U., Lashuel, H. A. and Reed, S. I. (1998). "Complete inhibition of Cdk/cyclin by one molecule of $p21^{Cip1}$." *Genes Dev* **12**: 3882-8.

Hengst, L. and Reed, S. I. (1998). "Inhibitors of the Cip/Kip family." *Curr Top Microbiol Immunol* **227**: 25-41.

Honig, B. (1999). "Protein folding: from the levinthal paradox to structure prediction." *J Mol Biol* **293**: 283-93.

Hooke, R. (1665). *Micrographia: Or some physiological descriptions of minute bodies made by magnifying glasses, with observations and inquiries thereupon.* J. Martyn and J. Allestry, London (facsimile edition, Culture et Civilization, Brussels).

Hunter, T. and Pines, J. (1994). "Cyclins and cancer. II: Cyclin D and CDK inhibitors come of age." *Cell* **79**: 573-82.

Inostroza, J. A., Mermelstein, F. H., Ha, I., Lane, W. S. and Reinberg, D. (1992). "Dr1, a TATA-binding protein-associated phosphoprotein and inhibitor of class II gene transcription." *Cell* **70**: 477-89.

Jeffrey, P. D., Russo, A. A., Polyak, K., Gibbs, E., Hurwitz, J., Massague, J. and Pavletich, N. P. (1995). "Mechanism of CDK activation revealed by the structure of a cyclinA-CDK2 complex." *Nature* **376**: 313-20.

Kaiser, E., Colescott, R. L., Bossinger, C. D. and Cook, P. I. (1970). "Color test for detection of free terminal amino groups in the solid- phase synthesis of peptides." *Anal Biochem* **34**: 595-8.

Kaldis, P. and Solomon, M. J. (2000). "Analysis of CAK activities from human cells." *Eur J Biochem* **267**: 4213-21.

Kaldis, P., Sutton, A. and Solomon, M. J. (1996). "The Cdk-activating kinase (CAK) from budding yeast." *Cell* **86**: 553-64.

Karaiskou, A., Jessus, C., Brassac, T. and Ozon, R. (1999). "Phosphatase 2A and polo kinase, two antagonistic regulators of cdc25 activation and MPF auto-amplification." *J Cell Sci* **112**: 3747-56.

Kiyokawa, H., Kineman, R. D., Manova-Todorova, K. O., Soares, V. C., Hoffman, E. S., Ono, M., Khanam, D., Hayday, A. C., Frohman, L. A. and Koff, A. (1996). "Enhanced growth of mice lacking the cyclin-dependent kinase inhibitor function of $p27^{Kip1}$." *Cell* **85**: 721-32.

Kiyokawa, H. and Koff, A. (1998). "Roles of cyclin-dependent kinase inhibitors: lessons from knockout mice." *Curr Top Microbiol Immunol* **227**: 105-20.

Kobayashi, N., Boyer, T. G. and Berk, A. J. (1995). "A class of activation domains interacts directly with TFIIA and stimulates TFIIA-TFIID-promoter complex assembly." *Mol Cell Biol* **15**: 6465-73.

Koepp, D. M., Harper, J. W. and Elledge, S. J. (1999). "How the cyclin became a cyclin: regulated proteolysis in the cell cycle." *Cell* **97**: 431-4.

Koff, A., Cross, F., Fisher, A., Schumacher, J., Leguellec, K., Philippe, M. and Roberts, J. M. (1991). "Human cyclin E, a new cyclin that interacts with two members of the CDC2 gene family." *Cell* **66**: 1217-28.

Koff, A., Giordano, A., Desai, D., Yamashita, K., Harper, J. W., Elledge, S., Nishimoto, T., Morgan, D. O., Franza, B. R. and Roberts, J. M. (1992). "Formation and activation of a cyclin E-Cdk2 complex during the G1 phase of the human cell cycle." *Science* **257**: 1689-94.

Kokubo, T., Swanson, M. J., Nishikawa, J. I., Hinnebusch, A. G. and Nakatani, Y. (1998). "The yeast TAF145 inhibitory domain and TFIIA competitively bind to TATA- binding protein." *Mol Cell Biol* **18**: 1003-12.

Kondo, M., Matsuoka, S., Uchida, K., Osada, H., Nagatake, M., Takagi, K., Harper, J. W., Takahashi, T. and Elledge, S. J. (1996). "Selective maternal-allele loss in human lung cancers of the maternally expressed $p57^{KIP2}$ gene at 11p15.5." *Oncogene* **12**: 1365-8.

Kriwacki, R. W., Hengst, L., Tennant, L., Reed, S. I. and Wright, P. E. (1996). "Structural studies of $p21^{Waf1/Cip1/Sdi1}$ in the free and Cdk2-bound state: conformational disorder mediates binding diversity." *Proc Natl Acad Sci U S A* **93**: 11504-9.

LaBaer, J., Garrett, M. D., Stevenson, L. F., Slingerland, J. M., Sandhu, C., Chou, H. S., Fattaey, A. and Harlow, E. (1997). "New functional activities for the p21 family of CDK inhibitors." *Genes Dev* **11**: 847-62.

Laue, T. M., Shah, B. D., Ridgeway, T. M. and Pelletier, S. (1992). Computer-aided interpretation of analytical sedimentation data for proteins. *Analytical ultracentrifugation in biochemistry and polymer science*. Eds., S. E. Harding, A. J. Rowe and J. C. Horton. The Royal Society of Chemistry, Cambridge, England.

Lawrie, A. M., Noble, M. E., Tunnah, P., Brown, N. R., Johnson, L. N. and Endicott, J. A. (1997). "Protein kinase inhibition by staurosporine revealed in details of the molecular interaction with CDK2." *Nature Struct Biol* **4**: 796-801.

Lee, J. C. and Timasheff, S. N. (1974). "The calculation of partial specific volumes of proteins in guanidine hydrochloride." *Arch Biochem Biophys* **165**: 268-73.

Lee, M. H., Nikolic, M., Baptista, C. A., Lai, E., Tsai, L. H. and Massague, J. (1996). "The brain-specific activator p35 allows Cdk5 to escape inhibition by $p27^{Kip1}$ in neurons." *Proc Natl Acad Sci U S A* **93**: 3259-63.

Lee, M. H., Reynisdottir, I. and Massague, J. (1995). "Cloning of $p57^{KIP2}$, a cyclin-dependent kinase inhibitor with unique domain structure and tissue distribution." *Genes Dev* **9**: 639-49.

Lees, E. M. and Harlow, E. (1993). "Sequences within the conserved cyclin box of human cyclin A are sufficient for binding to and activation of cdc2 kinase." *Mol Cell Biol* **13**: 1194-201.

Lemon, B. and Tjian, R. (2000). "Orchestrated response: a symphony of transcription factors for gene control." *Genes Dev* **14**: 2551-69.

Lew, D. J. and Kornbluth, S. (1996). "Regulatory roles of cyclin dependent kinase phosphorylation in cell cycle control." *Curr Opin Cell Biol* **8**: 795-804.

Lieberman, P. M. and Berk, A. J. (1994). "A mechanism for TAFs in transcriptional activation: activation domain enhancement of TFIID-TFIIA--promoter DNA complex formation." *Genes Dev* **8**: 995-1006.

Liu, D., Ishima, R., Tong, K. I., Bagby, S., Kokubo, T., Muhandiram, D. R., Kay, L. E., Nakatani, Y. and Ikura, M. (1998). "Solution structure of a TBP-TAF(II)230 complex: protein mimicry of the minor groove surface of the TATA box unwound by TBP." *Cell* **94**: 573-83.

Lumb, K. J., Carr, C. M. and Kim, P. S. (1994). "Subdomain folding of the coiled coil leucine zipper from the bZIP transcriptional activator GCN4." *Biochemistry* **33**: 7361-7.

Masui, Y. and Markert, C. L. (1971). "Cytoplasmic control of nuclear behavior during meiotic maturation of frog oocytes." *J Exp Zool* **177**: 129-45.

Matsuoka, S., Edwards, M. C., Bai, C., Parker, S., Zhang, P., Baldini, A., Harper, J. W. and Elledge, S. J. (1995). "p57KIP2, a structurally distinct member of the $p21^{CIP1}$ Cdk inhibitor family, is a candidate tumor suppressor gene." *Genes Dev* **9**: 650-62.

Matsuoka, S., Thompson, J. S., Edwards, M. C., Bartletta, J. M., Grundy, P., Kalikin, L. M., Harper, J. W., Elledge, S. J. and Feinberg, A. P. (1996). "Imprinting of the gene encoding a human cyclin-dependent kinase inhibitor, $p57^{KIP2}$, on chromosome 11p15." *Proc Natl Acad Sci U S A* **93**: 3026-30.

McRorie, D. K. and Voelker, P. J. (1993). *Self-associating systems in the analytical ultracentrifuge*. Beckman Instruments, Inc., Palo Alto, CA.

Meisterernst, M. and Roeder, R. G. (1991). "Family of proteins that interact with TFIID and regulate promoter activity." *Cell* **67**: 557-67.

Meisterernst, M., Roy, A. L., Lieu, H. M. and Roeder, R. G. (1991). "Activation of class II gene transcription by regulatory factors is potentiated by a novel activity." *Cell* **66**: 981-93.

Merino, A., Madden, K. R., Lane, W. S., Champoux, J. J. and Reinberg, D. (1993). "DNA topoisomerase I is involved in both repression and activation of transcription." *Nature* **365**: 227-32.

Minor, D. L., Jr. and Kim, P. S. (1996). "Context-dependent secondary structure formation of a designed protein sequence." *Nature* **380**: 730-4.

Morgan, D. O. (1997). "Cyclin-dependent kinases: engines, clocks, and microprocessors." *Annu Rev Cell Dev Biol* **13**: 261-91.

Munoz, V., Cronet, P., Lopez-Hernandez, E. and Serrano, L. (1996). "Analysis of the effect of local interactions on protein stability." *Fold Des* **1**: 167-78.

Munoz, V. and Serrano, L. (1997). "Development of the multiple sequence approximation within the AGADIR model of alpha-helix formation: comparison with Zimm-Bragg and Lifson- Roig formalisms." *Biopolymers* **41**: 495-509.

Murray, A. and Hunt, T. (1993). *The cell cycle: An introduction.* Oxford University Press, Oxford, England.

Nakayama, K., Ishida, N., Shirane, M., Inomata, A., Inoue, T., Shishido, N., Horii, I. and Loh, D. Y. (1996). "Mice lacking $p27^{Kip1}$ display increased body size, multiple organ hyperplasia, retinal dysplasia, and pituitary tumors." *Cell* **85**: 707-20.

Nevado, J., Gaudreau, L., Adam, M. and Ptashne, M. (1999). "Transcriptional activation by artificial recruitment in mammalian cells." *Proc Natl Acad Sci U S A* **96**: 2674-7.

Noda, A., Ning, Y., Venable, S. F., Pereira-Smith, O. M. and Smith, J. R. (1994). "Cloning of senescent cell-derived inhibitors of DNA synthesis using an expression screen." *Exp Cell Res* **211**: 90-8.

Oya, M. and Schulz, W. A. (2000). "Decreased expression of $p57^{KIP2}$ mRNA in human bladder cancer." *Br J Cancer* **83**: 626-31.

Ozer, J., Moore, P. A., Bolden, A. H., Lee, A., Rosen, C. A. and Lieberman, P. M. (1994). "Molecular cloning of the small (gamma) subunit of human TFIIA reveals functions critical for activated transcription." *Genes Dev* **8**: 2324-35.

Pace, C. N. (1986). Determination and analysis of urea and guanidine hydrochloride henaturation curves. *Methods in Enzymology: Enzyme*

Structure. C. H. W. Hirs and S. N. Timasheff. Orlando, Academic Press, Inc. **131:** 266-80.

Pace, C. N., Vajdos, F., Fee, L., Grimsley, G. and Gray, T. (1995). "How to measure and predict the molar absorption coefficient of a protein." *Protein Sci* **4**: 2411-23.

Pauly, J. E. e. (1987). Studying cells: from light to electrons. *The American Association of Anatomists, 1888-1987. Essays on the History of Anatomy in America and a Report on the Membership -- Past and Present.* Ed., J. E. Pauly. Baltimore, Williams & Wilkins: 33-42.

Pavletich, N. P. (1999). "Mechanisms of cyclin-dependent kinase regulation: structures of Cdks, their cyclin activators, and Cip and INK4 inhibitors." *J Mol Biol* **287**: 821-8.

Pines, J. (1995). "Cell cycle. Confirmational change." *Nature* **376**: 294-5.

Polyak, K., Lee, M. H., Erdjument-Bromage, H., Koff, A., Roberts, J. M., Tempst, P. and Massague, J. (1994). "Cloning of $p27^{Kip1}$, a cyclin-dependent kinase inhibitor and a potential mediator of extracellular antimitogenic signals." *Cell* **78**: 59-66.

Prakash, V. and Timasheff, S. N. (1981). "The calculation of partial specific volumes of proteins in 8 M urea solution." *Anal Biochem* **117**: 330-5.

Ranish, J. A., Lane, W. S. and Hahn, S. (1992). "Isolation of two genes that encode subunits of the yeast transcription factor IIA." *Science* **255**: 1127-9.

Reid, L. H., Crider-Miller, S. J., West, A., Lee, M. H., Massague, J. and Weissman, B. E. (1996). "Genomic organization of the human $p57^{KIP2}$ gene and its analysis in the G401 Wilms' tumor assay." *Cancer Res* **56**: 1214-8.

Reynaud, E. G., Leibovitch, M. P., Tintignac, L. A., Pelpel, K., Guillier, M. and Leibovitch, S. A. (2000). "Stabilization of MyoD by direct binding to $p57^{Kip2}$." *J Biol Chem* **275**: 18767-76.

Rochet, J. C. and Lansbury, P. T., Jr. (2000). "Amyloid fibrillogenesis: themes and variations." *Curr Opin Struct Biol* **10**: 60-8.

Romero, P., Obradovic, Z., Kissinger, C. R., Villafranca, J. E., Garner, E., Guilliot, S. and Dunker, A. K. (1998). "Thousands of proteins likely to have long disordered regions." *Pac Symp Biocomput*: 437-48.

Romero, P., Obradovic, Z., Li, X., Garner, E. C., Brown, C. J. and Dunker, A. K. (2001). "Sequence complexity of disordered protein." *Proteins* **42**: 38-48.

Rosenblatt, J., De Bondt, H., Jancarik, J., Morgan, D. O. and Kim, S. H. (1993). "Purification and crystallization of human cyclin-dependent kinase 2." *J Mol Biol* **230**: 1317-9.

Russell, P. and Nurse, P. (1986). "cdc25+ functions as an inducer in the mitotic control of fission yeast." *Cell* **45**: 145-53.

Russell, P. and Nurse, P. (1987). "Negative regulation of mitosis by wee1+, a gene encoding a protein kinase homolog." *Cell* **49**: 559-67.

Russo, A. A., Jeffrey, P. D., Patten, A. K., Massague, J. and Pavletich, N. P. (1996a). "Crystal structure of the $p27^{Kip1}$ cyclin-dependent-kinase inhibitor bound to the cyclin A-Cdk2 complex." *Nature* **382**: 325-31.

Russo, A. A., Jeffrey, P. D. and Pavletich, N. P. (1996b). "Structural basis of cyclin-dependent kinase activation by phosphorylation." *Nature Struct Biol* **3**: 696-700.

Russo, A. A., Tong, L., Lee, J. O., Jeffrey, P. D. and Pavletich, N. P. (1998). "Structural basis for inhibition of the cyclin-dependent kinase Cdk6 by the tumour suppressor $p16^{INK4a}$." *Nature* **395**: 237-43.

Schnolzer, M., Alewood, P., Jones, A., Alewood, D. and Kent, S. B. (1992). "In situ neutralization in Boc-chemistry solid phase peptide synthesis. Rapid, high yield assembly of difficult sequences." *Int J Pept Protein Res* **40**: 180-93.

Schulman, B. A., Lindstrom, D. L. and Harlow, E. (1998). "Substrate recruitment to cyclin-dependent kinase 2 by a multipurpose docking site on cyclin A." *Proc Natl Acad Sci U S A* **95**: 10453-8.

Selwyn, M. J. (1965). "A simple test for inactivation of an enzyme during assay." *Biochim Biophys Acta* **105**: 193-5.

Serrano, L. (2000). "The relationship between sequence and structure in elementary folding units." *Adv Protein Chem* **53**: 49-85.

Sherr, C. J. (1993). "Mammalian G1 cyclins." *Cell* **73**: 1059-65.

Sherr, C. J. and Roberts, J. M. (1999). "CDK inhibitors: positive and negative regulators of G1-phase progression." *Genes Dev* **13**: 1501-12.

Siegel, L. M. and Monty, K. J. (1966). "Determination of molecular weights and frictional ratios of proteins in impure systems by use of gel filtration and density gradient centrifugation. Application to crude

preparations of sulfite and hydroxylamine reductases." *Biochim Biophys Acta* **112**: 346-62.

Solomon, M. J., Harper, J. W. and Shuttleworth, J. (1993). "CAK, the $p34^{cdc2}$ activating kinase, contains a protein identical or closely related to $p40^{MO15}$." *EMBO J* **12**: 3133-42.

Songyang, Z., Blechner, S., Hoagland, N., Hoekstra, M. F., Piwnica-Worms, H. and Cantley, L. C. (1994). "Use of an oriented peptide library to determine the optimal substrates of protein kinases." *Curr Biol* **4**: 973-82.

Sreerama, N., Venyaminov, S. Y. and Woody, R. W. (2000). "Estimation of protein secondary structure from circular dichroism spectra: inclusion of denatured proteins with native proteins in the analysis." *Anal Biochem* **287**: 243-51.

Sreerama, N. and Woody, R. W. (2000). "Estimation of protein secondary structure from circular dichroism spectra: comparison of CONTIN, SELCON, and CDSSTR methods with an expanded reference Set." *Anal Biochem* **287**: 252-60.

Stargell, L. A., Ogg, R. C., Adkins, J. N., Robinson, M. M. and Lumb, K. J. (2001). "Transcription Activity of the TFIIA Four-Helix Bundle in vivo." *Proteins* **43**: 227-32.

Stewart, J. M. and Young, J. D. (1984). *Solid phase peptide synthesis*. New York, Pierce Chemical Company.

Sun, X., Ma, D., Sheldon, M., Yeung, K. and Reinberg, D. (1994). "Reconstitution of human TFIIA activity from recombinant polypeptides: a role in TFIID-mediated transcription." *Genes Dev* **8**: 2336-48.

Taddei, N., Chiti, F., Fiaschi, T., Bucciantini, M., Capanni, C., Stefani, M., Serrano, L., Dobson, C. M. and Ramponi, G. (2000). "Stabilisation of alpha-helices by site-directed mutagenesis reveals the importance of secondary structure in the transition state for acylphosphatase folding." *J Mol Biol* **300**: 633-47.

Takahashi, K., Kobayashi, T. and Kanayama, N. (2000). "$p57^{Kip2}$ regulates the proper development of labyrinthine and spongiotrophoblasts." *Mol Hum Reprod* **6**: 1019-25.

Tan, S., Hunziker, Y., Sargent, D. F. and Richmond, T. J. (1996). "Crystal structure of a yeast TFIIA/TBP/DNA complex." *Nature* **381**: 127-51.

Taylor, S. S. and Radzio-Andzelm, E. (1994). "Three protein kinase structures define a common motif." *Structure* **2**: 345-55.

Toyoshima, H. and Hunter, T. (1994). "p27, a novel inhibitor of G1 cyclin-Cdk protein kinase activity, is related to p21." *Cell* **78**: 67-74.

Tsugu, A., Sakai, K., Dirks, P. B., Jung, S., Weksberg, R., Fei, Y. L., Mondal, S., Ivanchuk, S., Ackerley, C., Hamel, P. A. and Rutka, J. T. (2000). "Expression of p57(KIP2) potently blocks the growth of human astrocytomas and induces cell senescence." *Am J Pathol* **157**: 919-32.

Urano, T., Hosoi, T., Shiraki, M., Toyoshima, H., Ouchi, Y. and Inoue, S. (2000). "Possible involvement of the $p57^{Kip2}$ gene in bone metabolism." *Biochem Biophys Res Commun* **269**: 422-6.

Uversky, V. N., Gillespie, J. R. and Fink, A. L. (2000). "Why are "natively unfolded" proteins unstructured under physiologic conditions?" *Proteins* **41**: 415-27.

Viguera, A. R., Villegas, V., Aviles, F. X. and Serrano, L. (1996). *Fold Des* **1**: 167-78.

Warbrick, E., Lane, D. P., Glover, D. M. and Cox, L. S. (1995). "A small peptide inhibitor of DNA replication defines the site of interaction between the cyclin-dependent kinase inhibitor $p21^{WAF1}$ and proliferating cell nuclear antigen." *Curr Biol* **5**: 275-82.

Watanabe, H., Pan, Z. Q., Schreiber-Agus, N., DePinho, R. A., Hurwitz, J. and Xiong, Y. (1998). "Suppression of cell transformation by the cyclin-dependent kinase inhibitor $p57^{KIP2}$ requires binding to proliferating cell nuclear antigen." *Proc Natl Acad Sci U S A* **95**: 1392-7.

Weinberg, R. A. (1995). "The retinoblastoma protein and cell cycle control." *Cell* **81**: 323-30.

West, M. W., Wang, W., Patterson, J., Mancias, J. D., Beasley, J. R. and Hecht, M. H. (1999). "De novo amyloid proteins from designed combinatorial libraries." *Proc Natl Acad Sci U S A* **96**: 11211-6.

Williamson, J. R. (2000). "Induced fit in RNA-protein recognition." *Nature Struct Biol* **7**: 834-7.

Wishart, D. S. and Sykes, B. D. (1994). "Chemical shifts as a tool for structure determination." *Methods Enzymol* **239**: 363-92.

Woody, R. W. (1992). Circular dichroism and conformation of unordered polypeptides. *Adv Biophys Chem* **2**: 37-9.

Woody, R. W. (1995). "Circular dichroism." *Methods Enzymol* **246**: 34-71.

Woody, R. W. and Dunker, A. K. (1996). *Circular Dichroism and the Conformational Analysis of Biomolecules.* G. D. Fasman. New York, Plenum Press.

Wright, P. E. and Dyson, H. J. (1999). "Intrinsically unstructured proteins: re-assessing the protein structure- function paradigm." *J Mol Biol* **293**: 321-31.

Xie, Q., Arnold, G. E., Romero, P., Obradovic, Z., Garner, E. and Dunker, A. K. (1998). "The sequence attribute method for determining relationships between sequence and protein disorder." *Genome Inform Ser Workshop Genome Inform* **9**: 193-200.

Xiong, Y., Hannon, G. J., Zhang, H., Casso, D., Kobayashi, R. and Beach, D. (1993). "p21 is a universal inhibitor of cyclin kinases." *Nature* **366**: 701-4.

Yan, Y., Frisen, J., Lee, M. H., Massague, J. and Barbacid, M. (1997). "Ablation of the CDK inhibitor p57Kip2 results in increased apoptosis and delayed differentiation during mouse development." *Genes Dev* **11**: 973-83.

Yang, J. and Kornbluth, S. (1999). "All aboard the cyclin train: subcellular trafficking of cyclins and their CDK partners." *Trends Cell Biol* **9**: 207-10.

Yokomori, K., Zeidler, M. P., Chen, J. L., Verrijzer, C. P., Mlodzik, M. and Tjian, R. (1994). "Drosophila TFIIA directs cooperative DNA binding with TBP and mediates transcriptional activation." *Genes Dev* **8**: 2313-23.

Zhang, H., Hannon, G. J. and Beach, D. (1994a). "p21-containing cyclin kinases exist in both active and inactive states." *Genes Dev* **8**: 1750-8.

Zhang, H., Hannon, G. J., Casso, D. and Beach, D. (1994b). "p21 is a component of active cell cycle kinases." *Cold Spring Harb Symp Quant Biol* **59**: 21-9.

Zhang, P., Liegeois, N. J., Wong, C., Finegold, M., Hou, H., Thompson, J. C., Silverman, A., Harper, J. W., DePinho, R. A. and Elledge, S. J. (1997). "Altered cell differentiation and proliferation in mice lacking p57KIP2 indicates a role in Beckwith-Wiedemann syndrome." *Nature* **387**: 151-8.

Zhu, X., Ohtsubo, M., Bohmer, R. M., Roberts, J. M. and Assoian, R. K. (1996). "Adhesion-dependent cell cycle progression linked to the expression of cyclin D1, activation of cyclin E-Cdk2, and phosphorylation of the retinoblastoma protein." *J Cell Biol* **133**: 391-403.

Zitzewitz, J. A., Ibarra-Molero, B., Fishel, D. R., Terry, K. L. and Matthews, C. R. (2000). "Preformed secondary structure drives the association reaction of GCN4- p1, a model coiled-coil system." *J Mol Biol* **296**: 1105-16.